Report #08032

# DIGHEM SURVEY
# FOR
# CORONATION MINERALS INC.
# WELLGREEN PROPERTY,
# YUKON TERRITORY

**NTS: 115G/5,6**

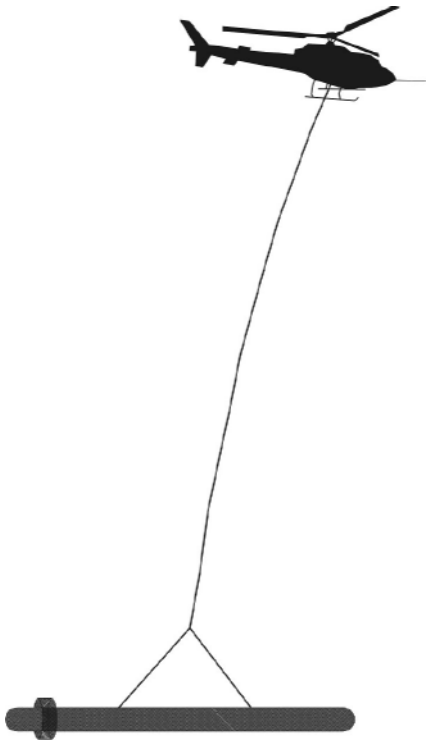

Fugro Airborne Surveys Corp.
Mississauga, Ontario

July 30, 2008

Fugro Airborne Surveys, 2270 Argentia Road, Unit 2, Mississauga, Ontario, Canada, L5N 6A6
Phone: 1 905 812 0212, Fax: 1 905 812 1504

## SUMMARY

This report describes the logistics, data acquisition, processing and presentation of results of a DIGHEM airborne geophysical survey carried out for Coronation Minerals Inc., over the Wellgreen property, located 30 kilometres west of Burwash Landing. Total coverage of the survey block amounted to 854 km. The survey was flown from May 8th to May 10th, 2008.

The purpose of the survey was to detect zones of conductive mineralization and to provide information that could be used to map the geology and structure of the survey area. This was accomplished by using a DIGHEM multi-coil, multi-frequency electromagnetic system, supplemented by a high sensitivity cesium magnetometer. The information from these sensors was processed to produce maps that display the magnetic and conductive properties of the survey area. A GPS electronic navigation system ensured accurate positioning of the geophysical data with respect to the base maps.

The survey data were processed and compiled in the Fugro Airborne Surveys Toronto office. Map products and digital data were provided in accordance with the scales and formats specified in the Survey Agreement.

The survey property contains several anomalous features, many of which are considered to be of moderate to high priority as exploration targets. Most of the inferred bedrock conductors appear to warrant further investigation using appropriate surface exploration techniques. Areas of interest may be assigned priorities on the basis of supporting

geophysical, geochemical and/or geological information. After initial investigations have been carried out, it may be necessary to re-evaluate the remaining anomalies based on information acquired from the follow-up program.

# CONTENTS

## APPENDICES

# 1. INTRODUCTION

A DIGHEM electromagnetic/magnetic survey was flown for Coronation Minerals Inc., from May 8th to May 10th, 2008, over the Wellgreen property, located 30 kilometres west of Burwash Landing, Yukon Territory. The survey area can be located on NTS map sheets 115G/5,6 (Figure 2).

Survey coverage consisted of approximately 854 line-km, including 71.5 line-km of tie lines. Flight lines were flown in an azimuthal direction of 20°/200° with a line separation of 100 metres. Tie lines were flown orthogonal to the traverse lines with a line separation of 1000 metres.

The survey employed the DIGHEM electromagnetic system. Ancillary equipment consisted of a magnetometer, radar altimeter, video camera, analog and digital recorders and an electronic navigation system. The instrumentation was installed in an AS350B3 turbine helicopter (Registration C-FQDA that was provided by Great Slave Helicopters Ltd. The helicopter flew at a mean airspeed of 85 km/h with a mean EM sensor height of approximately 47 metres.

In some portions of the survey area, the steep topography forced the pilot to exceed normal terrain clearance for reasons of safety. It is possible that some weak conductors may have escaped detection in areas where the bird height exceeded 120 m. In difficult areas where near-vertical climbs were necessary, the forward speed of the helicopter was

reduced to a level that permitted excessive bird swinging. This problem, combined with the severe stresses to which the bird was subjected, gave rise to aerodynamic noise levels that are slightly higher than normal on some lines. Where warranted, reflights were carried out to minimize these adverse effects.

Figure 1: Fugro Airborne Surveys DIGHEM EM bird with AS350-B3

# 2. SURVEY OPERATIONS

The base of operations for the survey was established at Destruction Bay, Yukon Territory.

The survey area can be located on NTS map sheets 115G/5,6 (Figure 2).

Table 2-1 lists the corner coordinates of the survey area in NAD83, UTM Zone 7, central meridian 141°W.

**Table 2-1**

| | X-UTM (E) | Y-UTM (N) |
|---|---|---|
| 1 | 570389 | 6818960 |
| 2 | 570853 | 6818957 |
| 3 | 570857 | 6819230 |
| 4 | 571790 | 6819202 |
| 5 | 571768 | 6818831 |
| 6 | 572082 | 6819022 |
| 7 | 572309 | 6818651 |
| 8 | 572701 | 6818888 |
| 9 | 573180 | 6818096 |
| 10 | 573203 | 6818123 |
| 11 | 573235 | 6818585 |
| 12 | 573617 | 6818560 |
| 13 | 573670 | 6818537 |
| 14 | 573910 | 6818137 |
| 15 | 574464 | 6818492 |
| 16 | 575069 | 6818436 |
| 17 | 575070 | 6818309 |
| 18 | 575278 | 6818540 |
| 19 | 576345 | 6817644 |
| 20 | 575748 | 6816931 |
| 21 | 576369 | 6816398 |

| | X-UTM (E) | Y-UTM (N) |
|---|---|---|
| 22 | 576576 | 6816722 |
| 23 | 576902 | 6816941 |
| 24 | 577105 | 6816976 |
| 25 | 577387 | 6817174 |
| 26 | 577639 | 6816797 |
| 27 | 577860 | 6817042 |
| 28 | 578388 | 6816576 |
| 29 | 578693 | 6816925 |
| 30 | 579309 | 6816389 |
| 31 | 580128 | 6815817 |
| 32 | 580242 | 6815912 |
| 33 | 580509 | 6815537 |
| 34 | 580874 | 6815794 |
| 35 | 581145 | 6815440 |
| 36 | 581403 | 6815414 |
| 37 | 581293 | 6814505 |
| 38 | 581442 | 6814486 |
| 39 | 581314 | 6814097 |
| 40 | 580955 | 6814196 |
| 41 | 580891 | 6813981 |
| 42 | 580760 | 6813906 |
| 43 | 580505 | 6813626 |
| 44 | 580443 | 6813508 |
| 45 | 580240 | 6813367 |
| 46 | 580283 | 6813271 |
| 47 | 580032 | 6813191 |
| 48 | 580034 | 6813086 |
| 49 | 580060 | 6813061 |
| 50 | 580047 | 6812889 |
| 51 | 580069 | 6812874 |
| 52 | 580086 | 6812500 |
| 53 | 579992 | 6812500 |
| 54 | 579553 | 6812374 |
| 55 | 579373 | 6812361 |
| 56 | 578741 | 6812223 |
| 57 | 578518 | 6812215 |
| 58 | 578260 | 6811993 |
| 59 | 578237 | 6811993 |
| 60 | 578149 | 6811875 |
| 61 | 578151 | 6811789 |

| | X-UTM (E) | Y-UTM (N) |
|---|---|---|
| 62 | 578032 | 6811498 |
| 63 | 578164 | 6811446 |
| 64 | 578300 | 6811379 |
| 65 | 578440 | 6811173 |
| 66 | 578517 | 6810940 |
| 67 | 578498 | 6810815 |
| 68 | 578566 | 6810724 |
| 69 | 578566 | 6810591 |
| 70 | 578492 | 6810508 |
| 71 | 578541 | 6810423 |
| 72 | 578565 | 6810284 |
| 73 | 578645 | 6810250 |
| 74 | 578712 | 6810191 |
| 75 | 578778 | 6810095 |
| 76 | 578846 | 6810088 |
| 77 | 578940 | 6809901 |
| 78 | 578966 | 6809901 |
| 79 | 579380 | 6809006 |
| 80 | 571007 | 6808991 |
| 81 | 571001 | 6812983 |
| 82 | 570078 | 6812983 |
| 83 | 570077 | 6815266 |
| 84 | 575527 | 6815282 |
| 85 | 575512 | 6815309 |
| 86 | 575681 | 6815531 |
| 87 | 573638 | 6816611 |
| 88 | 573579 | 6816492 |
| 89 | 571420 | 6817544 |
| 90 | 571566 | 6817840 |
| 91 | 570816 | 6817884 |
| 92 | 570811 | 6818017 |
| 93 | 570352 | 6818034 |

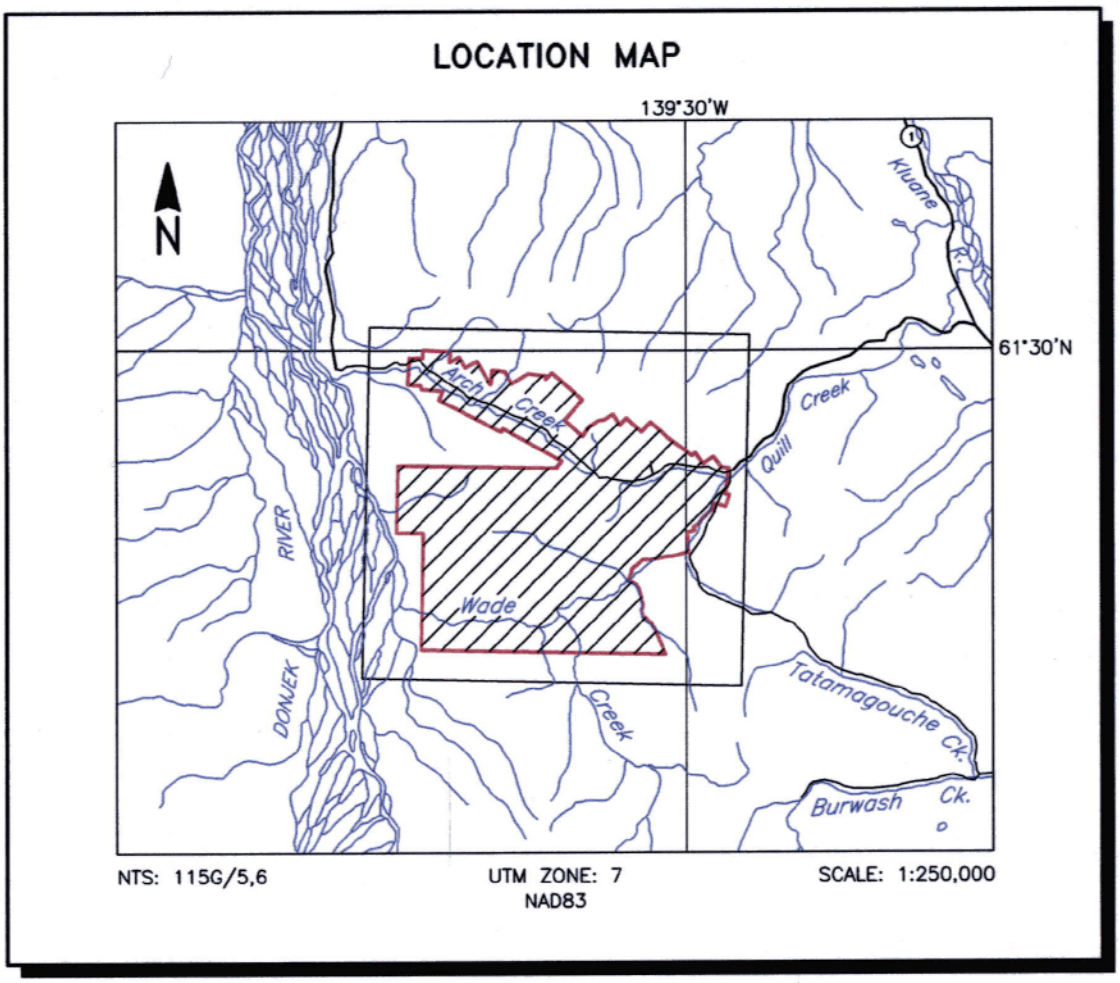


Figure 2
Location Map and Sheet Layout
Wellgreen Survey Area, Yukon Territory
Job # 08032

The survey specifications were as follows:

| Parameter | Specifications |
|---|---|
| Traverse line direction | Az 020 |
| Traverse line spacing | 100 m |
| Tie line direction | Az 110 |
| Tie line spacing | 1000 m |
| Sample interval | 10 Hz, 2.4 m @ 85 km/h |
| Aircraft mean terrain clearance | 74 m |
| EM sensor mean terrain clearance | 47 m |
| Mag sensor mean terrain clearance | 47 m |
| Average speed | 85 km/h |
| Navigation (guidance) | ±5 m, Real-time GPS |
| Post-survey flight path | ±2 m, Differential GPS |

# 3. SURVEY EQUIPMENT

This section provides a brief description of the geophysical instruments used to acquire the survey data and the calibration procedures employed. The geophysical equipment was installed in an AS350-B3 helicopter. This aircraft provides a safe and efficient platform for surveys of this type.

## Electromagnetic System

Model: DIGHEM

Type: Towed bird, symmetric dipole configuration operated at a nominal survey altitude of 30 metres. Coil separation is 8 metres for 900 Hz, 1000 Hz, 5500 Hz and 7200 Hz, and 6.3 metres for the 56,000 Hz coil-pair.

Coil orientations, frequencies and dipole moments

| $Atm^2$ | orientation | | nominal | actual |
|---|---|---|---|---|
| 211 | coaxial | / | 1000 Hz | 1125 Hz |
| 211 | coplanar | / | 900 Hz | 875 Hz |
| 67 | coaxial | / | 5500 Hz | 5454 Hz |
| 56 | coplanar | / | 7200 Hz | 7153 Hz |
| 15 | coplanar | / | 56,000 Hz | 56400 Hz |

Channels recorded: 5 in-phase channels
5 quadrature channels
2 monitor channels

Sensitivity: 0.06 ppm at 1000 Hz Cx
0.12 ppm at 900 Hz Cp
0.12 ppm at 5,500 Hz Cx
0.24 ppm at 7,200 Hz Cp
0.60 ppm at 56,000 Hz Cp

Sample rate: 10 per second, equivalent to 1 sample every 2.4 m, at a survey speed of 85 km/h.

## In-Flight EM System Calibration

Calibration of the system during the survey uses the Fugro AutoCal automatic, internal calibration process. At the beginning and end of each flight, and at intervals during the flight, the system is flown up to high altitude to remove it from any “ground effect” (response from the earth). Any remaining signal from the receiver coils (base level) is measured as the zero level, and is removed from the data collected until the time of the next calibration. Following the zero level setting, internal calibration coils, for which the response phase and amplitude have been determined at the factory, are automatically triggered – one for each frequency. The on-time of the coils is sufficient to determine an accurate response through any ambient noise. The receiver response to each calibration coil “event” is compared to the expected response (from the factory calibration) for both phase angle and amplitude, and any phase and gain corrections are automatically applied to bring the data to the correct value.

In addition, the outputs of the transmitter coils are continuously monitored during the survey, and the gains are adjusted to correct for any change in transmitter output.

Because the internal calibration coils are calibrated at the factory (on a resistive halfspace) ground calibrations using external calibration coils on-site are not necessary for system calibration. A check calibration may be carried out on-site to ensure all systems are working correctly. All system calibrations will be carried out in the air, at sufficient altitude that there will be no measurable response from the ground.

The internal calibration coils are rigidly positioned and mounted in the system relative to the transmitter and receiver coils. In addition, when the internal calibration coils are calibrated at the factory, a rigid jig is employed to ensure accurate response from the external coils.

Using real time Fast Fourier Transforms and the calibration procedures outlined above, the data are processed in real time, from measured total field at a high sampling rate, to in-phase and quadrature values at 10 samples per second.

## Airborne Magnetometer

| | |
|---|---|
| Model: | Fugro AM102 processor with Scintrex CS3 sensor |
| Type: | Optically pumped cesium vapour |
| Sensitivity: | 0.01 nT |
| Sample rate: | 10 per second |

The magnetometer sensor is housed in the EM bird, 27.7 m below the helicopter.

## Magnetic Base Station

Primary

| | | |
|---|---|---|
| Model: | Fugro CF1 base station with timing provided by integrated GPS | |
| Sensor type: | Scintrex CS-3 | |
| Counter specifications: | Accuracy: | ±0.1 nT |

| | | |
|---|---|---|
| | Resolution: | 0.01 nT |
| | Sample rate | 1 Hz |
| GPS specifications: | Model: | Marconi Allstar |
| | Type: | Code and carrier tracking of L1 band, 12-channel, C/A code at 1575.42 MHz |
| | Sensitivity: | -90 dBm, 1.0 second update |
| | Accuracy: | Manufacturer's stated accuracy for differential corrected GPS is 2 metres |

Environmental Monitor specifications:

Temperature:

- Accuracy: ±1.5ºC max
- Resolution: 0.0305ºC
- Sample rate: 1 Hz
- Range: -40ºC to +75ºC

Barometric pressure:

- Model: Motorola MPXA4115A
- Accuracy: ±3.0º kPa max (-20ºC to 105ºC temp. ranges)
- Resolution: 0.013 kPa
- Sample rate: 1 Hz
- Range: 55 kPa to 108 kPa

Backup

| | |
|---|---|
| Model: | GEM Systems GSM-19T |
| Type: | Digital recording proton precession |
| Sensitivity: | 0.10 nT |
| Sample rate: | 3 second intervals |

A digital recorder is operated in conjunction with the base station magnetometer to record the diurnal variations of the earth's magnetic field. The clock of the base station is synchronized with that of the airborne system, using GPS time, to permit subsequent removal of diurnal drift. The Fugro CF1 was the primary magnetic base station. It was

located at longitude138 48 12.75168 W, latitude 61 15 14.04266 N, 805.78 m above the WGS84 ellipsoid.

**Figure 3 Primary Magnetic Base Station**

## Navigation (Global Positioning System)

Airborne Receiver for Flight Path Recovery

| | |
|---|---|
| Model: | Novatel OEM-4 |
| Type: | Code and carrier tracking of L1-C/A code at 1575.42 MHz and L2-P code at 1227.0 MHz. Dual frequency, 24-channel. |
| Sample rate: | 10 Hz update. |
| Accuracy: | Better than 1 metre in differential mode. |
| Antenna: | Mounted on helicopter tail. |

Primary Base Station for Post-Survey Differential Correction

| | |
|---|---|
| Model: | Novatel OEM-4 |
| Type: | Code and carrier tracking of L1-C/A code at 1575.42 MHz and L2-P code at 1227.0 MHz. Dual frequency, 24-channel. |
| Sample rate: | 10 Hz update. |
| Accuracy: | Better than 1 metre in differential mode. |

The Novatel OEM-4 is a line of sight, satellite navigation system that utilizes time-coded signals from at least four of forty-eight available satellites. Both Russian GLONASS and American NAVSTAR satellite constellations are used to calculate the position and to provide real time guidance to the helicopter. The mobile and base station raw XYZ data were recorded, thereby permitting post-survey differential corrections for theoretical accuracies of better than 1 metre

Each base station receiver is able to calculate its latitude and longitude. For this survey, the primary GPS base station was located at longitude138 48 12.13546 W, latitude 61 15 14.44354 N, 807.81 m above the WGS84 ellipsoid. The GPS records data relative to the WGS84 ellipsoid, which is the basis of the revised North American Datum (NAD83). Conversion software is used to transform the WGS84 coordinates to the NAD83 UTM system displayed on the maps.

## Radar Altimeter

| | |
|---|---|
| Manufacturer: | Honeywell/Sperry |
| Model: | RT300 |
| Type: | Short pulse modulation, 4.3 GHz |
| Sensitivity: | 0.3 m |
| Sample rate: | 10 per second |

The radar altimeter measures the vertical distance between the helicopter and the ground. This information is used in the processing algorithm that determines conductor depth.

## Barometric Pressure and Temperature Sensors

| | | |
|---|---|---|
| Model: | DIGHEM D 1300 | |
| Type: | Motorola MPX4115AP analog pressure sensor<br>AD592AN high-impedance remote temperature sensors | |
| Sensitivity: | Pressure: | 150 mV/kPa |
| | Temperature: | 100 mV/°C or 10 mV/°C (selectable) |
| Sample rate: | 10 per second | |

The D1300 circuit is used in conjunction with one barometric sensor and up to three temperature sensors. Two sensors (baro and temp) are installed in the EM console in the aircraft, to monitor pressure (1KPA) and internal operating temperatures.

## Digital Data Acquisition System

| | |
|---|---|
| Manufacturer: | Fugro |
| Model: | HeliDAS |
| Recorder: | Compact flash card |

The stored data are downloaded to the field workstation PC at the survey base, for verification, backup and preparation of in-field products.

## Video Flight Path Recording System

Type: Axis 2420 Digital Network Camera

Recorder: Tablet computer

Fiducial numbers are recorded continuously and are displayed on the margin of each image. This procedure ensures accurate correlation of data with respect to visible features on the ground.

# 4. QUALITY CONTROL AND IN-FIELD PROCESSING

Digital data for each flight were transferred to the field workstation, in order to verify data quality and completeness. A database was created and updated using Geosoft Oasis Montaj and proprietary Fugro Atlas software. This allowed the field personnel to calculate, display and verify both the positional (flight path) and geophysical data on a screen or printer. A preliminary assessment of the data acquired is made on a flight by flight basis.

In-field processing of Fugro survey data consists of differential corrections to the airborne GPS data, verification of EM calibrations, drift correction of the raw airborne EM data, spike rejection and filtering of all geophysical and ancillary data, verification of flight videos, calculation of preliminary resistivity data, diurnal correction, and preliminary levelling of magnetic data.

All data, including base station records, were checked on a daily basis, to ensure compliance with the survey contract specifications. Reflights were required if any of the following specifications were not met.

Navigation - Positional (x,y) accuracy of better than 10 m, with a CEP (circular error of probability) of 95%.

Flight Path - No lines to exceed ±25% departure from nominal line spacing over a continuous distance of more than 1 km, except for reasons of safety.

Clearance - Mean terrain sensor clearance of 30 m, ±10 m, except where precluded by safety considerations, e.g., restricted or populated areas, severe topography, obstructions, tree canopy, aerodynamic limitations, etc. The rugged topography of most of the survey area required the pilot to tow the bird at an average terrain clearance of 47 m.

Airborne Mag - The non-normalized 4th difference will not exceed 1.6 nT over a continuous distance of 1 kilometre excluding areas where this specification is exceeded due to natural anomalies.

Base Mag - For acceptance of the magnetic data, non linear variations in the magnetic diurnal shall not exceed 10 nT per minute.

EM - Spheric pulses may occur having strong peaks but narrow widths. The EM data area considered acceptable when their occurrence is less than 10 spheric events exceeding the stated noise specification for a given frequency per 100 samples continuously over a distance of 2 000 metres.

| Frequency | Coil Orientation | Peak to Peak Noise Envelope (ppm) |
|---|---|---|
| 1000 Hz | vertical coaxial | 5.0 |
| 900 Hz | horizontal coplanar | 10.0 |
| 5 500 Hz | vertical coaxial | 10.0 |
| 7200 Hz | horizontal coplanar | 20.0 |
| 56 000 Hz | horizontal coplanar | 40.0 |

# 5. DATA PROCESSING

## Flight Path Recovery

Both the base and mobile GPS units simultaneously record the raw range data from at least four satellites. The geographic positions of both units, relative to the model ellipsoid, are calculated from this information. Differential corrections, which are obtained from the base station, are applied to the mobile unit data to provide a post-flight track of the aircraft, accurate to within 1 m. Speed checks of the flight path are also carried out to determine if there are any spikes or gaps in the data.

The corrected WGS84 latitude/longitude coordinates are transformed to the coordinate system used on the final maps. Images or plots are then created to provide a visual check of the flight path.

## Electromagnetic Data

EM data are processed at the recorded sample rate of 10 samples/second. Spheric rejection median and Hanning filters are then applied to reduce noise to acceptable levels. EM profiles are then examined on screen to allow the interpreter to select the most appropriate EM anomaly picking controls for a given survey area. The EM picking parameters depend on several factors but are primarily based on the dynamic range of the

resistivities within the survey area, and the types and expected geophysical responses of the targets being sought.

Anomalous electromagnetic responses are selected and analysed by computer to provide a preliminary electromagnetic anomaly map. The automatic selection algorithm is intentionally oversensitive to assure that no meaningful responses are missed. The computer-selected anomalies are superimposed on profiles of the em data, calculated resistivities and depths. These are displayed on large computer monitors along with flight path video and appropriate gridded data. With all these data on screen and linked the interpreter then classifies the anomalies according to their source and eliminates those that are not substantiated by the data. The final interpreted EM anomaly map includes bedrock, surficial and cultural conductors.

## Apparent Resistivity

The apparent resistivities in ohm-m are generated from the in-phase and quadrature EM components for all of the coplanar frequencies, using a pseudo-layer half-space model. The inputs to the resistivity algorithm are the in-phase and quadrature amplitudes of the secondary field. The algorithm calculates the apparent resistivity in ohm-m, and the apparent height of the bird above the conductive source. Any difference between the apparent height and the true height, as measured by the radar altimeter, is called the pseudo-layer and reflects the difference between the real geology and a homogeneous halfspace. This difference is often attributed to the presence of a highly resistive upper layer. Any errors in the altimeter reading, caused by heavy tree cover, are included in the

pseudo-layer and do not affect the resistivity calculation. The apparent depth estimates, however, will reflect the altimeter errors. Apparent resistivities calculated in this manner may differ from those calculated using other models.

In areas where the effects of magnetic permeability or dielectric permittivity have suppressed the in-phase responses, the calculated resistivities will be erroneously high. Various algorithms and inversion techniques can be used to partially correct for the effects of permeability and permittivity.

Apparent resistivity maps portray all of the information for a given frequency over the entire survey area. This full coverage contrasts with the electromagnetic anomaly map, which provides information only over interpreted conductors. The large dynamic range afforded by the multiple frequencies makes the apparent resistivity parameter an excellent mapping tool.

The preliminary apparent resistivity maps and images are carefully inspected to identify any lines or line segments that might require base level adjustments. Subtle changes between in-flight calibrations of the system can result in line-to-line differences that are more recognizable in resistive (low signal amplitude) areas. If required, manual level adjustments are carried out to eliminate or minimize resistivity differences that can be attributed, in part, to changes in operating temperatures. These levelling adjustments are usually very subtle, and do not result in the degradation of discrete anomalies.

After the manual levelling process is complete, revised resistivity grids are created. The resulting grids can be subjected to a microlevelling technique in order to smooth the data for contouring.

## Residual Magnetic Intensity

A Fugro CF-1 cesium vapour magnetometer was operated at the survey base for each area to record diurnal variations of the earth's magnetic field. The clock of the base station was synchronized with that of the airborne system to permit subsequent removal of diurnal drift. A GEM Systems GSM-19T proton precession magnetometer was also operated as a backup unit.

A fourth difference editing routine was applied to the magnetic data and this was examined along with the magnetic data on a line-by-line basis to detect and then remove any spikes. The aeromagnetic data were corrected for measured system lag, and then corrected for diurnal variations by subtraction of the digitally recorded base station magnetic data. The IGRF (model 2005) was then removed based on the survey date and aircraft height. Tie line levelling was attempted and rejected as inappropriate. Excessive magnetic gradients in the survey area caused the majority of the tie line traverse line intersections to be rejected. Instead manual adjustments were applied to any lines that required levelling, as indicated by shadowed images of the gridded vertical magnetic gradient data. The manually levelled data were then subjected to a microlevelling filter. The resulting data have been presented on the maps using a contour interval of 5 nT where gradients permit. The maps show the magnetic properties of the rock units underlying the survey area.

## Calculated Vertical Magnetic Gradient

The diurnally corrected residual magnetic field data were subjected to a processing algorithm that enhances the response of magnetic bodies in the upper 500 m and attenuates the response of deeper bodies. The resulting vertical gradient maps provide better definition and resolution of near-surface magnetic units. They also identify weak magnetic features that may not be evident on the residual magnetic field maps. Regional magnetic variations and changes in lithology, however, may be better defined on the residual magnetic field maps. The resulting data have been presented on the maps using a contour interval of 0.05 nT/m where gradients permit.

## Digital Elevation (optional)

The radar altimeter values (ALTRAD_BIRD + aircraft to ground clearance) are subtracted from the differentially corrected and de-spiked Z values to produce profiles of the height above the ellipsoid along the survey lines. These values are gridded to produce contour maps showing approximate elevations within the survey area ith respect to the WGS84 spheroid. The calculated digital terrain data are then tie-line levelled. Any remaining subtle line-to-line discrepancies are manually removed. After the manual corrections are applied, the digital terrain data are filtered with a microlevelling algorithm.

The accuracy of the elevation calculation is directly dependent on the accuracy of the two input parameters, ALTRAD_BIRD and Z. The ALTRAD_BIRD value may be erroneous in areas of heavy tree cover, where the altimeter reflects the distance to the tree canopy rather than the ground. The Z value is primarily dependent on the number of available satellites. Although post-processing of GPS data will yield X and Y accuracies in the order of 1 metre, the accuracy of the Z value is usually much less, sometimes in the ±10 metre range. Further inaccuracies may be introduced during the interpolation and gridding process.

Because of the inherent inaccuracies of this method, no guarantee is made or implied that the information displayed is a true representation of the height above sea level. Although this product may be of some use as a general reference, THIS PRODUCT MUST NOT BE USED FOR NAVIGATION PURPOSES.

## Contour, Colour and Shadow Map Displays

The geophysical data are interpolated onto a regular grid using a modified Akima spline technique. The resulting grid is suitable for image processing and generation of contour maps. The grid cell size is 20% of the line interval.

Colour maps are produced by interpolating the grid down to the pixel size. The parameter is then incremented with respect to specific amplitude ranges to provide colour "contour" maps.

Monochromatic shadow maps or images are generated by employing an artificial sun to cast shadows on a surface defined by the geophysical grid. There are many variations in the shadowing technique. These techniques can be applied to total field or enhanced magnetic data, magnetic derivatives, resistivity, etc. The shadowing technique is also used as a quality control method to detect subtle changes between lines.

## Multi-channel Stacked Profiles

Distance-based profiles of the digitally recorded geophysical data are generated and plotted at an appropriate scale. These profiles also contain the calculated parameters that are used in the interpretation process. These are viewed on screen as part of the interpretation process, and are also presented as final paper copies if requested. The profiles display electromagnetic anomalies with their respective interpretive symbols. Table 5-1 shows the parameters and scales for the multi-channel stacked profiles.

In Table 5-1, the log resistivity scale of 0.06 decade/mm means that the resistivity changes by an order of magnitude in 16.6 mm. The resistivities at 0, 33 and 67 mm up from the bottom of the digital profile are respectively 1, 100 and 10,000 ohm-m.

## Table 5-1. Multi-channel Stacked Profiles

| Channel Name (Freq) | Observed Parameters | Scale Units/mm |
|---|---|---|
| MAG | residual magnetic intensity (fine) | 10 nT |
| MAG | residiual magnetic intensity (coarse) | 50 nT |
| ALTRAD_BIRD | EM sensor height above ground | 6 m |
| CXI1000 | vertical coaxial coil-pair in-phase (1000 Hz) | 1 ppm |
| CXQ1000 | vertical coaxial coil-pair quadrature (1000 Hz) | 1 ppm |
| CPI900 | horizontal coplanar coil-pair in-phase (900 Hz) | 4 ppm |
| CPQ900 | horizontal coplanar coil-pair quadrature (900 Hz) | 4 ppm |
| CXI5500 | vertical coaxial coil-pair in-phase (5500 Hz) | 5 ppm |
| CXQ5500 | vertical coaxial coil-pair quadrature (5500 Hz) | 5 ppm |
| CPI7200 | horizontal coplanar coil-pair in-phase (7200 Hz) | 10 ppm |
| CPQ7200 | horizontal coplanar coil-pair quadrature (7200 Hz) | 10 ppm |
| CPI56K | horizontal coplanar coil-pair in-phase (56,000 Hz) | 10 ppm |
| CPQ56K | horizontal coplanar coil-pair quadrature (56,000 Hz) | 10 ppm |
| CXSP | coaxial spherics monitor | |
| CPPL | coplanar powerline monitor | |
| | | |
| | Computed Parameters | |
| DIFI ( mid freq.) | difference function in-phase from CXI and CPI | 5 ppm |
| DIFQ ( mid freq.) | difference function quadrature from CXQ and CPQ | 5 ppm |
| RES900 | log resistivity | .06 decade |
| RES7200 | log resistivity | .06 decade |
| RES56K | log resistivity | .06 decade |
| DEP900 | apparent depth | 6 m |
| DEP7200 | apparent depth | 6 m |
| DEP56K | apparent depth | 6 m |
| Anom_Grade | Local amplitude | 1 grade |

# 6. PRODUCTS

This section lists the final maps and products that have been provided under the terms of the survey agreement. Other products can be prepared from the existing dataset, if requested. These include magnetic enhancements or derivatives, percent magnetite, resistivities corrected for magnetic permeability and/or dielectric permittivity, digital terrain, resistivity-depth sections, inversions, and overburden thickness. Most parameters can be displayed as contours, profiles, or in colour.

## Base Maps

Base maps of the survey area were by scanning published topographic maps to a bitmap (.bmp) format. This process provides a relatively accurate, distortion-free base that facilitates correlation of the navigation data to the map coordinate system. The topographic files were combined with geophysical data for plotting the final maps. All maps were created using the following parameters:

Projection Description:

| | |
|---|---|
| Datum: | NAD83 |
| Ellipsoid: | GRS80 |
| Projection: | UTM (Zone: 7N) |
| Central Meridian: | 141 W |
| False Northing: | 0 |
| False Easting: | 500000 |
| Scale Factor: | 0.9996 |
| WGS84 to Local Conversion: | Molodensky |
| Datum Shifts: | DX: 0 DY: 0 DZ: 0 |

The following parameters are presented on one map sheet, at a scale of 1:20,000. All maps include flight lines and topography, unless otherwise indicated. Preliminary products are not listed.

## Final Products

| | Colour |
|---|---|
| EM Anomalies | 2 |
| Residual Magnetic Intensity | 2 |
| Calculated Vertical Magnetic Gradient | 2 |
| Apparent Resistivity 7200 Hz | 2 |
| Apparent Resistivity 56,000 Hz | 2 |
| Digital Elevation Model | 2 |

Additional Products

| | |
|---|---|
| Digital Archive (see Archive Description) | 1 DVD |
| Survey Report | PDF on DVD |
| Multi-channel Stacked Profiles | All lines |
| Flight Path Video | DVD |

# 7. SURVEY RESULTS

## General Discussion

Table 7-1 summarizes the EM responses in the survey area, with respect to conductance grade and interpretation. The apparent conductance and depth values in the full EM anomaly database on the final DVD archive have been calculated from “local” in-phase and quadrature amplitudes of the coaxial 5500 Hz frequency. The picking and interpretation procedure relies on several parameters and calculated functions. For this survey, the Coaxial 5500 Hz responses and the mid-frequency difference channels were used as two of the main picking criteria. The 7200 Hz coplanar results were also weighted to provide picks over wider or flat-dipping sources. The quadrature channels provided picks in areas where the in-phase responses might have been suppressed by magnetite.

The anomalies shown on the electromagnetic anomaly maps are based on a near-vertical, half plane model. This model best reflects "discrete" bedrock conductors. Wide bedrock conductors or flat-lying conductive units, whether from surficial or bedrock sources, may give rise to very broad anomalous responses on the EM profiles. These may not appear on the electromagnetic anomaly map if they have a regional character rather than a locally anomalous character.

# TABLE 7-1 EM ANOMALY STATISTICS

## WELLGREEN PROPERTY, YUKON TERRITORY

| CONDUCTOR GRADE | CONDUCTANCE RANGE SIEMENS (MHOS) | NUMBER OF RESPONSES |
|---|---|---|
| 7 | >100 | 1 |
| 6 | 50 - 100 | 0 |
| 5 | 20 - 50 | 6 |
| 4 | 10 - 20 | 8 |
| 3 | 5 - 10 | 31 |
| 2 | 1 - 5 | 234 |
| 1 | <1 | 538 |
| * | INDETERMINATE | 473 |
| TOTAL | | 1291 |

| CONDUCTOR MODEL | MOST LIKELY SOURCE | NUMBER OF RESPONSES |
|---|---|---|
| D | DISCRETE BEDROCK CONDUCTOR | 28 |
| B | DISCRETE BEDROCK CONDUCTOR | 218 |
| S | CONDUCTIVE COVER | 1044 |
| H | ROCK UNIT OR THICK COVER | 0 |
| E | EDGE OF WIDE CONDUCTOR | 1 |
| L | CULTURE | 0 |
| TOTAL | | 1291 |

(SEE EM MAP LEGEND FOR EXPLANATIONS)

These broad conductors, which more closely approximate a half-space model, will be maximum coupled to the horizontal (coplanar) coil-pair and should be more evident on the resistivity parameter. Resistivity maps, therefore, may be more valuable than the electromagnetic anomaly maps, in areas where broad or flat-lying conductors are considered to be of importance.

Excellent resolution and discrimination of conductors was accomplished by using a fast sampling rate of 0.1 sec and by employing a “common” frequency (5500/7200 Hz) on two orthogonal coil-pairs (coaxial and coplanar). The resulting difference channel parameters often permit differentiation of bedrock and surficial conductors, even though they may exhibit similar conductance values.

Anomalies that occur near the ends of the survey lines (i.e., outside the survey area), should be viewed with caution. Some of the weaker anomalies could be due to aerodynamic noise, i.e., bird bending, which is created by abnormal stresses to which the bird is subjected during the climb and turn of the aircraft between lines. Such aerodynamic noise is usually manifested by an anomaly on the coaxial in-phase channel only, although severe stresses can affect the coplanar in-phase channels as well.

## Magnetic Data

A Fugro CF-1 cesium vapour magnetometer was operated at the survey base to record diurnal variations of the earth's magnetic field. The clock of the base station was synchronized with that of the airborne system to permit subsequent removal of diurnal drift.

There is abundant evidence on the magnetic maps to suggest that the survey area has been subjected to deformation and/or alteration. These structural complexities are evident on the contour maps as variations in magnetic intensity, irregular patterns, and as offsets or changes in strike direction.

If a specific magnetic intensity can be assigned to the rock type that is believed to host the target mineralization, it may be possible to select areas of higher priority on the basis of the residual magnetic intensity data. This is based on the assumption that the magnetite content of the host rocks will give rise to a limited range of contour values that will permit differentiation of various lithological units.

The magnetic results, in conjunction with the other geophysical parameters, have provided valuable information that can be used to effectively map the geology and structure in the survey area.

## Apparent Resistivity

Apparent resistivity maps, which display the conductive properties of the survey area, were produced from the 7200 Hz and 56,000 Hz coplanar data. Resistivity values were capped at maximum values for each frequency These cutoffs eliminate the erratic higher resistivities that would result from unstable ratios of very small EM amplitudes.

In general, the resistivity patterns show agreement with the magnetic trends. This suggests that many of the resistivity lows are probably related to bedrock features, rather than conductive overburden. There are some areas, however, where contour patterns appear to be strongly influenced by conductive surficial material.

## Electromagnetic Anomalies

The EM anomalies resulting from this survey appear to fall within one of two general categories. The first type consists of discrete, well-defined anomalies that yield marked inflections on the difference channels. These anomalies are usually attributed to conductive sulphides or graphite and are generally given a "B", "T" or "D" interpretive symbol, denoting a bedrock source.

The second class of anomalies comprises moderately broad responses that exhibit the characteristics of a half-space and do not yield well-defined inflections on the difference channels. Anomalies in this category are usually given an "S" or "H" interpretive symbol.

The lack of a difference channel response usually implies a broad or flat-lying conductive source such as overburden. Some of these anomalies could reflect conductive rock units, zones of deep weathering, or the weathered tops of kimberlite pipes, all of which can yield “non-discrete” signatures.

The effects of conductive overburden are evident over portions of the survey area(s). Although the difference channels (DIFI and DIFQ) are extremely valuable in detecting bedrock conductors that are partially masked by conductive overburden, sharp undulations in the bedrock/overburden interface can yield anomalies in the difference channels which may be interpreted as possible bedrock conductors. Such anomalies usually fall into the "S?" or "B?" classification but may also be given an "E" interpretive symbol, denoting a resistivity contrast at the edge of a conductive unit.

The "?" symbol does not question the validity of an anomaly, but instead indicates some degree of uncertainty as to which is the most appropriate EM source model. This ambiguity results from the combination of effects from two or more conductive sources, such as overburden and bedrock, gradational changes, or moderately shallow dips. The presence of a conductive upper layer has a tendency to mask or alter the characteristics of bedrock conductors, making interpretation difficult. This problem is further exacerbated in the presence of magnetite.

Magnetite can cause suppression or polarity reversals of the in-phase components, particularly at the lower frequencies in resistive areas. The effects of magnetite-rich rock

units are usually evident on the multi-parameter geophysical data profiles as negative excursions of the lower frequency in-phase channels.

In areas where EM responses are evident primarily on the quadrature components, zones of poor conductivity are indicated. Where these responses are coincident with magnetic anomalies, it is possible that the effects of magnetite have suppressed the in-phase component amplitudes. Poorly conductive magnetic features can give rise to resistivity anomalies that are only slightly below or slightly above background. If it is expected that poorly conductive economic mineralization could be associated with magnetite-rich units, most of these weakly anomalous features will be of interest. In areas where magnetite causes the in-phase components to become negative, the apparent conductance and depth of EM anomalies will be unreliable. Magnetite effects usually give rise to overstated (higher) resistivity values and understated (shallow) depth calculations.

As potential targets within the area may be associated with massive to weakly disseminated sulphides, which may or may not be hosted by magnetite-rich rocks, it is impractical to assess the relative merits of EM anomalies on the basis of conductance. It is recommended that an attempt be made to compile a suite of geophysical "signatures" over any known areas of interest. Anomaly characteristics are clearly defined on the multi-parameter geophysical data profiles that are supplied as one of the survey products.

The electromagnetic anomaly maps show the anomaly locations with the interpreted conductor type, dip and conductance being indicated by symbols. Direct magnetic

correlation is also shown if it exists. The strike direction and length of the conductors are indicated only where anomalies can be correlated from line to line with a reasonable degree of confidence.

In areas where several conductors or conductive trends appear to be related to a common geological unit, these have been outlined as "zones" on the EM anomaly map. The zone outlines usually approximate the limits of conductive units defined by the resistivity contours, but may also be related to distinct rock units that can be inferred from the magnetic data.

## Wellgreen Area

The area shows several zones where magnetic data correlate with conductivity. Zone 1 appears as a higher magnetic gradient area that corresponds to a resistive area. The shape of the zone differs from the strike of local stratigraphy indicating it may be a zone of alteration or an intrusive body. Parallel to the northeast boundary of zone 1 and wrapping around the northern edge of Zone 1 are two trends of bedrock conductors, A1 and A2 that should be investigated. These conductors continue across lines along the edge of Zone 1. They have a narrow coaxial inphase response that corresponds to a dip in the coplanar inphase indicating a bedrock source. To the northwest of Zone 1 is a highly conductive area containing many bedrock conductors. Local geology indicates the rocks in this area to be shale and argillite of the McCarthy formation. Shale is very conductive and is

characterized by high amplitude bedrock conductors and that is probably the source of these.

To the northeast alternating areas of low and high gradient magnetic data correspond with areas of low and high resistivity parallel to stratigraphy likely indicating different lithologies of the McCarthy and Hansen Creek formations. Ground follow-up or detailed knowledge of the geology of the area will allow the rock types responsible for these geophysical responses to be interpreted. Conductor axis A3 is located along a magnetic low coincident with a river valley. Usually conductors in a valley are created by conductive overburden but these anomalies show the characteristics of a bedrock source. Possibly they are caused by a contact between two lithologies or a fault that is reflected in the topography. Axis A4 runs parallel to the topography bounding the high ground to the north of the Maple Creek/Quill Creek valley and like A3 shows characteristics of a bedrock source. To the north of the A4 axis there is a sudden drop in the magnetic intensity along M1, which corresponds to a conductive response in the resistivity data. The EM anomalies along M1 are mostly surficial and geophysically this structural break could be a faulted contact between rock types. To the north of M1 there are two conductive zones in an area of high magnetic gradient. Both these zones possess many bedrock conductors scattered throughout the zone. These zones appear to coincide with the locations of the Wellgreen Property Main Zone and West Zone but detailed knowledge of the locations of the properties will allow for a more accurate interpretation. These zones are associated with a magnetic feature that is almost 4000 nT higher than the rest of the area. This intense magnetic field suppresses the inphase response especially on the lower frequencies

making the interpretation more difficult but the width and amplitude of the quadrature responses indicate a bedrock origin for these anomalies. To the northwest of these zones along strike there is a potentially related northwest trending magnetic feature that is offset several times by northeast trending structural breaks. At A5 and A6 this magnetic feature is associated with conductor axes composed of many bedrock anomalies. The source of these should be investigated.

# 8. CONCLUSIONS AND RECOMMENDATIONS

This report provides a brief description of the survey results and the equipment, data processing procedures and logistics of the survey.

The survey was successful in locating several conductors that may warrant additional work. The various maps included with this report display the magnetic and conductive properties of the survey area. It is recommended that a complete assessment and detailed evaluation of the survey results be carried out, in conjunction with all available geophysical, geological and geochemical information. Particular reference should be made to the multi-parameter data profiles that clearly define the characteristics of the individual anomalies.

The interpreted bedrock conductors and anomalous targets defined by the survey should be subjected to further investigation, using appropriate surface exploration techniques. Anomalies that are currently considered to be of moderately low priority may require upgrading if follow-up results are favourable.

It is also recommended that image processing of existing geophysical data be considered, in order to extract the maximum amount of information from the survey results. Current software and imaging techniques often provide valuable information on structure and lithology, which may not be clearly evident on the contour and colour maps. These techniques can yield images that define subtle, but significant, structural details.

Respectfully submitted,

**FUGRO AIRBORNE SURVEYS CORP.**

# APPENDIX A

# LIST OF PERSONNEL

The following personnel were involved in the acquisition, processing, interpretation and presentation of data, relating to a DIGHEM airborne geophysical survey carried out for Coronation Minerals Inc., near Burwash Landing, Yukon Territory.

| | |
|---|---|
| Emily Farquhar | Manager Geophysical Services |
| David Miles | Manager Geophysical Projects |
| Graham Konieczny | Manager, Data Processing and Interpretation |
| Lesley Minty | Project Manager |
| Amit Praharaj | Geophysical Operator |
| Darren Hamill | Field Geophysicist |
| Len Joa | Pilot (Great Slave Helicopters Ltd.) |
| Russell Imrie | Interpretation Geophysicist |
| Lyn Vanderstarren | Drafting Supervisor |
| Albina Tonello | Secretary/Expeditor |

The survey consisted of 854 km of coverage, flown from May 8 to May 10, 2008.

All personnel are employees of Fugro Airborne Surveys, except where indicated.

# APPENDIX B

# BACKGROUND INFORMATION

# BACKGROUND INFORMATION

## Electromagnetics

Fugro electromagnetic responses fall into two general classes, discrete and broad. The discrete class consists of sharp, well-defined anomalies from discrete conductors such as sulphide lenses and steeply dipping sheets of graphite and sulphides. The broad class consists of wide anomalies from conductors having a large horizontal surface such as flatly dipping graphite or sulphide sheets, saline water-saturated sedimentary formations, conductive overburden and rock, kimberlite pipes and geothermal zones. A vertical conductive slab with a width of 200 m would straddle these two classes.

The vertical sheet (half plane) is the most common model used for the analysis of discrete conductors. All anomalies plotted on the geophysical maps are analyzed according to this model. The following section entitled **Discrete Conductor Analysis** describes this model in detail, including the effect of using it on anomalies caused by broad conductors such as conductive overburden.

The conductive earth (half-space) model is suitable for broad conductors. Resistivity contour maps result from the use of this model. A later section entitled **Resistivity Mapping** describes the method further, including the effect of using it on anomalies caused by discrete conductors such as sulphide bodies.

## Geometric Interpretation

The geophysical interpreter attempts to determine the geometric shape and dip of the conductor. Figure B-1 shows typical HEM anomaly shapes which are used to guide the geometric interpretation.

## Discrete Conductor Analysis

The EM anomalies appearing on the electromagnetic map are analyzed by computer to give the conductance (i.e., conductivity-thickness product) in siemens (mhos) of a vertical sheet model. This is done regardless of the interpreted geometric shape of the conductor. This is not an unreasonable procedure, because the computed conductance increases as the electrical quality of the conductor increases, regardless of its true shape. DIGHEM anomalies are divided into seven grades of conductance, as shown in Table B-1. The conductance in siemens (mhos) is the reciprocal of resistance in ohms.

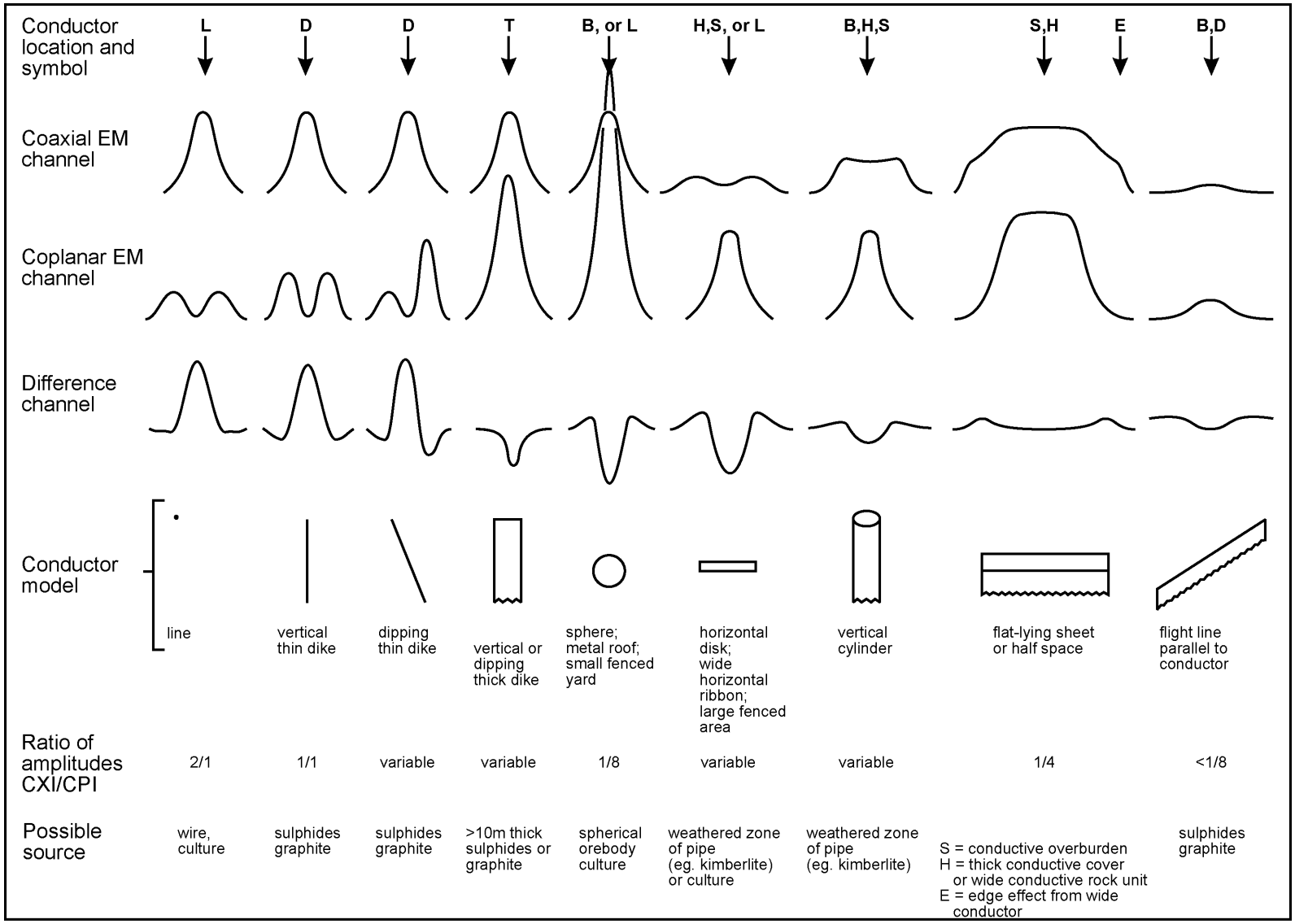


**Typical HEM anomaly shapes**
**Figure B-1**

The conductance value is a geological parameter because it is a characteristic of the conductor alone. It generally is independent of frequency, flying height or depth of burial, apart from the averaging over a greater portion of the conductor as height increases. Small anomalies from deeply buried strong conductors are not confused with small anomalies from shallow weak conductors because the former will have larger conductance values.

## Table B-1. EM Anomaly Grades

| Anomaly Grade | Siemens |
|---|---|
| 7 | > 100 |
| 6 | 50 - 100 |
| 5 | 20 - 50 |
| 4 | 10 - 20 |
| 3 | 5 - 10 |
| 2 | 1 - 5 |
| 1 | < 1 |

Conductive overburden generally produces broad EM responses which may not be shown as anomalies on the geophysical maps. However, patchy conductive overburden in otherwise resistive areas can yield discrete anomalies with a conductance grade (cf. Table B-1) of 1, 2 or even 3 for conducting clays which have resistivities as low as 50 ohm-m. In areas where ground resistivities are below 10 ohm-m, anomalies caused by weathering variations and similar causes can have any conductance grade. The anomaly shapes from the multiple coils often allow such conductors to be recognized, and these are indicated by the letters S, H, and sometimes E on the geophysical maps (see EM legend on maps).

For bedrock conductors, the higher anomaly grades indicate increasingly higher conductances. Examples: the New Insco copper discovery (Noranda, Canada) yielded a grade 5 anomaly, as did the neighbouring copper-zinc Magusi River ore body; Mattabi (copper-zinc, Sturgeon Lake, Canada) and Whistle (nickel, Sudbury, Canada) gave grade 6; and the Montcalm nickel-copper discovery (Timmins, Canada) yielded a grade 7 anomaly. Graphite and sulphides can span all grades but, in any particular survey area, field work may show that the different grades indicate different types of conductors.

Strong conductors (i.e., grades 6 and 7) are characteristic of massive sulphides or graphite. Moderate conductors (grades 4 and 5) typically reflect graphite or sulphides of a less massive character, while weak bedrock conductors (grades 1 to 3) can signify poorly connected graphite or heavily disseminated sulphides. Grades 1 and 2 conductors may not respond to ground EM equipment using frequencies less than 2000 Hz.

The presence of sphalerite or gangue can result in ore deposits having weak to moderate conductances. As an example, the three million ton lead-zinc deposit of Restigouche Mining Corporation near Bathurst, Canada, yielded a well-defined grade 2 conductor. The 10 percent by volume of sphalerite occurs as a coating around the fine grained massive

pyrite, thereby inhibiting electrical conduction. Faults, fractures and shear zones may produce anomalies that typically have low conductances (e.g., grades 1 to 3). Conductive rock formations can yield anomalies of any conductance grade. The conductive materials in such rock formations can be salt water, weathered products such as clays, original depositional clays, and carbonaceous material.

For each interpreted electromagnetic anomaly on the geophysical maps, a letter identifier and an interpretive symbol are plotted beside the EM grade symbol. The horizontal rows of dots, under the interpretive symbol, indicate the anomaly amplitude on the flight record. The vertical column of dots, under the anomaly letter, gives the estimated depth. In areas where anomalies are crowded, the letter identifiers, interpretive symbols and dots may be obliterated. The EM grade symbols, however, will always be discernible, and the obliterated information can be obtained from the anomaly listing appended to this report.

The purpose of indicating the anomaly amplitude by dots is to provide an estimate of the reliability of the conductance calculation. Thus, a conductance value obtained from a large ppm anomaly (3 or 4 dots) will tend to be accurate whereas one obtained from a small ppm anomaly (no dots) could be quite inaccurate. The absence of amplitude dots indicates that the anomaly from the coaxial coil-pair is 5 ppm or less on both the in-phase and quadrature channels. Such small anomalies could reflect a weak conductor at the surface or a stronger conductor at depth. The conductance grade and depth estimate illustrates which of these possibilities fits the recorded data best.

The conductance measurement is considered more reliable than the depth estimate. There are a number of factors that can produce an error in the depth estimate, including the averaging of topographic variations by the altimeter, overlying conductive overburden, and the location and attitude of the conductor relative to the flight line. Conductor location and attitude can provide an erroneous depth estimate because the stronger part of the conductor may be deeper or to one side of the flight line, or because it has a shallow dip. A heavy tree cover can also produce errors in depth estimates. This is because the depth estimate is computed as the distance of bird from conductor, minus the altimeter reading. The altimeter can lock onto the top of a dense forest canopy. This situation yields an erroneously large depth estimate but does not affect the conductance estimate.

Dip symbols are used to indicate the direction of dip of conductors. These symbols are used only when the anomaly shapes are unambiguous, which usually requires a fairly resistive environment.

A further interpretation is presented on the EM map by means of the line-to-line correlation of bedrock anomalies, which is based on a comparison of anomaly shapes on adjacent lines. This provides conductor axes that may define the geological structure over portions of the survey area. The absence of conductor axes in an area implies that anomalies could not be correlated from line to line with reasonable confidence.

The electromagnetic anomalies are designed to provide a correct impression of conductor quality by means of the conductance grade symbols. The symbols can stand alone with

geology when planning a follow-up program. The actual conductance values are printed in the attached anomaly list for those who wish quantitative data. The anomaly ppm and depth are indicated by inconspicuous dots which should not distract from the conductor patterns, while being helpful to those who wish this information. The map provides an interpretation of conductors in terms of length, strike and dip, geometric shape, conductance, depth, and thickness. The accuracy is comparable to an interpretation from a high quality ground EM survey having the same line spacing.

The appended EM anomaly list provides a tabulation of anomalies in ppm, conductance, and depth for the vertical sheet model. No conductance or depth estimates are shown for weak anomalous responses that are not of sufficient amplitude to yield reliable calculations.

Since discrete bodies normally are the targets of EM surveys, local base (or zero) levels are used to compute local anomaly amplitudes. This contrasts with the use of true zero levels which are used to compute true EM amplitudes. Local anomaly amplitudes are shown in the EM anomaly list and these are used to compute the vertical sheet parameters of conductance and depth.

## Questionable Anomalies

The EM maps may contain anomalous responses that are displayed as asterisks (*). These responses denote weak anomalies of indeterminate conductance, which may reflect one of the following: a weak conductor near the surface, a strong conductor at depth (e.g., 100 to 120 m below surface) or to one side of the flight line, or aerodynamic noise. Those responses that have the appearance of valid bedrock anomalies on the flight profiles are indicated by appropriate interpretive symbols (see EM legend on maps). The others probably do not warrant further investigation unless their locations are of considerable geological interest.

## The Thickness Parameter

A comparison of coaxial and coplanar shapes can provide an indication of the thickness of a steeply dipping conductor. The amplitude of the coplanar anomaly (e.g., CPI channel) increases relative to the coaxial anomaly (e.g., CXI) as the apparent thickness increases, i.e., the thickness in the horizontal plane. (The thickness is equal to the conductor width if the conductor dips at 90 degrees and strikes at right angles to the flight line.) This report refers to a conductor as thin when the thickness is likely to be less than 3 m, and thick when in excess of 10 m. Thick conductors are indicated on the EM map by parentheses "( )". For base metal exploration in steeply dipping geology, thick conductors can be high priority targets because many massive sulphide ore bodies are thick. The system cannot sense the thickness when the strike of the conductor is subparallel to the flight line, when the conductor has a shallow dip, when the anomaly amplitudes are small, or when the resistivity of the environment is below 100 ohm-m.

## Resistivity Mapping

Resistivity mapping is useful in areas where broad or flat lying conductive units are of interest. One example of this is the clay alteration which is associated with Carlin-type deposits in the south west United States. The resistivity parameter was able to identify the clay alteration zone over the Cove deposit. The alteration zone appeared as a strong resistivity low on the 900 Hz resistivity parameter. The 7,200 Hz and 56,000 Hz resistivities showed more detail in the covering sediments, and delineated a range front fault. This is typical in many areas of the south west United States, where conductive near surface sediments, which may sometimes be alkalic, attenuate the higher frequencies.

Resistivity mapping has proven successful for locating diatremes in diamond exploration. Weathering products from relatively soft kimberlite pipes produce a resistivity contrast with the unaltered host rock. In many cases weathered kimberlite pipes were associated with thick conductive layers that contrasted with overlying or adjacent relatively thin layers of lake bottom sediments or overburden.

Areas of widespread conductivity are commonly encountered during surveys. These conductive zones may reflect alteration zones, shallow-dipping sulphide or graphite-rich units, saline ground water, or conductive overburden. In such areas, EM amplitude changes can be generated by decreases of only 5 m in survey altitude, as well as by increases in conductivity. The typical flight record in conductive areas is characterized by in-phase and quadrature channels that are continuously active. Local EM peaks reflect either increases in conductivity of the earth or decreases in survey altitude. For such conductive areas, apparent resistivity profiles and contour maps are necessary for the correct interpretation of the airborne data. The advantage of the resistivity parameter is that anomalies caused by altitude changes are virtually eliminated, so the resistivity data reflect only those anomalies caused by conductivity changes. The resistivity analysis also helps the interpreter to differentiate between conductive bedrock and conductive overburden. For example, discrete conductors will generally appear as narrow lows on the contour map and broad conductors (e.g., overburden) will appear as wide lows.

The apparent resistivity is calculated using the pseudo-layer (or buried) half-space model defined by Fraser (1978)[1]. This model consists of a resistive layer overlying a conductive half-space. The depth channels give the apparent depth below surface of the conductive material. The apparent depth is simply the apparent thickness of the overlying resistive layer. The apparent depth (or thickness) parameter will be positive when the upper layer is more resistive than the underlying material, in which case the apparent depth may be quite close to the true depth.

---

[1] Resistivity mapping with an airborne multicoil electromagnetic system: Geophysics, v. 43, p.144-172

The apparent depth will be negative when the upper layer is more conductive than the underlying material, and will be zero when a homogeneous half-space exists. The apparent depth parameter must be interpreted cautiously because it will contain any errors that might exist in the measured altitude of the EM bird (e.g., as caused by a dense tree cover). The inputs to the resistivity algorithm are the in-phase and quadrature components of the coplanar coil-pair. The outputs are the apparent resistivity of the conductive half-space (the source) and the sensor-source distance. The flying height is not an input variable, and the output resistivity and sensor-source distance are independent of the flying height when the conductivity of the measured material is sufficient to yield significant in-phase as well as quadrature responses. The apparent depth, discussed above, is simply the sensor-source distance minus the measured altitude or flying height. Consequently, errors in the measured altitude will affect the apparent depth parameter but not the apparent resistivity parameter.

The apparent depth parameter is a useful indicator of simple layering in areas lacking a heavy tree cover. Depth information has been used for permafrost mapping, where positive apparent depths were used as a measure of permafrost thickness. However, little quantitative use has been made of negative apparent depths because the absolute value of the negative depth is not a measure of the thickness of the conductive upper layer and, therefore, is not meaningful physically. Qualitatively, a negative apparent depth estimate usually shows that the EM anomaly is caused by conductive overburden. Consequently, the apparent depth channel can be of significant help in distinguishing between overburden and bedrock conductors.

## Interpretation in Conductive Environments

Environments having low background resistivities (e.g., below 30 ohm-m for a 900 Hz system) yield very large responses from the conductive ground. This usually prohibits the recognition of discrete bedrock conductors. However, Fugro data processing techniques produce three parameters that contribute significantly to the recognition of bedrock conductors in conductive environments. These are the in-phase and quadrature difference channels (DIFI and DIFQ, which are available only on systems with “common” frequencies on orthogonal coil pairs), and the resistivity and depth channels (RES and DEP) for each coplanar frequency.

The EM difference channels (DIFI and DIFQ) eliminate most of the responses from conductive ground, leaving responses from bedrock conductors, cultural features (e.g., telephone lines, fences, etc.) and edge effects. Edge effects often occur near the perimeter of broad conductive zones. This can be a source of geologic noise. While edge effects yield anomalies on the EM difference channels, they do not produce resistivity anomalies. Consequently, the resistivity channel aids in eliminating anomalies due to edge effects. On the other hand, resistivity anomalies will coincide with the most highly conductive sections of conductive ground, and this is another source of geologic noise. The recognition of a bedrock conductor in a conductive environment therefore is based on the anomalous responses of the two difference channels (DIFI and DIFQ) and the

resistivity channels (RES). The most favourable situation is where anomalies coincide on all channels.

The DEP channels, which give the apparent depth to the conductive material, also help to determine whether a conductive response arises from surficial material or from a conductive zone in the bedrock. When these channels ride above the zero level on the depth profiles (i.e., depth is negative), it implies that the EM and resistivity profiles are responding primarily to a conductive upper layer, i.e., conductive overburden. If the DEP channels are below the zero level, it indicates that a resistive upper layer exists, and this usually implies the existence of a bedrock conductor. If the low frequency DEP channel is below the zero level and the high frequency DEP is above, this suggests that a bedrock conductor occurs beneath conductive cover.

## Reduction of Geologic Noise

Geologic noise refers to unwanted geophysical responses. For purposes of airborne EM surveying, geologic noise refers to EM responses caused by conductive overburden and magnetic permeability. It was mentioned previously that the EM difference channels (i.e., channel DIFI for in-phase and DIFQ for quadrature) tend to eliminate the response of conductive overburden.

Magnetite produces a form of geological noise on the in-phase channels. Rocks containing less than 1% magnetite can yield negative in-phase anomalies caused by magnetic permeability. When magnetite is widely distributed throughout a survey area, the in-phase EM channels may continuously rise and fall, reflecting variations in the magnetite percentage, flying height, and overburden thickness. This can lead to difficulties in recognizing deeply buried bedrock conductors, particularly if conductive overburden also exists. However, the response of broadly distributed magnetite generally vanishes on the in-phase difference channel DIFI. This feature can be a significant aid in the recognition of conductors that occur in rocks containing accessory magnetite.

## EM Magnetite Mapping

The information content of HEM data consists of a combination of conductive eddy current responses and magnetic permeability responses. The secondary field resulting from conductive eddy current flow is frequency-dependent and consists of both in-phase and quadrature components, which are positive in sign. On the other hand, the secondary field resulting from magnetic permeability is independent of frequency and consists of only an in-phase component which is negative in sign. When magnetic permeability manifests itself by decreasing the measured amount of positive in-phase, its presence may be difficult to recognize. However, when it manifests itself by yielding a negative in-phase anomaly (e.g., in the absence of eddy current flow), its presence is assured. In this latter case, the negative component can be used to estimate the percent magnetite content.

A magnetite mapping technique, based on the low frequency coplanar data, can be complementary to magnetometer mapping in certain cases. Compared to magnetometry,

it is far less sensitive but is more able to resolve closely spaced magnetite zones, as well as providing an estimate of the amount of magnetite in the rock. The method is sensitive to 1/4% magnetite by weight when the EM sensor is at a height of 30 m above a magnetiitic half-space. It can individually resolve steep dipping narrow magnetite-rich bands that are separated by 60 m. Unlike magnetometry, the EM magnetite method is unaffected by remanent magnetism or magnetic latitude.

The EM magnetite mapping technique provides estimates of magnetite content that are usually correct within a factor of 2 when the magnetite is fairly uniformly distributed. EM magnetite maps can be generated when magnetic permeability is evident as negative in-phase responses on the data profiles.

Like magnetometry, the EM magnetite method maps only bedrock features, provided that the overburden is characterized by a general lack of magnetite. This contrasts with resistivity mapping which portrays the combined effect of bedrock and overburden.

## The Susceptibility Effect

When the host rock is conductive, the positive conductivity response will usually dominate the secondary field, and the susceptibility effect[2] will appear as a reduction in the in-phase, rather than as a negative value. The in-phase response will be lower than would be predicted by a model using zero susceptibility. At higher frequencies the in-phase conductivity response also gets larger, so a negative magnetite effect observed on the low frequency might not be observable on the higher frequencies, over the same body. The susceptibility effect is most obvious over discrete magnetite-rich zones, but also occurs over uniform geology such as a homogeneous half-space.

High magnetic susceptibility will affect the calculated apparent resistivity, if only conductivity is considered. Standard apparent resistivity algorithms use a homogeneous half-space model, with zero susceptibility. For these algorithms, the reduced in-phase response will, in most cases, make the apparent resistivity higher than it should be. It is important to note that there is nothing wrong with the data, nor is there anything wrong with the processing algorithms. The apparent difference results from the fact that the simple geological model used in processing does not match the complex geology.

---

[2] Magnetic susceptibility and permeability are two measures of the same physical property. Permeability is generally given as relative permeability, $\mu_r$, which is the permeability of the substance divided by the permeability of free space ($4 \pi \times 10^{-7}$). Magnetic susceptibility $k$ is related to permeability by $k=\mu^r-1$. Susceptibility is a unitless measurement, and is usually reported in units of $10^{-6}$. The typical range of susceptibilities is –1 for quartz, 130 for pyrite, and up to $5 \times 10^5$ for magnetite, in $10^{-6}$ units (Telford et al, 1986).

## Measuring and Correcting the Magnetite Effect

Theoretically, it is possible to calculate (forward model) the combined effect of electrical conductivity and magnetic susceptibility on an EM response in all environments. The difficulty lies, however, in separating out the susceptibility effect from other geological effects when deriving resistivity and susceptibility from EM data.

Over a homogeneous half-space, there is a precise relationship between in-phase, quadrature, and altitude. These are often resolved as phase angle, amplitude, and altitude. Within a reasonable range, any two of these three parameters can be used to calculate the half space resistivity. If the rock has a positive magnetic susceptibility, the in-phase component will be reduced and this departure can be recognized by comparison to the other parameters.

The algorithm used to calculate apparent susceptibility and apparent resistivity from HEM data, uses a homogeneous half-space geological model. Non half-space geology, such as horizontal layers or dipping sources, can also distort the perfect half-space relationship of the three data parameters. While it may be possible to use more complex models to calculate both rock parameters, this procedure becomes very complex and time-consuming. For basic HEM data processing, it is most practical to stick to the simplest geological model.

Magnetite reversals (reversed in-phase anomalies) have been used for many years to calculate an “FeO” or magnetite response from HEM data (Fraser, 1981). However, this technique could only be applied to data where the in-phase was observed to be negative, which happens when susceptibility is high and conductivity is low.

## Applying Susceptibility Corrections

Resistivity calculations done with susceptibility correction may change the apparent resistivity. High-susceptibility conductors, that were previously masked by the susceptibility effect in standard resistivity algorithms, may become evident. In this case the susceptibility corrected apparent resistivity is a better measure of the actual resistivity of the earth. However, other geological variations, such as a deep resistive layer, can also reduce the in-phase by the same amount. In this case, susceptibility correction would not be the best method. Different geological models can apply in different areas of the same data set. The effects of susceptibility, and other effects that can create a similar response, must be considered when selecting the resistivity algorithm.

## Susceptibility from EM vs Magnetic Field Data

The response of the EM system to magnetite may not match that from a magnetometer survey. First, HEM-derived susceptibility is a rock property measurement, like resistivity. Magnetic data show the total magnetic field, a measure of the potential field, not the

rock property. Secondly, the shape of an anomaly depends on the shape and direction of the source magnetic field. The electromagnetic field of HEM is much different in shape from the earth's magnetic field. Total field magnetic anomalies are different at different magnetic latitudes; HEM susceptibility anomalies have the same shape regardless of their location on the earth.

In far northern latitudes, where the magnetic field is nearly vertical, the total magnetic field measurement over a thin vertical dike is very similar in shape to the anomaly from the HEM-derived susceptibility (a sharp peak over the body). The same vertical dike at the magnetic equator would yield a negative magnetic anomaly, but the HEM susceptibility anomaly would show a positive susceptibility peak.

## Effects of Permeability and Dielectric Permittivity

Resistivity algorithms that assume free-space magnetic permeability and dielectric permittivity, do not yield reliable values in highly magnetic or highly resistive areas. Both magnetic polarization and displacement currents cause a decrease in the in-phase component, often resulting in negative values that yield erroneously high apparent resistivities. The effects of magnetite occur at all frequencies, but are most evident at the lowest frequency. Conversely, the negative effects of dielectric permittivity are most evident at the higher frequencies, in resistive areas.

The table below shows the effects of varying permittivity over a resistive (10,000 ohm-m) half space, at frequencies of 56,000 Hz (DIGHEM$^V$) and 102,000 Hz (RESOLVE).

### Apparent Resistivity Calculations
### Effects of Permittivity on In-phase/Quadrature/Resistivity

| Freq (Hz) | Coil | Sep (m) | Thres (ppm) | Alt (m) | In Phase | Quad Phase | App Res | App Depth (m) | Permittivity |
|---|---|---|---|---|---|---|---|---|---|
| 56,000 | CP | 6.3 | 0.1 | 30 | 7.3 | 35.3 | 10118 | -1.0 | 1 Air |
| 56,000 | CP | 6.3 | 0.1 | 30 | 3.6 | 36.6 | 19838 | -13.2 | 5 Quartz |
| 56,000 | CP | 6.3 | 0.1 | 30 | -1.1 | 38.3 | 81832 | -25.7 | 10 Epidote |
| 56,000 | CP | 6.3 | 0.1 | 30 | -10.4 | 42.3 | 76620 | -25.8 | 20 Granite |
| 56,000 | CP | 6.3 | 0.1 | 30 | -19.7 | 46.9 | 71550 | -26.0 | 30 Diabase |
| 56,000 | CP | 6.3 | 0.1 | 30 | -28.7 | 52.0 | 66787 | -26.1 | 40 Gabbro |
| 102,000 | CP | 7.86 | 0.1 | 30 | 32.5 | 117.2 | 9409 | -0.3 | 1 Air |
| 102,000 | CP | 7.86 | 0.1 | 30 | 11.7 | 127.2 | 25956 | -16.8 | 5 Quartz |
| 102,000 | CP | 7.86 | 0.1 | 30 | -14.0 | 141.6 | 97064 | -26.5 | 10 Epidote |
| 102,000 | CP | 7.86 | 0.1 | 30 | -62.9 | 176.0 | 83995 | -26.8 | 20 Granite |
| 102,000 | CP | 7.86 | 0.1 | 30 | -107.5 | 215.8 | 73320 | -27.0 | 30 Diabase |
| 102,000 | CP | 7.86 | 0.1 | 30 | -147.1 | 259.2 | 64875 | -27.2 | 40 Gabbro |

Methods have been developed (Huang and Fraser, 2000, 2001) to correct apparent resistivities for the effects of permittivity and permeability. The corrected resistivities yield more credible values than if the effects of permittivity and permeability are disregarded.

## Recognition of Culture

Cultural responses include all EM anomalies caused by man-made metallic objects. Such anomalies may be caused by inductive coupling or current gathering. The concern of the interpreter is to recognize when an EM response is due to culture. Points of consideration used by the interpreter, when coaxial and coplanar coil-pairs are operated at a common frequency, are as follows:

1. Channels CXPL and CPPL monitor 60 Hz radiation. An anomaly on these channels shows that the conductor is radiating power. Such an indication is normally a guarantee that the conductor is cultural. However, care must be taken to ensure that the conductor is not a geologic body that strikes across a power line, carrying leakage currents.

2. A flight that crosses a "line" (e.g., fence, telephone line, etc.) yields a centre-peaked coaxial anomaly and an m-shaped coplanar anomaly.[3] When the flight crosses the cultural line at a high angle of intersection, the amplitude ratio of coaxial/coplanar response is 2. Such an EM anomaly can only be caused by a line. The geologic body that yields anomalies most closely resembling a line is the vertically dipping thin dike. Such a body, however, yields an amplitude ratio of 1 rather than 2. Consequently, an m-shaped coplanar anomaly with a CXI/CPI amplitude ratio of 2 is virtually a guarantee that the source is a cultural line.

3. A flight that crosses a sphere or horizontal disk yields centre-peaked coaxial and coplanar anomalies with a CXI/CPI amplitude ratio (i.e., coaxial/coplanar) of 1/8. In the absence of geologic bodies of this geometry, the most likely conductor is a metal roof or small fenced yard.[4] Anomalies of this type are virtually certain to be cultural if they occur in an area of culture.

4. A flight that crosses a horizontal rectangular body or wide ribbon yields an m-shaped coaxial anomaly and a centre-peaked coplanar anomaly. In the absence of geologic bodies of this geometry, the most likely conductor is a large fenced area.[5] Anomalies of this type are virtually certain to be cultural if they occur in an area of culture.

---

[3] See Figure B-1 presented earlier.

[4] It is a characteristic of EM that geometrically similar anomalies are obtained from: (1) a planar conductor, and (2) a wire which forms a loop having dimensions identical to the perimeter of the equivalent planar conductor.

5. EM anomalies that coincide with culture, as seen on the camera film or video display, are usually caused by culture. However, care is taken with such coincidences because a geologic conductor could occur beneath a fence, for example. In this example, the fence would be expected to yield an m-shaped coplanar anomaly as in case #2 above. If, instead, a centre-peaked coplanar anomaly occurred, there would be concern that a thick geologic conductor coincided with the cultural line.

6. The above description of anomaly shapes is valid when the culture is not conductively coupled to the environment. In this case, the anomalies arise from inductive coupling to the EM transmitter. However, when the environment is quite conductive (e.g., less than 100 ohm-m at 900 Hz), the cultural conductor may be conductively coupled to the environment. In this latter case, the anomaly shapes tend to be governed by current gathering. Current gathering can completely distort the anomaly shapes, thereby complicating the identification of cultural anomalies. In such circumstances, the interpreter can only rely on the radiation channels and on the camera film or video records.

# Magnetic Responses

The residual magnetic intensity provides information on the magnetic properties of the earth materials in the survey area. The information can be used to locate magnetic bodies of direct interest for exploration, and for structural and lithological mapping.

The residual magnetic intensity reflects the abundance of magnetic material in the source. Magnetite is the most common magnetic mineral. Other minerals such as ilmenite, pyrrhotite, franklinite, chromite, hematite, arsenopyrite, limonite and pyrite are also magnetic, but to a lesser extent than magnetite on average.

In some geological environments, an EM anomaly with magnetic correlation has a greater likelihood of being produced by sulphides than one which is non-magnetic. However, sulphide ore bodies may be non-magnetic (e.g., the Kidd Creek deposit near Timmins, Canada) as well as magnetic (e.g., the Mattabi deposit near Sturgeon Lake, Canada).

Iron ore deposits will be anomalously magnetic in comparison to surrounding rock due to the concentration of iron minerals such as magnetite, ilmenite and hematite.

Changes in magnetic susceptibility often allow rock units to be differentiated based on the total field magnetic response. Geophysical classifications may differ from geological classifications if various magnetite levels exist within one general geological classification. Geometric considerations of the source such as shape, dip and depth, inclination of the earth's field and remanent magnetization will complicate such an analysis.

In general, mafic lithologies contain more magnetite and are therefore more magnetic than many sediments which tend to be weakly magnetic. Metamorphism and alteration can also increase or decrease the magnetization of a rock unit.

Textural differences on residual magnetic intensity contour, colour or shadow map due to the frequency of activity of the magnetic parameter resulting from inhomogeneities in the distribution of magnetite within the rock, may define certain lithologies. For example, near surface volcanics may display highly complex contour patterns with little line-to-line correlation.

Rock units may be differentiated based on the plan shapes of their residual magnetic intensity responses. Mafic intrusive plugs can appear as isolated "bulls-eye" anomalies. Granitic intrusives appear as sub-circular zones, and may have contrasting rings due to contact metamorphism. Generally, granitic terrain will lack a pronounced strike direction, although granite gneiss may display strike.

Linear north-south units are theoretically not well-definedon residual magnetic intensity maps in equatorial regions due to the low inclination of the earth's magnetic field. However, most stratigraphic units will have variations in composition along strike that will cause the units to appear as a series of alternating magnetic highs and lows.

Faults and shear zones may be characterized by alteration that causes destruction of magnetite (e.g., weathering) that produces a contrast with surrounding rock. Structural breaks may be filled by magnetite-rich, fracture filling material as is the case with diabase dikes, or by non-magnetic felsic material.

Faulting can also be identified by patterns in the residual magnetic intensity contours or colours. Faults and dikes tend to appear as lineaments and often have strike lengths of several kilometres. Offsets in narrow, magnetic, stratigraphic trends also delineate structure. Sharp contrasts in magnetic lithologies may arise due to large displacements along strike-slip or dip-slip faults.

# APPENDIX C

# DATA ARCHIVE DESCRIPTION

# APPENDIX C

# ARCHIVE DESCRIPTION

This archive contains preliminary data archives of the airborne geophysical survey conducted by FUGRO AIRBORNE SURVEYS CORP. over the Wellgreen Property, Yukon on behalf of Coronation Minerals Inc. from May 8, 2008 to ay 10, 2008

Job # 08032

---

******* Disc 1 of 1 *******

| | |
|---|---|
| \README.TXT | - this file |
| GRIDS\ | |
| | Preliminary Grids in Geosoft format with corresponding .GI files |
| CVG.GRD | - Calculated Vertical Gradient of MAG.GRD nT/m |
| DTM.GRD | - Digital Terrain Model |
| MAG.GRD | - ResidualTotal Magnetic Intensity -IGRF plane removed nT |
| RES56K.GRD | - Apparent Resistivity 56400 kHz coplanar |
| RES900.GRD | - Apparent Resistivity 875 Hz coplanar |
| RES7200.GRD | - Apparent Resistivity 7153 Hz coplanar |
| LINEDATA\ | |
| ARC.XYZ | - Geosoft ASCII Format final profile archive |
| AN08032.XYZ | - Geosoft ASCII Format EM anomaly archive |
| AN08032.TXT | - EM anomaly archive description for AN08032.XYZ |
| PDF\ | |
| | PDF files of final map products |
| PLAEM.GRD | - Interpretation and EM Anomaly map |
| PLCVG.GRD | - Calculated Vertical Gradient |
| PLDTM.GRD | - Digital Terrain Model |
| PLMAG.GRD | - Residual Magnetic Intensity |
| PLRES56K.GRD | - Apparent Resistivity 56400 kHz coplanar |
| PLRES7200.GRD | - Apparent Resistivity 7153 Hz coplanar REPORT\ |
| REPORT\ | |
| REP08032.PDF | -Interpretation and Logistics report |

The ARC.XYZ file contains the following data channels:

| | |
|---|---|
| 1 – X | UTM EASTING NAD 83 ZONE 7N (METRES) |
| 2 – Y | UTM NORTHING NAD 83 ZONE 7N (METRES) |
| 3 – FID | FIDUCIAL |
| 4 – LATITUDE | LATITUDE WGS84 (degrees) |
| 5 – LONGITUDE | LONGITUDE WGS84 (degrees) |
| 6 – FLIGHT | FLIGHT NUMBER |
| 7 – DATE | FLIGHT DATE (yyyy/mm/dd) |
| 8 - ALTRAD_BIRD | BIRD HEIGHT FROM RADAR ALTIMETER (m) |
| 9 - ALTRAD_HELI | HELICOPTER HEIGHT FROM RADAR ALTIMETER (m) |
| 10 - Z | HEIGHT OF HELI ABOVE WGS84 SPHEROID (METRES) |
| 11 – DTM | DIGITAL TERRAIN MODEL Z-ALTRAD_HELI (METRES) |
| 12 – MAGSP | DESPIKED TOTAL MAGNETIC INTENSITY (nT) |
| 13 - MAG_LAG | DESPIKED LAGGED TOTAL MAGNETIC INTENSITY (nT) |
| 14 - DIURNAL_FILT | DIURNAL MAGNETIC VARIATION (nT) |
| 15 - DIURNAL_COR | BASE REMOVED DIURNAL MAGNETIC VARIATION (nT) |
| 16 – MAGLD | LAGGED DIURNAL CORRECTED TOTAL MAGNETIC INTENSITY (nT) |
| 17 – IGRF | INTERNATIONAL GEOMAGNETIC REFERENCE FIELD (nT) |
| 18 - MAG | LEVELED RESIDUAL MAGNETIC INTENSITY (nT) |
| 19 - CPI900_R | UNLEVELED COPLANAR INPHASE 875 Hz (PPM) |
| 20 - CPQ900_R | UNLEVELED COPLANAR QUADRATURE 875 Hz (PPM) |
| 21 - CXI1000_R | UNLEVELED COAXIAL INPHASE 1125 Hz (PPM) |
| 22 - CXQ1000_R | UNLEVELED COAXIAL QUADRATURE 1125 Hz (PPM) |
| 23 - CXI5500_R | UNLEVELED COAXIAL INPHASE 5454 Hz (PPM) |
| 24 - CXQ5500_R | UNLEVELED COAXIAL QUADRATURE 5454 Hz (PPM) |
| 25 - CPI7200_R | UNLEVELED COPLANAR INPHASE 7153 Hz (PPM) |
| 26 - CPQ7200_R | UNLEVELED COPLANAR QUADRATURE 7153 Hz (PPM) |
| 27 - CPI56K_R | UNLEVELED COPLANAR INPHASE 56400 Hz (PPM) |
| 28 - CPQ56K_R | UNLEVELED COPLANAR QUADRATURE 56400 Hz (PPM) |
| 29 - CPI900 | LEVELED COPLANAR INPHASE 875 Hz (PPM) |
| 30 - CPQ900 | LEVELED COPLANAR QUADRATURE 875 Hz (PPM) |
| 31 - CXI1000 | LEVELED COAXIAL INPHASE 1125 Hz (PPM) |
| 32 - CXQ1000 | LEVELED COAXIAL QUADRATURE 1125 Hz (PPM) |
| 33 - CXI5500 | LEVELED COAXIAL INPHASE 5454 Hz (PPM) |
| 34 - CXQ5500 | LEVELED COAXIAL QUADRATURE 5454 Hz (PPM) |
| 35 - CPI7200 | LEVELED COPLANAR INPHASE 7153 Hz (PPM) |
| 36 - CPQ7200 | LEVELED COPLANAR QUADRATURE 7153 Hz (PPM) |
| 37 - CPI56K | LEVELED COPLANAR INPHASE 56400 Hz (PPM) |
| 38 - CPQ56K | LEVELED COPLANAR QUADRATURE 56400 Hz (PPM) |
| 39 - RES900 | APPARENT RESISTIVITY 875 Hz COPLANAR (OHM*M) |
| 40 - RES7200 | APPARENT RESISTIVITY 7153 Hz COPLANAR (OHM*M) |
| 41 - RES56K | APPARENT RESISTIVITY 56400 Hz COPLANAR (OHM*M) |
| 42 - DEP900 | APPARENT DEPTH 878 Hz COPLANAR (M) |
| 43 - DEP7200 | APPARENT DEPTH 7153 Hz COPLANAR (M) |
| 44 - DEP56K | APPARENT DEPTH 56400 Hz COPLANAR (M) |
| 45 – CPPL | COPLANAR POWERLINE MONITOR |
| 46 – CXSP | COAXIAL SPHERICS MONITOR |

---

All EM data in the archive is presented in the standard normalization convention for the coplanar coils. The ratio of coplanar to coaxial amplitudes for the same frequency is 4:1 over a layered earth.

Resistivity is calculated using a proprietary pseudo-layer half-space algorithm.

---

The coordinate system for all grids and XYZ files is projected as follows

| | | |
|---|---|---|
| Datum | NAD 83 | |
| Spheroid | GRS80 | |
| Projection | UTM | |
| Central meridian | 141 West | |
| False easting | 500000 | |
| False northing | 0 | |
| Scale factor | 0.9996 | |
| Northern parallel | N/A | |
| Base parallel | N/A | |
| WGS84 to local conversion method | | Molodensky |
| Delta X shift | +0 | |
| Delta Y shift | +0 | |
| Delta Z shift | +0 | |

# APPENDIX D

# DATA PROCESSING FLOWCHARTS

# APPENDIX D

## Processing Flow Chart - Electromagnetic Data

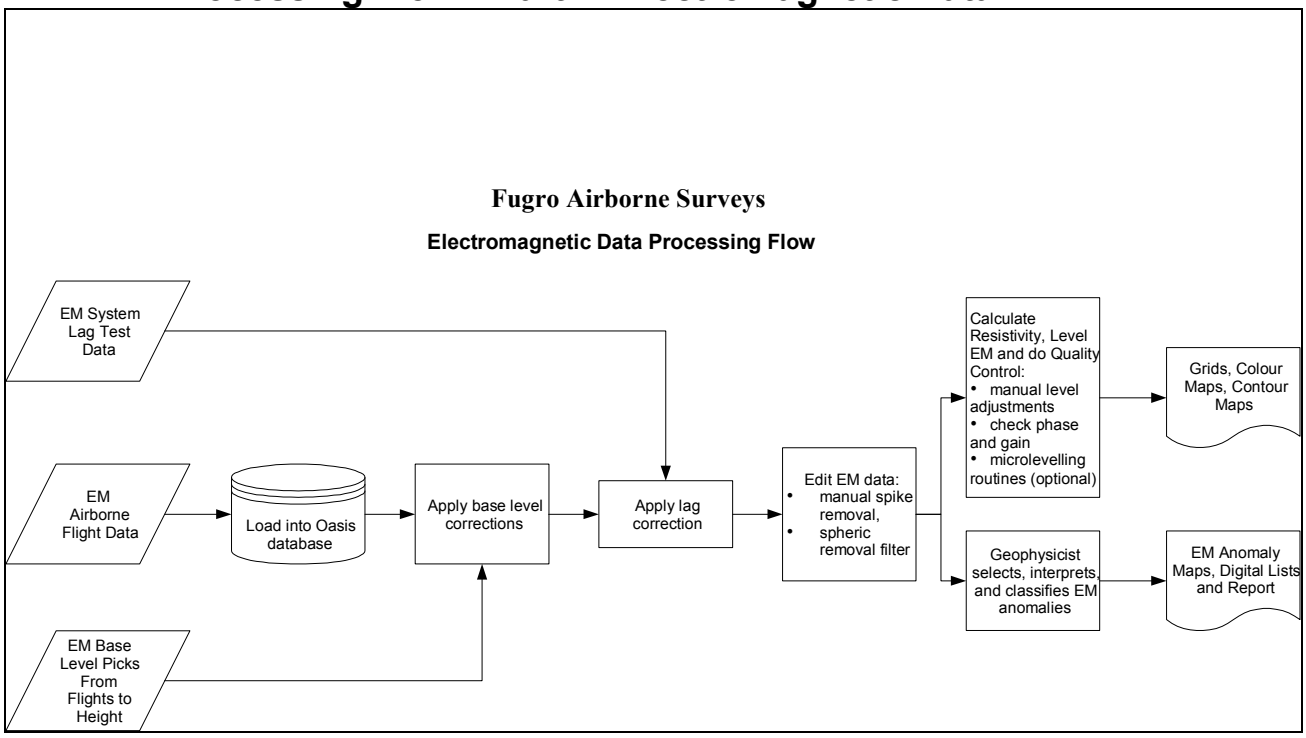


## Processing Flow Chart - Magnetic Data

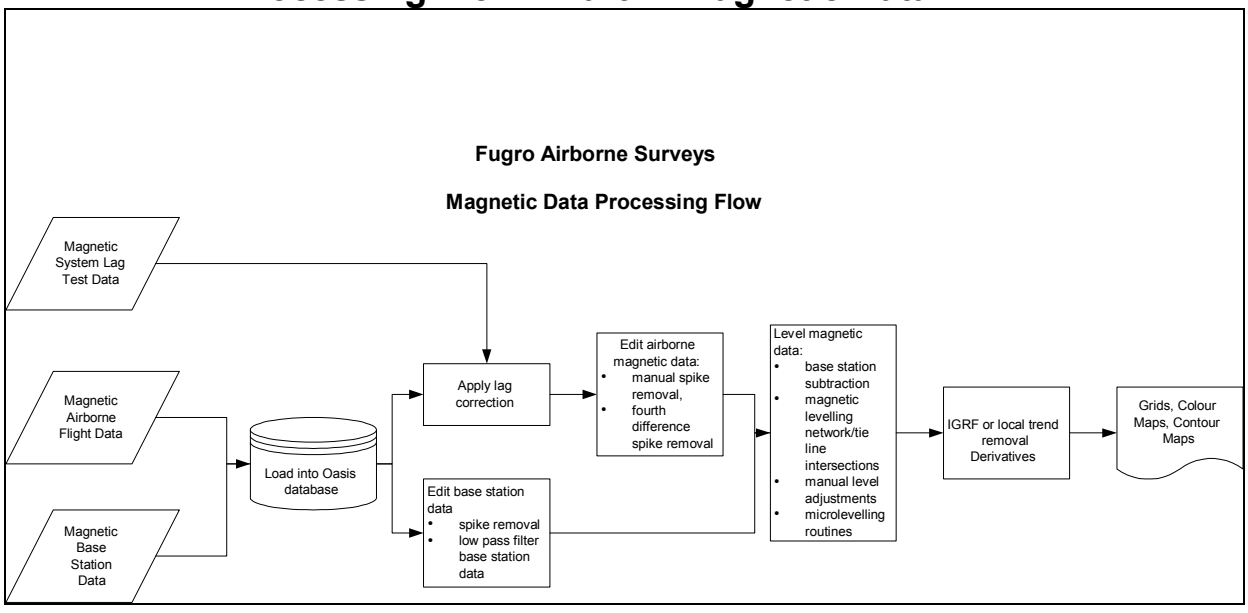

# APPENDIX E

# GLOSSARY

# APPENDIX E

# GLOSSARY OF AIRBORNE GEOPHYSICAL TERMS

Note: The definitions given in this glossary refer to the common terminology as used in airborne geophysics.

**altitude attenuation**: the absorption of gamma rays by the atmosphere between the earth and the detector. The number of gamma rays detected by a system decreases as the altitude increases.

**apparent- :** the ***physical parameters*** of the earth measured by a geophysical system are normally expressed as apparent, as in "apparent ***resistivity***". This means that the measurement is limited by assumptions made about the geology in calculating the response measured by the geophysical system. Apparent resistivity calculated with ***HEM***, for example, generally assumes that the earth is a ***homogeneous half-space*** – not layered.

**amplitude**: The strength of the total electromagnetic field. In ***frequency domain*** it is most often the sum of the squares of ***in-phase*** and ***quadrature*** components. In multi-component electromagnetic surveys it is generally the sum of the squares of all three directional components.

**analytic signal**: The total amplitude of all the directions of magnetic ***gradient***. Calculated as the sum of the squares.

**anisotropy**: Having different ***physical parameters*** in different directions. This can be caused by layering or fabric in the geology. Note that a unit can be anisotropic, but still **homogeneous**.

**anomaly**: A localized change in the geophysical data characteristic of a discrete source, such as a conductive or magnetic body: something locally different from the **background**.

**B-field**: In time-domain **electromagnetic** surveys, the magnetic field component of the (electromagnetic) **field**. This can be measured directly, although more commonly it is calculated by integrating the time rate of change of the magnetic field **dB/dt**, as measured with a receiver coil.

**background**: The "normal" response in the geophysical data – that response observed over most of the survey area. **Anomalies** are usually measured relative to the background. In airborne gamma-ray spectrometric surveys the term defines the **cosmic**, radon, and aircraft responses in the absence of a signal from the ground.

**base-level**: The measured values in a geophysical system in the absence of any outside signal. All geophysical data are measured relative to the system base level.

**base frequency**: The frequency of the pulse repetition for a ***time-domain electromagnetic*** system. Measured between subsequent positive pulses.

**bird**: A common name for the pod towed beneath or behind an aircraft, carrying the geophysical sensor array.

**bucking**: The process of removing the strong ***signal*** from the ***primary field*** at the ***receiver*** from the data, to measure the ***secondary field***. It can be done electronically or mathematically. This is done in ***frequency-domain EM***, and to measure ***on-time*** in ***time-domain EM***.

**calibration coil**: A wire coil of known size and dipole moment, which is used to generate a field of known ***amplitude*** and ***phase*** in the receiver, for system calibration. Calibration coils can be external, or internal to the system. Internal coils may be called Q-coils.

**coaxial coils**: **[CX]** Coaxial coils in an HEM system are in the vertical plane, with their axes horizontal and collinear in the flight direction. These are most sensitive to vertical conductive objects in the ground, such as thin, steeply dipping conductors perpendicular to the flight direction. Coaxial coils generally give the sharpest anomalies over localized conductors. (See also ***coplanar coils***)

**coil**: A multi-turn wire loop used to transmit or detect electromagnetic fields. Time varying ***electromagnetic*** fields through a coil induce a voltage proportional to the strength of the field and the rate of change over time.

**compensation**: Correction of airborne geophysical data for the changing effect of the aircraft. This process is generally used to correct data in ***fixed-wing time-domain electromagnetic*** surveys (where the transmitter is on the aircraft and the receiver is moving), and magnetic surveys (where the sensor is on the aircraft, turning in the earth's magnetic field.

**component**: In ***frequency domain electromagnetic*** surveys this is one of the two **phase** measurements – ***in-phase or quadrature***. In "multi-component" electromagnetic surveys it is also used to define the measurement in one geometric direction (vertical, horizontal in-line and horizontal transverse – the Z, X and Y components).

**Compton scattering**: gamma ray photons will bounce off electrons as they pass through the earth and atmosphere, reducing their energy and then being detected by ***radiometric*** sensors at lower energy levels. See also ***stripping***.

**conductance**: See ***conductivity thickness***

**conductivity**: [σ] The facility with which the earth or a geological formation conducts electricity. Conductivity is usually measured in milli-Siemens per metre (mS/m). It is the reciprocal of ***resistivity***.

**conductivity-depth imaging**: see ***conductivity-depth transform***.

**conductivity-depth transform**: A process for converting electromagnetic measurements to an approximation of the conductivity distribution vertically in the earth, assuming a ***layered earth***. (Macnae and Lamontagne, 1987; Wolfgram and Karlik, 1995)

**conductivity thickness**: [σ**t**] The product of the ***conductivity***, and thickness of a large, tabular body. (It is also called the "conductivity-thickness product") In electromagnetic geophysics, the response of a thin plate-like conductor is proportional to the conductivity multiplied by thickness. For example a 10 metre thickness of 20 Siemens/m mineralization will be equivalent to 5 metres of 40 S/m; both have 200 S conductivity thickness. Sometimes referred to as conductance.

**conductor**: Used to describe anything in the ground more conductive than the surrounding geology. Conductors are most often clays or graphite, or hopefully some type of mineralization, but may also be man-made objects, such as fences or pipelines.

**coplanar coils**: **[CP]** In HEM, the coplanar coils lie in the horizontal plane with their axes vertical, and parallel. These coils are most sensitive to massive conductive bodies, horizontal layers, and the ***halfspace***.

**cosmic ray**: High energy sub-atomic particles from outer space that collide with the earth's atmosphere to produce a shower of gamma rays (and other particles) at high energies.

**counts (per second)**: The number of ***gamma-rays*** detected by a gamma-ray ***spectrometer.*** The rate depends on the geology, but also on the size and sensitivity of the detector.

**culture**: A term commonly used to denote any man-made object that creates a geophysical anomaly. Includes, but not limited to, power lines, pipelines, fences, and buildings.

**current channelling**: See current gathering.

**current gathering**: The tendency of electrical currents in the ground to channel into a conductive formation. This is particularly noticeable at higher frequencies or early time channels when the formation is long and parallel to the direction of current flow. This tends to enhance anomalies relative to inductive currents (see also ***induction***). Also known as current channelling.

**daughter products**: The radioactive natural sources of gamma-rays decay from the original "parent" element (commonly potassium, uranium, and thorium) to one or more lower-energy "daughter" elements. Some of these lower energy elements are also radioactive and decay further. ***Gamma-ray spectrometry*** surveys may measure the gamma rays given off by the original element or by the decay of the daughter products.

**dB/dt**: As the ***secondary electromagnetic field*** changes with time, the magnetic field [**B**] component induces a voltage in the receiving ***coil***, which is proportional to the rate of change of the magnetic field over time.

**decay**: In ***time-domain electromagnetic*** theory, the weakening over time of the ***eddy currents*** in the ground, and hence the ***secondary field*** after the ***primary field*** electromagnetic pulse is turned off. In ***gamma-ray spectrometry***, the radioactive breakdown of an element, generally potassium, uranium, thorium, or one of their ***daughter*** products.

**decay constant**: see time constant.

**decay series**: In ***gamma-ray spectrometry***, a series of progressively lower energy ***daughter products*** produced by the radioactive breakdown of uranium or thorium.

**depth of exploration**: The maximum depth at which the geophysical system can detect the target. The depth of exploration depends very strongly on the type and size of the target, the contrast of the target with the surrounding geology, the homogeneity of the surrounding geology, and the type of geophysical system. One measure of the maximum depth of exploration for an electromagnetic system is the depth at which it can detect the strongest conductive target – generally a highly conductive horizontal layer.

**differential resistivity**: A process of transforming ***apparent resistivity*** to an approximation of layer resistivity at each depth. The method uses multi-frequency HEM data and approximates the effect of shallow layer ***conductance*** determined from higher frequencies to estimate the deeper conductivities (Huang and Fraser, 1996)

**dipole moment**: [NIA] For a transmitter, the product of the area of a ***coil***, the number of turns of wire, and the current flowing in the coil. At a distance significantly larger than the size of the coil, the magnetic field from a coil will be the same if the dipole moment product is the same. For a receiver coil, this is the product of the area and the number of turns. The sensitivity to a magnetic field (assuming the source is far away) will be the same if the dipole moment is the same.

**diurnal**: The daily variation in a natural field, normally used to describe the natural fluctuations (over hours and days) of the earth's magnetic field.

**dielectric permittivity**: **[$\varepsilon$]** The capacity of a material to store electrical charge, this is most often measured as the relative permittivity [$\varepsilon_r$], or ratio of the material dielectric to that of free space. The effect of high permittivity may be seen in HEM data at high

frequencies over highly resistive geology as a reduced or negative ***in-phase***, and higher ***quadrature*** data.

**drape**: To fly a survey following the terrain contours, maintaining a constant altitude above the local ground surface. Also applied to re-processing data collected at varying altitudes above ground to simulate a survey flown at constant altitude.

**drift**: Long-time variations in the base-level or calibration of an instrument.

**eddy currents**: The electrical currents induced in the ground, or other conductors, by a time-varying ***electromagnetic field*** (usually the ***primary field***). Eddy currents are also induced in the aircraft's metal frame and skin; a source of ***noise*** in EM surveys.

**electromagnetic**: **[EM]** Comprised of a time-varying electrical and magnetic field. Radio waves are common electromagnetic fields. In geophysics, an electromagnetic system is one which transmits a time-varying ***primary field*** to induce ***eddy currents*** in the ground, and then measures the ***secondary field*** emitted by those eddy currents.

**energy window**: A broad spectrum of ***gamma-ray*** energies measured by a spectrometric survey. The energy of each gamma-ray is measured and divided up into numerous discrete energy levels, called windows.

**equivalent** (thorium or uranium): The amount of radioelement calculated to be present, based on the gamma-rays measured from a **daughter** element. This assumes that the ***decay series*** is in equilibrium – progressing normally.

**exposure rate**: in radiometric surveys, a calculation of the total exposure rate due to gamma rays at the ground surface. It is used as a measurement of the concentration of all the **radioelements** at the surface. See also: **natural exposure rate**.

**fiducial, or fid**: Timing mark on a survey record. Originally these were timing marks on a profile or film; now the term is generally used to describe 1-second interval timing records in digital data, and on maps or profiles.

**Figure of Merit**: **(FOM)** A sum of the 12 distinct magnetic noise variations measured by each of four flight directions, and executing three aircraft attitude variations (yaw, pitch, and roll) for each direction. The flight directions are generally parallel and perpendicular to planned survey flight directions. The FOM is used as a measure of the **manoeuvre noise** before and after **compensation.**

**fixed-wing**: Aircraft with wings, as opposed to "rotary wing" helicopters.

**footprint**: This is a measure of the area of sensitivity under the aircraft of an airborne geophysical system. The footprint of an ***electromagnetic*** system is dependent on the altitude of the system, the orientation of the transmitter and receiver and the separation between the receiver and transmitter, and the conductivity of the ground. The footprint

of a ***gamma-ray spectrometer*** depends mostly on the altitude. For all geophysical systems, the footprint also depends on the strength of the contrasting ***anomaly***.

**frequency domain**: An ***electromagnetic*** system which transmits a ***primary field*** that oscillates smoothly over time (sinusoidal), inducing a similarly varying electrical current in the ground. These systems generally measure the changes in the ***amplitude*** and ***phase*** of the ***secondary field*** from the ground at different frequencies by measuring the **in-phase** and **quadrature** phase components. See also ***time-domain***.

**full-stream data**: Data collected and recorded continuously at the highest possible sampling rate. Normal data are stacked (see ***stacking***) over some time interval before recording.

**gamma-ray**: A very high-energy photon, emitted from the nucleus of an atom as it undergoes a change in energy levels.

**gamma-ray spectrometry**: Measurement of the number and energy of natural (and sometimes man-made) gamma-rays across a range of photon energies.

**gradient**: In magnetic surveys, the gradient is the change of the magnetic field over a distance, either vertically or horizontally in either of two directions. Gradient data is often measured, or calculated from the total magnetic field data because it changes more quickly over distance than the ***total magnetic field***, and so may provide a more precise measure of the location of a source. See also ***analytic signal***.

***ground effect***: The response from the earth. A common calibration procedure in many geophysical surveys is to fly to altitude high enough to be beyond any measurable response from the ground, and there establish ***base levels*** or ***backgrounds***.

**half-space**: A mathematical model used to describe the earth – as infinite in width, length, and depth below the surface. The most common halfspace models are ***homogeneous*** and ***layered earth***.

**heading error**: A slight change in the magnetic field measured when flying in opposite directions.

**HEM**: Helicopter ElectroMagnetic, This designation is most commonly used for helicopter-borne, ***frequency-domain*** electromagnetic systems. At present, the transmitter and receivers are normally mounted in a ***bird*** carried on a sling line beneath the helicopter.

**herringbone pattern**: A pattern created in geophysical data by an asymmetric system, where the **anomaly** may be extended to either side of the source, in the direction of flight. Appears like fish bones, or like the teeth of a comb, extending either side of centre, each tooth an alternate flight line.

**homogeneous**: This is a geological unit that has the same ***physical parameters*** throughout its volume. This unit will create the same response to an HEM system anywhere, and the HEM system will measure the same apparent ***resistivity*** anywhere. The response may change with system direction (see ***anisotropy***).

**HTEM**: Helicopter Time-domain ElectroMagnetic, This designation is used for the new generation of helicopter-borne, ***time-domain*** electromagnetic systems.

**in-phase**: the component of the measured ***secondary field*** that has the same phase as the transmitter and the ***primary field***. The in-phase component is stronger than the ***quadrature*** phase over relatively higher ***conductivity***.

**induction**: Any time-varying electromagnetic field will induce (cause) electrical currents to flow in any object with non-zero ***conductivity***. (see ***eddy currents***)

**induction number:** also called the "response parameter", this number combines many of the most significant parameters affecting the ***EM*** response into one parameter against which to compare responses. For a ***layered earth*** the response parameter is $\mu\omega\sigma h^2$ and for a large, flat, ***conductor*** it is $\mu\omega\sigma th$, where $\mu$ is the ***magnetic permeability***, $\omega$ is the angular ***frequency***, $\sigma$ is the **conductivity**, t is the thickness (for the flat conductor) and h is the height of the system above the conductor.

**inductive limit**: When the frequency of an EM system is very high, or the **conductivity** of the target is very high, the response measured will be entirely **in-phase** with no **quadrature** (**phase** angle =0). The in-phase response will remain constant with further increase in conductivity or frequency. The system can no longer detect changes in conductivity of the target.

**infinite**: In geophysical terms, an "infinite' dimension is one much greater than the ***footprint*** of the system, so that the system does not detect changes at the edges of the object.

**International Geomagnetic Reference Field**: **[IGRF]** An approximation of the smooth magnetic field of the earth, in the absence of variations due to local geology. Once the IGRF is subtracted from the measured magnetic total field data, any remaining variations are assumed to be due to local geology. The IGRF also predicts the slow changes of the field up to five years in the future.

**inversion**, or **inverse modeling**: A process of converting geophysical data to an earth model, which compares theoretical models of the response of the earth to the data measured, and refines the model until the response closely fits the measured data (Huang and Palacky, 1991)

**layered earth**: A common geophysical model which assumes that the earth is horizontally layered – the ***physical parameters*** are constant to ***infinite*** distance horizontally, but change vertically.

**magnetic permeability**: **[μ]** This is defined as the ratio of magnetic induction to the inducing magnetic field. The relative magnetic permeability [$\mu_r$] is often quoted, which is the ratio of the rock permeability to the permeability of free space. In geology and geophysics, the ***magnetic susceptibility*** is more commonly used to describe rocks.

**magnetic susceptibility**: **[k]** A measure of the degree to which a body is magnetized. In SI units this is related to relative ***magnetic permeability*** by $k=\mu_r-1$, and is a dimensionless unit. For most geological material, susceptibility is influenced primarily by the percentage of magnetite. It is most often quoted in units of $10^{-6}$. In HEM data this is most often apparent as a negative ***in-phase*** component over high susceptibility, high ***resistivity*** geology such as diabase dikes.

**manoeuvre noise:** variations in the magnetic field measured caused by changes in the relative positions of the magnetic sensor and magnetic objects or electrical currents in the aircraft. This type of noise is generally corrected by magnetic **compensation**.

**model**: Geophysical theory and applications generally have to assume that the geology of the earth has a form that can be easily defined mathematically, called the model. For example steeply dipping **conductor**s are generally modeled as being **infinite** in horizontal and depth extent, and very thin. The earth is generally modeled as horizontally layered, each layer infinite in extent and uniform in characteristic. These models make the mathematics to describe the response of the (normally very complex) earth practical. As theory advances, and computers become more powerful, the useful models can become more complex.

**natural exposure rate**: in radiometric surveys, a calculation of the total exposure rate due to natural-source gamma rays at the ground surface. It is used as a measurement of the concentration of all the natural **radioelements** at the surface. See also: **exposure rate**.

**noise**: That part of a geophysical measurement that the user does not want. Typically this includes electronic interference from the system, the atmosphere (***sferics***), and man-made sources. This can be a subjective judgment, as it may include the response from geology other than the target of interest. Commonly the term is used to refer to high frequency (short period) interference. See also ***drift***.

**Occam's inversion**: an ***inversion*** process that matches the measured ***electromagnetic*** data to a theoretical model of many, thin layers with constant thickness and varying resistivity (Constable et al, 1987).

**off-time**: In a ***time-domain electromagnetic*** survey, the time after the end of the ***primary field pulse***, and before the start of the next pulse.

**on-time**: In a ***time-domain electromagnetic*** survey, the time during the ***primary field pulse***.

**overburden**: In engineering and mineral exploration terms, this most often means the soil on top of the unweathered bedrock. It may be sand, glacial till, or weathered rock.

**Phase, phase angle**: The angular difference in time between a measured sinusoidal electromagnetic field and a reference – normally the primary field. The phase is calculated from $\tan^{-1}$(***in-phase / quadrature***).

**physical parameters**: These are the characteristics of a geological unit. For electromagnetic surveys, the important parameters are ***conductivity***, ***magnetic permeability*** (or ***susceptibility***) and ***dielectric permittivity***; for magnetic surveys the parameter is magnetic susceptibility, and for gamma ray spectrometric surveys it is the concentration of the major radioactive elements: potassium, uranium, and thorium.

**permittivity**: see ***dielectric permittivity***.

**permeability**: see ***magnetic permeability***.

**primary field**: the EM field emitted by a transmitter. This field induces ***eddy currents*** in (energizes) the conductors in the ground, which then create their own ***secondary fields***.

**pulse**: In time-domain EM surveys, the short period of intense ***primary*** field transmission. Most measurements (the ***off-time***) are measured after the pulse. **On-time** measurements may be made during the pulse.

**quadrature**: that component of the measured ***secondary field*** that is phase-shifted 90° from the ***primary field***. The quadrature component tends to be stronger than the ***in-phase*** over relatively weaker ***conductivity***.

**Q-coils**: see ***calibration coil***.

**radioelements**: This normally refers to the common, naturally-occurring radioactive elements: potassium (K), uranium (U), and thorium (Th). It can also refer to man-made radioelements, most often cobalt (Co) and cesium (Cs)

**radiometric**: Commonly used to refer to ***gamma ray*** spectrometry.

**radon**: A radioactive daughter product of uranium and thorium, radon is a gas which can leak into the atmosphere, adding to the non-geological background of a gamma-ray spectrometric survey.

**receiver**: the ***signal*** detector of a geophysical system. This term is most often used in active geophysical systems – systems that transmit some kind of signal. In airborne ***electromagnetic*** surveys it is most often a ***coil***. (see also, ***transmitter***)

**resistivity**: **[ρ]** The strength with which the earth or a geological formation resists the flow of electricity, typically the flow induced by the ***primary field*** of the electromagnetic transmitter. Normally expressed in ohm-metres, it is the reciprocal of ***conductivity***.

**resistivity-depth transforms**: similar to ***conductivity depth transforms***, but the calculated ***conductivity*** has been converted to ***resistivity***.

**resistivity section**: an approximate vertical section of the resistivity of the layers in the earth. The resistivities can be derived from the ***apparent resistivity***, the ***differential resistivities***, ***resistivity-depth transforms***, or ***inversions***.

**Response parameter**: another name for the **induction number**.

**secondary field**: The field created by conductors in the ground, as a result of electrical currents induced by the ***primary field*** from the ***electromagnetic*** transmitter. Airborne ***electromagnetic*** systems are designed to create and measure a secondary field.

**Sengpiel section**: a ***resistivity section*** derived using the ***apparent resistivity*** and an approximation of the depth of maximum sensitivity for each frequency.

**sferic**: Lightning, or the ***electromagnetic*** signal from lightning, it is an abbreviation of "atmospheric discharge". These appear to magnetic and electromagnetic sensors as sharp "spikes" in the data. Under some conditions lightning storms can be detected from hundreds of kilometres away. (see ***noise***)

**signal**: That component of a measurement that the user wants to see – the response from the targets, from the earth, etc. (See also ***noise***)

**skin depth**: A measure of the depth of penetration of an electromagnetic field into a material. It is defined as the depth at which the primary field decreases to 1/e of the field at the surface. It is calculated by approximately 503 x √(resistivity/frequency ). Note that depth of penetration is greater at higher ***resistivity*** and/or lower ***frequency***.

**spectrometry**: Measurement across a range of energies, where ***amplitude*** and energy are defined for each measurement. In gamma-ray spectrometry, the number of gamma rays are measured for each energy ***window***, to define the ***spectrum***.

**spectrum**: In ***gamma ray spectrometry***, the continuous range of energy over which gamma rays are measured. In ***time-domain electromagnetic*** surveys, the spectrum is the energy of the **pulse** distributed across an equivalent, continuous range of frequencies.

**spheric**: see ***sferic***.

**stacking**: Summing repeat measurements over time to enhance the repeating ***signal***, and minimize the random ***noise***.

**stripping**: Estimation and correction for the gamma ray photons of higher and lower energy that are observed in a particular ***energy window***. See also ***Compton scattering***.

**susceptibility**: See ***magnetic susceptibility***.

**tau**: [$\tau$] Often used as a name for the ***time constant***.

**TDEM**: ***time domain electromagnetic***.

**thin sheet**: A standard model for electromagnetic geophysical theory. It is usually defined as a thin, flat-lying conductive sheet, ***infinite*** in both horizontal directions. (see also ***vertical plate***)

**tie-line**: A survey line flown across most of the ***traverse lines***, generally perpendicular to them, to assist in measuring ***drift*** and ***diurnal*** variation. In the short time required to fly a tie-line it is assumed that the drift and/or diurnal will be minimal, or at least changing at a constant rate.

**time constant**: The time required for an ***electromagnetic*** field to decay to a value of 1/e of the original value. In ***time-domain*** electromagnetic data, the time constant is proportional to the size and ***conductance*** of a tabular conductive body. Also called the decay constant.

**Time channel**: In ***time-domain electromagnetic*** surveys the decaying ***secondary field*** is measured over a period of time, and the divided up into a series of consecutive discrete measurements over that time.

**time-domain**: ***Electromagnetic*** system which transmits a pulsed, or stepped ***electromagnetic*** field. These systems induce an electrical current (***eddy current***) in the ground that persists after the ***primary field*** is turned off, and measure the change over time of the ***secondary field*** created as the currents ***decay***. See also ***frequency-domain***.

**total energy envelope**: The sum of the squares of the three ***components*** of the ***time-domain electromagnetic secondary field***. Equivalent to the ***amplitude*** of the secondary field.

**transient**: Time-varying. Usually used to describe a very short period pulse of ***electromagnetic*** field.

***transmitter***: The source of the ***signa***l to be measured in a geophysical survey. In airborne ***EM*** it is most often a **coil** carrying a time-varying electrical current, transmitting the ***primary field***. (see also ***receiver***)

**traverse line**: A normal geophysical survey line. Normally parallel traverse lines are flown across the property in spacing of 50 m to 500 m, and generally perpendicular to the target geology.

**vertical plate**: A standard model for electromagnetic geophysical theory. It is usually defined as thin conductive sheet, ***infinite*** in horizontal dimension and depth extent. (see also ***thin shee***t)

**waveform**: The shape of the ***electromagnetic pulse*** from a ***time-domain*** electromagnetic transmitter.

**window**: A discrete portion of a ***gamma-ray spectrum*** or ***time-domain electromagnetic decay***. The continuous energy spectrum or ***full-stream*** data are grouped into windows to reduce the number of samples, and reduce ***noise***.

Version 1.5, November 29, 2005
Greg Hodges,
Chief Geophysicist
Fugro Airborne Surveys, Toronto

**Common Symbols and Acronyms**

**k** Magnetic susceptibility
$\varepsilon$ Dielectric permittivity
$\mu$, $\mu_r$ Magnetic permeability, relative permeability
$\rho$, $\rho_a$ Resistivity, apparent resistivity
$\sigma$,$\sigma_a$ Conductivity, apparent conductivity
$\sigma$**t** Conductivity thickness
$\tau$ Tau, or time constant
$\Omega$**m** ohm-metres, units of resistivity
**AGS** Airborne gamma ray spectrometry.
**CDT** Conductivity-depth transform, conductivity-depth imaging (Macnae and Lamontagne, 1987; Wolfgram and Karlik, 1995)
**CPI, CPQ** Coplanar in-phase, quadrature
**CPS** Counts per second
**CTP** Conductivity thickness product
**CXI, CXQ** Coaxial, in-phase, quadrature
**FOM** Figure of Merit
**fT** femtoteslas, normal unit for measurement of B-Field
**EM** Electromagnetic
**keV** kilo electron volts – a measure of gamma-ray energy
**MeV** mega electron volts – a measure of gamma-ray energy 1MeV = 1000keV
**NIA** dipole moment: turns x current x Area
**nT** nanotesla, a measure of the strength of a magnetic field
nG/h nanoGreys/hour – gamma ray dose rate at ground level
**ppm** parts per million – a measure of secondary field or noise relative to the primary or radioelement concentration.
**pT/s** picoteslas per second: Units of decay of secondary field, dB/dt
**S** siemens – a unit of conductance
**x**: the horizontal component of an EM field parallel to the direction of flight.
**y**: the horizontal component of an EM field perpendicular to the direction of flight.
**z**: the vertical component of an EM field.

**References:**

Constable, S.C., Parker, R.L., And Constable, C.G., 1987, Occam's inversion: a practical algorithm for generating smooth models from electromagnetic sounding data: Geophysics, 52, 289-300

Huang, H. and Fraser, D.C, 1996. The differential parameter method for muiltifrequency airborne resistivity mapping. Geophysics, 55, 1327-1337

Huang, H. and Palacky, G.J., 1991, Damped least-squares inversion of time-domain airborne EM data based on singular value decomposition: Geophysical Prospecting, v.39, 827-844

Macnae, J. and Lamontagne, Y., 1987, Imaging quasi-layered conductive structures by simple processing of transient electromagnetic data: Geophysics, v52, 4, 545-554.

Sengpiel, K-P. 1988, Approximate inversion of airborne EM data from a multi-layered ground. Geophysical Prospecting, 36, 446-459

Wolfgram, P. and Karlik, G., 1995, Conductivity-depth transform of GEOTEM data: Exploration Geophysics, 26, 179-185.

Yin, C. and Fraser, D.C. (2002), The effect of the electrical anisotropy on the responses of helicopter-borne frequency domain electromagnetic systems, Submitted to *Geophysical Prospecting*

095044

RECEIVED AUG. 20, 2008

Assay Samples collected on Rory Claims by Reading Party

| | | |
|---|---|---|
| WG-01 | 576337E x 6810910N | Rusty (Py) zone in vesicular basaltic. |
| WG-02 | 574218E x 6810110N | Powdered rock (Py) in washout below evident dyke (diorite?). |
| WG-03 | 574889E x 6809889N | Massive pyrrhotite float. |
| WG-04 | 574842E x 6809915N | Massive pyrrhotite float. |
| WG-05 | 575184E x 6809830N | Massive pyrrhotite from scree below cliff exposure of lense! |
| WG-06 | 575888E x 6810233N | Massive pyrrhotite from lense in canyon wall. |
| WG-07 | 575888E x 6810233N | Another sample from nearby in the same lense. |
| WG-08 | 575888E x 6810233N | Massive pyrrhotite from a lense higher in the canyon wall not far from the previous. |
| WG-09 | 573292E x 6814696N | Py in rusty gossan in basalt. |
| WG-10 | 572837E x 6813836N | Pyrrhotite dissem in limestone. |
| WG-11 | 573820E x 6812521N | Py dissem in basaltic lense in seds. |
| WG-12 | 573820E x 6812611N | Py dissem in siltstone (A-2 conductor!). |
| WG-13 | 571399E x 6813006N | Pyritized float in streambed. |
| WG-14 | 573820E x 6812611N | Additional sample of WG-12 rock. |
| WG-15 | 573820E x 6812611N | Same material, site of WG-12 |
| WG-16 | 575155E x 6811466N | Py dissem in diorite. |
| WG-17 | 575155E x 6811466N | Another sample from site WG-16. |
| WG-18 | 575155E x 6811466N | A 3rd sample from site WG-16. |
| WG-19 | 574268E x 6810xxxN | Rory exposure, washed rock. |

Alec;

Above are the loc's and brief descriptions of assay samples collected to date. The 1st 8 were shipped some time ago for Ni, Cu, Au and Pt - though I think Au is the likeliest possible in them.

We have encountered no Cu other than the powdery malachite fracture-coating at Rory's occurrence and there it is very local, restricted to a single lensoid area on a very very steep slope; adjacent ravines exhibit so sign of copper or related oxides. Diorite occurs below the Cu thing and a great thickness of limestone above it.

GROUND TRUTHING RESULTS FOR ZONE 1 FOUND BY FUGRO'S AIRBORNE SURVEY

**FUGRO AIRBORNE SURVEYS CORP.**

Fugro Airborne Surveys Corp.
2505 Meadowvale Boulevard
Mississauga, Ontario
Canada L5N 5S2
Phone : +1-905-812-0212
Fax : +1-905-812-1504
Website : www.fugroairborne.com

095044

Re: Fugro project 08032 - Yukon for Coronation Minerals Inc.

# STATEMENT OF QUALIFICATIONS

I, Russell Dean Imrie, of the City of Bolton, Province of Ontario, do hereby certify that:

1. I am a geologist who graduated from the University of Toronto in 1984 with a Bachelor of Science degree.
2. I have been actively engaged in geophysical data processing; quality control of geophysical maps from electromagnetic, magnetic and radiometric data; designed survey missions; conducted geological sampling, mapping, writing technical reports, and worked with several geophysical exploration companies as well as geophysical airborne survey companies since 1984.
3. I am presently employed by Fugro Airborne Surveys Corporation as an Interpretation Geophysicist, reporting directly to the Manager of Data Processing and Interpretation.
4. I have provided over 500,000 line kilometers of EM and magnetic data to clients while at Fugro.
5. I have no direct and indirect financial interest in the property described in this report.
6. The statements made in this report represent my best opinion and judgement.

Russell Dean Imrie
Geophysicist - Interpretation

Confirmed:

Graham Konieczny
Manager Data Processing and Interpretation

List of Claims

| Map | District | GrantNumb | RegType | ClaimNam | ClaimNbr | Claim Own | OperationF | ClaimExpir |
|---|---|---|---|---|---|---|---|---|
| Go to map | Whitehorse | YC65957 | Quartz | RORY | 1 | Coronation | 10/3/2007 | 10/3/2013 |
| Go to map | Whitehorse | YC65958 | Quartz | RORY | 2 | Coronation | 10/3/2007 | 10/3/2013 |
| Go to map | Whitehorse | YC65959 | Quartz | RORY | 3 | Coronation | 10/3/2007 | 10/3/2013 |
| Go to map | Whitehorse | YC65960 | Quartz | RORY | 4 | Coronation | 10/3/2007 | 10/3/2013 |
| Go to map | Whitehorse | YC65961 | Quartz | RORY | 5 | Coronation | 10/3/2007 | 10/3/2013 |
| Go to map | Whitehorse | YC65962 | Quartz | RORY | 6 | Coronation | 10/3/2007 | 10/3/2013 |
| Go to map | Whitehorse | YC65963 | Quartz | RORY | 7 | Coronation | 10/3/2007 | 10/3/2013 |
| Go to map | Whitehorse | YC65964 | Quartz | RORY | 8 | Coronation | 10/3/2007 | 10/3/2013 |
| Go to map | Whitehorse | YC65965 | Quartz | RORY | 9 | Coronation | 10/3/2007 | 10/3/2013 |
| Go to map | Whitehorse | YC65966 | Quartz | RORY | 10 | Coronation | 10/3/2007 | 10/3/2013 |
| Go to map | Whitehorse | YC65967 | Quartz | RORY | 11 | Coronation | 10/3/2007 | 10/3/2013 |
| Go to map | Whitehorse | YC65968 | Quartz | RORY | 12 | Coronation | 10/3/2007 | 10/3/2013 |
| Go to map | Whitehorse | YC65969 | Quartz | RORY | 13 | Coronation | 10/3/2007 | 10/3/2013 |
| Go to map | Whitehorse | YC65970 | Quartz | RORY | 14 | Coronation | 10/3/2007 | 10/3/2013 |
| Go to map | Whitehorse | YC65971 | Quartz | RORY | 15 | Coronation | 10/3/2007 | 10/3/2013 |
| Go to map | Whitehorse | YC65972 | Quartz | RORY | 16 | Coronation | 10/3/2007 | 10/3/2013 |
| Go to map | Whitehorse | YC65973 | Quartz | RORY | 17 | Coronation | 10/3/2007 | 10/3/2013 |
| Go to map | Whitehorse | YC65974 | Quartz | RORY | 18 | Coronation | 10/3/2007 | 10/3/2013 |
| Go to map | Whitehorse | YC65975 | Quartz | RORY | 19 | Coronation | 10/3/2007 | 10/3/2013 |
| Go to map | Whitehorse | YC65976 | Quartz | RORY | 20 | Coronation | 10/3/2007 | 10/3/2013 |
| Go to map | Whitehorse | YC65977 | Quartz | RORY | 21 | Coronation | 10/3/2007 | 10/3/2013 |
| Go to map | Whitehorse | YC65978 | Quartz | RORY | 22 | Coronation | 10/3/2007 | 10/3/2013 |
| Go to map | Whitehorse | YC65979 | Quartz | RORY | 23 | Coronation | 10/3/2007 | 10/3/2013 |
| Go to map | Whitehorse | YC65980 | Quartz | RORY | 24 | Coronation | 10/3/2007 | 10/3/2013 |
| Go to map | Whitehorse | YC65981 | Quartz | RORY | 25 | Coronation | 10/3/2007 | 10/3/2013 |
| Go to map | Whitehorse | YC65982 | Quartz | RORY | 26 | Coronation | 10/3/2007 | 10/3/2013 |
| Go to map | Whitehorse | YC65983 | Quartz | RORY | 27 | Coronation | 10/3/2007 | 10/3/2013 |
| Go to map | Whitehorse | YC65984 | Quartz | RORY | 28 | Coronation | 10/3/2007 | 10/3/2013 |
| Go to map | Whitehorse | YC65985 | Quartz | RORY | 29 | Coronation | 10/3/2007 | 10/3/2013 |
| Go to map | Whitehorse | YC65986 | Quartz | RORY | 30 | Coronation | 10/3/2007 | 10/3/2013 |
| Go to map | Whitehorse | YC65987 | Quartz | RORY | 31 | Coronation | 10/3/2007 | 10/3/2013 |
| Go to map | Whitehorse | YC65988 | Quartz | RORY | 32 | Coronation | 10/3/2007 | 10/3/2013 |
| Go to map | Whitehorse | YC65989 | Quartz | RORY | 33 | Coronation | 10/3/2007 | 10/3/2013 |
| Go to map | Whitehorse | YC65990 | Quartz | RORY | 34 | Coronation | 10/3/2007 | 10/3/2013 |
| Go to map | Whitehorse | YC65991 | Quartz | RORY | 35 | Coronation | 10/3/2007 | 10/3/2013 |
| Go to map | Whitehorse | YC65992 | Quartz | RORY | 36 | Coronation | 10/3/2007 | 10/3/2013 |
| Go to map | Whitehorse | YC65993 | Quartz | RORY | 37 | Coronation | 10/3/2007 | 10/3/2013 |
| Go to map | Whitehorse | YC65994 | Quartz | RORY | 38 | Coronation | 10/3/2007 | 10/3/2013 |
| Go to map | Whitehorse | YC65995 | Quartz | RORY | 39 | Coronation | 10/3/2007 | 10/3/2013 |
| Go to map | Whitehorse | YC65996 | Quartz | RORY | 40 | Coronation | 10/3/2007 | 10/3/2013 |
| Go to map | Whitehorse | YC65997 | Quartz | RORY | 41 | Coronation | 10/3/2007 | 10/3/2013 |
| Go to map | Whitehorse | YC65998 | Quartz | RORY | 42 | Coronation | 10/3/2007 | 10/3/2013 |
| Go to map | Whitehorse | YC65999 | Quartz | RORY | 43 | Coronation | 10/3/2007 | 10/3/2013 |
| Go to map | Whitehorse | YC66000 | Quartz | RORY | 44 | Coronation | 10/3/2007 | 10/3/2013 |
| Go to map | Whitehorse | YC66001 | Quartz | RORY | 45 | Coronation | 10/3/2007 | 10/3/2013 |
| Go to map | Whitehorse | YC66002 | Quartz | RORY | 46 | Coronation | 10/3/2007 | 10/3/2013 |
| Go to map | Whitehorse | YC66003 | Quartz | RORY | 47 | Coronation | 10/3/2007 | 10/3/2013 |

| | | | | | | | | |
|---|---|---|---|---|---|---|---|---|
| Go to map | Whitehorse | YC66004 | Quartz | RORY | 48 | Coronation | 10/3/2007 | 10/3/2013 |
| Go to map | Whitehorse | YC66005 | Quartz | RORY | 49 | Coronation | 10/3/2007 | 10/3/2013 |
| Go to map | Whitehorse | YC66006 | Quartz | RORY | 50 | Coronation | 10/3/2007 | 10/3/2013 |
| Go to map | Whitehorse | YC66007 | Quartz | RORY | 51 | Coronation | 10/3/2007 | 10/3/2013 |
| Go to map | Whitehorse | YC66008 | Quartz | RORY | 52 | Coronation | 10/3/2007 | 10/3/2013 |
| Go to map | Whitehorse | YC66009 | Quartz | RORY | 53 | Coronation | 10/3/2007 | 10/3/2013 |
| Go to map | Whitehorse | YC66010 | Quartz | RORY | 54 | Coronation | 10/3/2007 | 10/3/2013 |
| Go to map | Whitehorse | YC66011 | Quartz | RORY | 55 | Coronation | 10/3/2007 | 10/3/2013 |
| Go to map | Whitehorse | YC66012 | Quartz | RORY | 56 | Coronation | 10/3/2007 | 10/3/2013 |
| Go to map | Whitehorse | YC66013 | Quartz | RORY | 57 | Coronation | 10/3/2007 | 10/3/2013 |
| Go to map | Whitehorse | YC66014 | Quartz | RORY | 58 | Coronation | 10/3/2007 | 10/3/2013 |
| Go to map | Whitehorse | YC66015 | Quartz | RORY | 59 | Coronation | 10/3/2007 | 10/3/2013 |
| Go to map | Whitehorse | YC66016 | Quartz | RORY | 60 | Coronation | 10/3/2007 | 10/3/2013 |
| Go to map | Whitehorse | YC66017 | Quartz | RORY | 61 | Coronation | 10/3/2007 | 10/3/2013 |
| Go to map | Whitehorse | YC66018 | Quartz | RORY | 62 | Coronation | 10/3/2007 | 10/3/2013 |
| Go to map | Whitehorse | YC66019 | Quartz | RORY | 63 | Coronation | 10/3/2007 | 10/3/2013 |
| Go to map | Whitehorse | YC66020 | Quartz | RORY | 64 | Coronation | 10/3/2007 | 10/3/2013 |
| Go to map | Whitehorse | YC66021 | Quartz | RORY | 65 | Coronation | 10/3/2007 | 10/3/2013 |
| Go to map | Whitehorse | YC66022 | Quartz | RORY | 66 | Coronation | 10/3/2007 | 10/3/2013 |
| Go to map | Whitehorse | YC66023 | Quartz | RORY | 67 | Coronation | 10/3/2007 | 10/3/2013 |
| Go to map | Whitehorse | YC66024 | Quartz | RORY | 68 | Coronation | 10/3/2007 | 10/3/2013 |
| Go to map | Whitehorse | YC66025 | Quartz | RORY | 69 | Coronation | 10/3/2007 | 10/3/2013 |
| Go to map | Whitehorse | YC66026 | Quartz | RORY | 70 | Coronation | 10/3/2007 | 10/3/2013 |
| Go to map | Whitehorse | YC66027 | Quartz | RORY | 71 | Coronation | 10/3/2007 | 10/3/2013 |
| Go to map | Whitehorse | YC66028 | Quartz | RORY | 72 | Coronation | 10/3/2007 | 10/3/2013 |
| Go to map | Whitehorse | YC66029 | Quartz | RORY | 73 | Coronation | 10/3/2007 | 10/3/2013 |
| Go to map | Whitehorse | YC66030 | Quartz | RORY | 74 | Coronation | 10/3/2007 | 10/3/2013 |
| Go to map | Whitehorse | YC66031 | Quartz | RORY | 75 | Coronation | 10/3/2007 | 10/3/2013 |
| Go to map | Whitehorse | YC66032 | Quartz | RORY | 76 | Coronation | 10/3/2007 | 10/3/2013 |
| Go to map | Whitehorse | YC66033 | Quartz | RORY | 77 | Coronation | 10/3/2007 | 10/3/2013 |
| Go to map | Whitehorse | YC66034 | Quartz | RORY | 78 | Coronation | 10/3/2007 | 10/3/2013 |
| Go to map | Whitehorse | YC66035 | Quartz | RORY | 79 | Coronation | 10/3/2007 | 10/3/2013 |
| Go to map | Whitehorse | YC66036 | Quartz | RORY | 80 | Coronation | 10/3/2007 | 10/3/2013 |
| Go to map | Whitehorse | YC66037 | Quartz | RORY | 81 | Coronation | 10/3/2007 | 10/3/2013 |
| Go to map | Whitehorse | YC66038 | Quartz | RORY | 82 | Coronation | 10/3/2007 | 10/3/2013 |
| Go to map | Whitehorse | YC66039 | Quartz | RORY | 83 | Coronation | 10/3/2007 | 10/3/2013 |
| Go to map | Whitehorse | YC66040 | Quartz | RORY | 84 | Coronation | 10/3/2007 | 10/3/2013 |
| Go to map | Whitehorse | YC66041 | Quartz | RORY | 85 | Coronation | 10/3/2007 | 10/3/2013 |
| Go to map | Whitehorse | YC66042 | Quartz | RORY | 86 | Coronation | 10/3/2007 | 10/3/2013 |
| Go to map | Whitehorse | YC66043 | Quartz | RORY | 87 | Coronation | 10/3/2007 | 10/3/2013 |
| Go to map | Whitehorse | YC66044 | Quartz | RORY | 88 | Coronation | 10/3/2007 | 10/3/2013 |
| Go to map | Whitehorse | YC66045 | Quartz | RORY | 89 | Coronation | 10/3/2007 | 10/3/2013 |
| Go to map | Whitehorse | YC66046 | Quartz | RORY | 90 | Coronation | 10/3/2007 | 10/3/2013 |
| Go to map | Whitehorse | YC66047 | Quartz | RORY | 91 | Coronation | 10/3/2007 | 10/3/2013 |
| Go to map | Whitehorse | YC66048 | Quartz | RORY | 92 | Coronation | 10/3/2007 | 10/3/2013 |
| Go to map | Whitehorse | YC66049 | Quartz | RORY | 93 | Coronation | 10/3/2007 | 10/3/2013 |
| Go to map | Whitehorse | YC66050 | Quartz | RORY | 94 | Coronation | 10/3/2007 | 10/3/2013 |
| Go to map | Whitehorse | YC66051 | Quartz | RORY | 95 | Coronation | 10/3/2007 | 10/3/2013 |
| Go to map | Whitehorse | YC66052 | Quartz | RORY | 96 | Coronation | 10/3/2007 | 10/3/2013 |
| Go to map | Whitehorse | YC66053 | Quartz | RORY | 97 | Coronation | 10/3/2007 | 10/3/2013 |
| Go to map | Whitehorse | YC66054 | Quartz | RORY | 98 | Coronation | 10/3/2007 | 10/3/2013 |
| Go to map | Whitehorse | YC66055 | Quartz | RORY | 99 | Coronation | 10/3/2007 | 10/3/2013 |

| | | | | | | | |
|---|---|---|---|---|---|---|---|
| Go to map | Whitehorse | YC66056 | Quartz | RORY | 100 | Coronation | 10/3/2007 | 10/3/2013 |
| Go to map | Whitehorse | YC66057 | Quartz | RORY | 101 | Coronation | 10/3/2007 | 10/3/2013 |
| Go to map | Whitehorse | YC66058 | Quartz | RORY | 102 | Coronation | 10/3/2007 | 10/3/2013 |
| Go to map | Whitehorse | YC66059 | Quartz | RORY | 103 | Coronation | 10/3/2007 | 10/3/2013 |
| Go to map | Whitehorse | YC66060 | Quartz | RORY | 104 | Coronation | 10/3/2007 | 10/3/2013 |
| Go to map | Whitehorse | YC66061 | Quartz | RORY | 105 | Coronation | 10/3/2007 | 10/3/2013 |
| Go to map | Whitehorse | YC66062 | Quartz | RORY | 106 | Coronation | 10/3/2007 | 10/3/2013 |
| Go to map | Whitehorse | YC66063 | Quartz | RORY | 107 | Coronation | 10/3/2007 | 10/3/2013 |
| Go to map | Whitehorse | YC66064 | Quartz | RORY | 108 | Coronation | 10/3/2007 | 10/3/2013 |
| Go to map | Whitehorse | YC66065 | Quartz | RORY | 109 | Coronation | 10/3/2007 | 10/3/2013 |
| Go to map | Whitehorse | YC66066 | Quartz | RORY | 110 | Coronation | 10/3/2007 | 10/3/2013 |
| Go to map | Whitehorse | YC66067 | Quartz | RORY | 111 | Coronation | 10/3/2007 | 10/3/2013 |
| Go to map | Whitehorse | YC66068 | Quartz | RORY | 112 | Coronation | 10/3/2007 | 10/3/2013 |
| Go to map | Whitehorse | YC66069 | Quartz | RORY | 113 | Coronation | 10/3/2007 | 10/3/2013 |
| Go to map | Whitehorse | YC66070 | Quartz | RORY | 114 | Coronation | 10/3/2007 | 10/3/2013 |
| Go to map | Whitehorse | YC66071 | Quartz | RORY | 115 | Coronation | 10/3/2007 | 10/3/2013 |
| Go to map | Whitehorse | YC66072 | Quartz | RORY | 116 | Coronation | 10/3/2007 | 10/3/2013 |
| Go to map | Whitehorse | YC66073 | Quartz | RORY | 117 | Coronation | 10/3/2007 | 10/3/2013 |
| Go to map | Whitehorse | YC66074 | Quartz | RORY | 118 | Coronation | 10/3/2007 | 10/3/2013 |
| Go to map | Whitehorse | YC66075 | Quartz | RORY | 119 | Coronation | 10/3/2007 | 10/3/2013 |
| Go to map | Whitehorse | YC66076 | Quartz | RORY | 120 | Coronation | 10/3/2007 | 10/3/2013 |
| Go to map | Whitehorse | YC66077 | Quartz | RORY | 121 | Coronation | 10/3/2007 | 10/3/2013 |
| Go to map | Whitehorse | YC66078 | Quartz | RORY | 122 | Coronation | 10/3/2007 | 10/3/2013 |
| Go to map | Whitehorse | YC66079 | Quartz | RORY | 123 | Coronation | 10/3/2007 | 10/3/2013 |
| Go to map | Whitehorse | YC66080 | Quartz | RORY | 124 | Coronation | 10/3/2007 | 10/3/2013 |
| Go to map | Whitehorse | YC66081 | Quartz | RORY | 125 | Coronation | 10/3/2007 | 10/3/2013 |
| Go to map | Whitehorse | YC66082 | Quartz | RORY | 126 | Coronation | 10/3/2007 | 10/3/2013 |
| Go to map | Whitehorse | YC66083 | Quartz | RORY | 127 | Coronation | 10/3/2007 | 10/3/2013 |
| Go to map | Whitehorse | YC66084 | Quartz | RORY | 128 | Coronation | 10/3/2007 | 10/3/2013 |
| Go to map | Whitehorse | YC66085 | Quartz | RORY | 129 | Coronation | 10/3/2007 | 10/3/2013 |
| Go to map | Whitehorse | YC66086 | Quartz | RORY | 130 | Coronation | 10/3/2007 | 10/3/2013 |
| Go to map | Whitehorse | YC66087 | Quartz | RORY | 131 | Coronation | 10/3/2007 | 10/3/2013 |
| Go to map | Whitehorse | YC66088 | Quartz | RORY | 132 | Coronation | 10/3/2007 | 10/3/2013 |
| Go to map | Whitehorse | YC66089 | Quartz | RORY | 133 | Coronation | 10/3/2007 | 10/3/2013 |
| Go to map | Whitehorse | YC66090 | Quartz | RORY | 134 | Coronation | 10/3/2007 | 10/3/2013 |
| Go to map | Whitehorse | YC66091 | Quartz | RORY | 135 | Coronation | 10/3/2007 | 10/3/2013 |
| Go to map | Whitehorse | YC66092 | Quartz | RORY | 136 | Coronation | 10/3/2007 | 10/3/2013 |
| Go to map | Whitehorse | YC66093 | Quartz | RORY | 137 | Coronation | 10/3/2007 | 10/3/2013 |
| Go to map | Whitehorse | YC66094 | Quartz | RORY | 138 | Coronation | 10/3/2007 | 10/3/2013 |
| Go to map | Whitehorse | YC66095 | Quartz | RORY | 139 | Coronation | 10/3/2007 | 10/3/2013 |
| Go to map | Whitehorse | YC66096 | Quartz | RORY | 140 | Coronation | 10/3/2007 | 10/3/2013 |
| Go to map | Whitehorse | YC66097 | Quartz | RORY | 141 | Coronation | 10/3/2007 | 10/3/2013 |
| Go to map | Whitehorse | YC66098 | Quartz | RORY | 142 | Coronation | 10/3/2007 | 10/3/2013 |
| Go to map | Whitehorse | YC66099 | Quartz | RORY | 143 | Coronation | 10/3/2007 | 10/3/2013 |
| Go to map | Whitehorse | YC66100 | Quartz | RORY | 144 | Coronation | 10/3/2007 | 10/3/2013 |
| Go to map | Whitehorse | YC66101 | Quartz | RORY | 145 | Coronation | 10/3/2007 | 10/3/2013 |
| Go to map | Whitehorse | YC66102 | Quartz | RORY | 146 | Coronation | 10/3/2007 | 10/3/2013 |
| Go to map | Whitehorse | YC66103 | Quartz | RORY | 147 | Coronation | 10/3/2007 | 10/3/2013 |
| Go to map | Whitehorse | YC66104 | Quartz | RORY | 148 | Coronation | 10/3/2007 | 10/3/2013 |
| Go to map | Whitehorse | YC66105 | Quartz | RORY | 149 | Coronation | 10/3/2007 | 10/3/2013 |
| Go to map | Whitehorse | YC66106 | Quartz | RORY | 150 | Coronation | 10/3/2007 | 10/3/2013 |
| Go to map | Whitehorse | YC66107 | Quartz | RORY | 151 | Coronation | 10/3/2007 | 10/3/2013 |

| | | | | | | | |
|---|---|---|---|---|---|---|---|
| Go to map | Whitehorse | YC66108 | Quartz | RORY | 152 | Coronation | 10/3/2007 10/3/2013 |
| Go to map | Whitehorse | YC66109 | Quartz | RORY | 153 | Coronation | 10/3/2007 10/3/2013 |
| Go to map | Whitehorse | YC66110 | Quartz | RORY | 154 | Coronation | 10/3/2007 10/3/2013 |
| Go to map | Whitehorse | YC66111 | Quartz | RORY | 155 | Coronation | 10/3/2007 10/3/2013 |
| Go to map | Whitehorse | YC66112 | Quartz | RORY | 156 | Coronation | 10/3/2007 10/3/2013 |
| Go to map | Whitehorse | YC66113 | Quartz | RORY | 157 | Coronation | 10/3/2007 10/3/2013 |
| Go to map | Whitehorse | YC66114 | Quartz | RORY | 158 | Coronation | 10/3/2007 10/3/2013 |
| Go to map | Whitehorse | YC66115 | Quartz | RORY | 159 | Coronation | 10/3/2007 10/3/2013 |
| Go to map | Whitehorse | YC66116 | Quartz | RORY | 160 | Coronation | 10/3/2007 10/3/2013 |
| Go to map | Whitehorse | YC66117 | Quartz | RORY | 161 | Coronation | 10/3/2007 10/3/2013 |
| Go to map | Whitehorse | YC66118 | Quartz | RORY | 162 | Coronation | 10/3/2007 10/3/2013 |
| Go to map | Whitehorse | YC66119 | Quartz | RORY | 163 | Coronation | 10/3/2007 10/3/2013 |
| Go to map | Whitehorse | YC66120 | Quartz | RORY | 164 | Coronation | 10/3/2007 10/3/2013 |
| Go to map | Whitehorse | YC66121 | Quartz | RORY | 165 | Coronation | 10/3/2007 10/3/2013 |
| Go to map | Whitehorse | YC66122 | Quartz | RORY | 166 | Coronation | 10/3/2007 10/3/2013 |
| Go to map | Whitehorse | YC66123 | Quartz | RORY | 167 | Coronation | 10/3/2007 10/3/2013 |
| Go to map | Whitehorse | YC66124 | Quartz | RORY | 168 | Coronation | 10/3/2007 10/3/2013 |
| Go to map | Whitehorse | YC66125 | Quartz | RORY | 169 | Coronation | 10/3/2007 10/3/2013 |
| Go to map | Whitehorse | YC66126 | Quartz | RORY | 170 | Coronation | 10/3/2007 10/3/2013 |
| Go to map | Whitehorse | YC66127 | Quartz | RORY | 171 | Coronation | 10/3/2007 10/3/2013 |
| Go to map | Whitehorse | YC66128 | Quartz | RORY | 172 | Coronation | 10/3/2007 10/3/2013 |
| Go to map | Whitehorse | YC66129 | Quartz | RORY | 173 | Coronation | 10/3/2007 10/3/2013 |
| Go to map | Whitehorse | YC66130 | Quartz | RORY | 174 | Coronation | 10/3/2007 10/3/2013 |
| Go to map | Whitehorse | YC66131 | Quartz | RORY | 175 | Coronation | 10/3/2007 10/3/2013 |
| Go to map | Whitehorse | YC66132 | Quartz | RORY | 176 | Coronation | 10/3/2007 10/3/2013 |
| Go to map | Whitehorse | YC66133 | Quartz | RORY | 177 | Coronation | 10/3/2007 10/3/2013 |
| Go to map | Whitehorse | YC66134 | Quartz | RORY | 178 | Coronation | 10/3/2007 10/3/2013 |
| Go to map | Whitehorse | YC66135 | Quartz | RORY | 179 | Coronation | 10/3/2007 10/3/2013 |
| Go to map | Whitehorse | YC66136 | Quartz | RORY | 180 | Coronation | 10/3/2007 10/3/2013 |
| Go to map | Whitehorse | YC66137 | Quartz | RORY | 181 | Coronation | 10/3/2007 10/3/2013 |
| Go to map | Whitehorse | YC66138 | Quartz | RORY | 182 | Coronation | 10/3/2007 10/3/2013 |
| Go to map | Whitehorse | YC66139 | Quartz | RORY | 183 | Coronation | 10/3/2007 10/3/2013 |
| Go to map | Whitehorse | YC66140 | Quartz | RORY | 184 | Coronation | 10/3/2007 10/3/2013 |
| Go to map | Whitehorse | YC66141 | Quartz | RORY | 185 | Coronation | 10/3/2007 10/3/2013 |
| Go to map | Whitehorse | YC66142 | Quartz | RORY | 186 | Coronation | 10/3/2007 10/3/2013 |
| Go to map | Whitehorse | YC66143 | Quartz | RORY | 187 | Coronation | 10/3/2007 10/3/2013 |
| Go to map | Whitehorse | YC66144 | Quartz | RORY | 188 | Coronation | 10/3/2007 10/3/2013 |
| Go to map | Whitehorse | YC66145 | Quartz | RORY | 189 | Coronation | 10/3/2007 10/3/2013 |
| Go to map | Whitehorse | YC66146 | Quartz | RORY | 190 | Coronation | 10/3/2007 10/3/2013 |
| Go to map | Whitehorse | YC66147 | Quartz | RORY | 191 | Coronation | 10/3/2007 10/3/2013 |
| Go to map | Whitehorse | YC66148 | Quartz | RORY | 192 | Coronation | 10/3/2007 10/3/2013 |
| Go to map | Whitehorse | YC66149 | Quartz | RORY | 193 | Coronation | 10/3/2007 10/3/2013 |
| Go to map | Whitehorse | YC66150 | Quartz | RORY | 194 | Coronation | 10/3/2007 10/3/2013 |
| Go to map | Whitehorse | YC66151 | Quartz | RORY | 195 | Coronation | 10/3/2007 10/3/2013 |
| Go to map | Whitehorse | YC66152 | Quartz | RORY | 196 | Coronation | 10/3/2007 10/3/2013 |
| Go to map | Whitehorse | YC66153 | Quartz | RORY | 197 | Coronation | 10/3/2007 10/3/2013 |
| Go to map | Whitehorse | YC66154 | Quartz | RORY | 198 | Coronation | 10/3/2007 10/3/2013 |
| Go to map | Whitehorse | YC66155 | Quartz | RORY | 199 | Coronation | 10/3/2007 10/3/2013 |
| Go to map | Whitehorse | YC66156 | Quartz | RORY | 200 | Coronation | 10/3/2007 10/3/2013 |
| Go to map | Whitehorse | YC66157 | Quartz | RORY | 201 | Coronation | 10/3/2007 10/3/2013 |
| Go to map | Whitehorse | YC66158 | Quartz | RORY | 202 | Coronation | 10/3/2007 10/3/2013 |
| Go to map | Whitehorse | YC66159 | Quartz | RORY | 203 | Coronation | 10/3/2007 10/3/2013 |

| | | | | | | | |
|---|---|---|---|---|---|---|---|
| Go to map | Whitehorse | YC66160 | Quartz | RORY | 204 | Coronation | 10/3/2007 | 10/3/2013 |
| Go to map | Whitehorse | YC66161 | Quartz | RORY | 205 | Coronation | 10/3/2007 | 10/3/2013 |
| Go to map | Whitehorse | YC66162 | Quartz | RORY | 206 | Coronation | 10/3/2007 | 10/3/2013 |
| Go to map | Whitehorse | YC66163 | Quartz | RORY | 207 | Coronation | 10/3/2007 | 10/3/2013 |
| Go to map | Whitehorse | YC66164 | Quartz | RORY | 208 | Coronation | 10/3/2007 | 10/3/2013 |
| Go to map | Whitehorse | YC66165 | Quartz | RORY | 209 | Coronation | 10/3/2007 | 10/3/2013 |
| Go to map | Whitehorse | YC66166 | Quartz | RORY | 210 | Coronation | 10/3/2007 | 10/3/2013 |
| Go to map | Whitehorse | YC66167 | Quartz | RORY | 211 | Coronation | 10/3/2007 | 10/3/2013 |
| Go to map | Whitehorse | YC66168 | Quartz | RORY | 212 | Coronation | 10/3/2007 | 10/3/2013 |
| Go to map | Whitehorse | YC66169 | Quartz | RORY | 213 | Coronation | 10/3/2007 | 10/3/2013 |
| Go to map | Whitehorse | YC66170 | Quartz | RORY | 214 | Coronation | 10/3/2007 | 10/3/2013 |
| Go to map | Whitehorse | YC66171 | Quartz | RORY | 215 | Coronation | 10/3/2007 | 10/3/2013 |
| Go to map | Whitehorse | YC66172 | Quartz | RORY | 216 | Coronation | 10/3/2007 | 10/3/2013 |
| Go to map | Whitehorse | YC66173 | Quartz | RORY | 217 | Coronation | 10/3/2007 | 10/3/2013 |
| Go to map | Whitehorse | YC66174 | Quartz | RORY | 218 | Coronation | 10/3/2007 | 10/3/2013 |
| Go to map | Whitehorse | YC66175 | Quartz | RORY | 219 | Coronation | 10/3/2007 | 10/3/2013 |
| Go to map | Whitehorse | YC66176 | Quartz | RORY | 220 | Coronation | 10/3/2007 | 10/3/2013 |
| Go to map | Whitehorse | YC66177 | Quartz | RORY | 221 | Coronation | 10/3/2007 | 10/3/2013 |
| Go to map | Whitehorse | YC66178 | Quartz | RORY | 222 | Coronation | 10/3/2007 | 10/3/2013 |
| Go to map | Whitehorse | YC66179 | Quartz | RORY | 223 | Coronation | 10/3/2007 | 10/3/2013 |
| Go to map | Whitehorse | YC66180 | Quartz | RORY | 224 | Coronation | 10/3/2007 | 10/3/2013 |
| Go to map | Whitehorse | YC66181 | Quartz | RORY | 225 | Coronation | 10/3/2007 | 10/3/2013 |
| Go to map | Whitehorse | YC66182 | Quartz | RORY | 226 | Coronation | 10/3/2007 | 10/3/2013 |
| Go to map | Whitehorse | YC66183 | Quartz | RORY | 227 | Coronation | 10/3/2007 | 10/3/2013 |
| Go to map | Whitehorse | YC66184 | Quartz | RORY | 228 | Coronation | 10/3/2007 | 10/3/2013 |
| Go to map | Whitehorse | YC66185 | Quartz | RORY | 229 | Coronation | 10/3/2007 | 10/3/2013 |
| Go to map | Whitehorse | YC66186 | Quartz | RORY | 230 | Coronation | 10/3/2007 | 10/3/2013 |
| Go to map | Whitehorse | YC66187 | Quartz | RORY | 231 | Coronation | 10/3/2007 | 10/3/2013 |
| Go to map | Whitehorse | YC66188 | Quartz | RORY | 232 | Coronation | 10/3/2007 | 10/3/2013 |
| Go to map | Whitehorse | YC66189 | Quartz | RORY | 233 | Coronation | 10/3/2007 | 10/3/2013 |
| Go to map | Whitehorse | YC66190 | Quartz | RORY | 234 | Coronation | 10/3/2007 | 10/3/2013 |
| Go to map | Whitehorse | YC66191 | Quartz | RORY | 235 | Coronation | 10/3/2007 | 10/3/2013 |
| Go to map | Whitehorse | YC66192 | Quartz | RORY | 236 | Coronation | 10/3/2007 | 10/3/2013 |
| Go to map | Whitehorse | YC66193 | Quartz | RORY | 237 | Coronation | 10/3/2007 | 10/3/2013 |
| Go to map | Whitehorse | YC66194 | Quartz | RORY | 238 | Coronation | 10/3/2007 | 10/3/2013 |
| Go to map | Whitehorse | YC66195 | Quartz | RORY | 239 | Coronation | 10/3/2007 | 10/3/2013 |
| Go to map | Whitehorse | YC66196 | Quartz | RORY | 240 | Coronation | 10/3/2007 | 10/3/2013 |
| Go to map | Whitehorse | YC66197 | Quartz | RORY | 241 | Coronation | 10/3/2007 | 10/3/2013 |
| Go to map | Whitehorse | YC66198 | Quartz | RORY | 242 | Coronation | 10/3/2007 | 10/3/2013 |
| Go to map | Whitehorse | YC66199 | Quartz | RORY | 243 | Coronation | 10/3/2007 | 10/3/2013 |
| Go to map | Whitehorse | YC66200 | Quartz | RORY | 244 | Coronation | 10/3/2007 | 10/3/2013 |
| Go to map | Whitehorse | YC66201 | Quartz | RORY | 245 | Coronation | 10/3/2007 | 10/3/2013 |
| Go to map | Whitehorse | YC66202 | Quartz | RORY | 246 | Coronation | 10/3/2007 | 10/3/2013 |
| Go to map | Whitehorse | YC66203 | Quartz | RORY | 247 | Coronation | 10/3/2007 | 10/3/2013 |
| Go to map | Whitehorse | YC66204 | Quartz | RORY | 248 | Coronation | 10/3/2007 | 10/3/2013 |
| Go to map | Whitehorse | YC66205 | Quartz | RORY | 249 | Coronation | 10/3/2007 | 10/3/2013 |
| Go to map | Whitehorse | YC66206 | Quartz | RORY | 250 | Coronation | 10/3/2007 | 10/3/2013 |
| Go to map | Whitehorse | YC66207 | Quartz | RORY | 251 | Coronation | 10/3/2007 | 10/3/2013 |
| Go to map | Whitehorse | YC66208 | Quartz | RORY | 252 | Coronation | 10/3/2007 | 10/3/2013 |
| Go to map | Whitehorse | YC66209 | Quartz | RORY | 253 | Coronation | 10/3/2007 | 10/3/2013 |
| Go to map | Whitehorse | YC66210 | Quartz | RORY | 254 | Coronation | 10/3/2007 | 10/3/2013 |
| Go to map | Whitehorse | YC66211 | Quartz | RORY | 255 | Coronation | 10/3/2007 | 10/3/2013 |

| | | | | | | | | |
|---|---|---|---|---|---|---|---|---|
| Go to map | Whitehorse | YC66212 | Quartz | RORY Frac | 256 | Coronation | 10/3/2007 | 10/3/2013 |
| Go to map | Whitehorse | YC66213 | Quartz | RORY | 257 | Coronation | 10/3/2007 | 10/3/2013 |
| Go to map | Whitehorse | YC66214 | Quartz | RORY | 258 | Coronation | 10/3/2007 | 10/3/2013 |
| Go to map | Whitehorse | YC66215 | Quartz | RORY | 259 | Coronation | 10/3/2007 | 10/3/2013 |
| Go to map | Whitehorse | YC66216 | Quartz | RORY | 260 | Coronation | 10/3/2007 | 10/3/2013 |
| Go to map | Whitehorse | YC66217 | Quartz | RORY | 261 | Coronation | 10/3/2007 | 10/3/2013 |
| Go to map | Whitehorse | YC66218 | Quartz | RORY | 262 | Coronation | 10/3/2007 | 10/3/2013 |
| Go to map | Whitehorse | YC66219 | Quartz | RORY | 263 | Coronation | 10/3/2007 | 10/3/2013 |
| Go to map | Whitehorse | YC66220 | Quartz | RORY Frac | 264 | Coronation | 10/3/2007 | 10/3/2013 |
| Go to map | Whitehorse | YC66221 | Quartz | RORY Frac | 265 | Coronation | 10/3/2007 | 10/3/2013 |

report total:

| Map | District | GrantNuml | RegType | ClaimNam | ClaimNbr | Claim Own | OperationF | ClaimExpir |
|---|---|---|---|---|---|---|---|---|
| Go to map | Whitehorse | YA94966 | Quartz | MUS | 5 | Arch Joint ' | 6/12/1986 | 2/11/2014 |
| Go to map | Whitehorse | YA94967 | Quartz | MUS | 6 | Arch Joint ' | 6/12/1986 | 2/11/2014 |
| Go to map | Whitehorse | YA94968 | Quartz | BARNY | 1 | Arch Joint ' | 6/12/1986 | 2/11/2014 |
| Go to map | Whitehorse | YA94969 | Quartz | BARNY | 2 | Arch Joint ' | 6/12/1986 | 2/11/2014 |
| Go to map | Whitehorse | YA94970 | Quartz | BARNY | 3 | Arch Joint ' | 6/12/1986 | 2/11/2014 |
| Go to map | Whitehorse | YA94971 | Quartz | BARNY | 4 | Arch Joint ' | 6/12/1986 | 2/11/2014 |
| Go to map | Whitehorse | YA94972 | Quartz | BARNY | 5 | Arch Joint ' | 6/12/1986 | 2/11/2014 |
| Go to map | Whitehorse | YA94973 | Quartz | BARNY | 6 | Arch Joint ' | 6/12/1986 | 2/11/2014 |
| Go to map | Whitehorse | YA96002 | Quartz | BARNY | 7 | Arch Joint ' | 8/22/1986 | 2/11/2014 |
| Go to map | Whitehorse | YA96003 | Quartz | BARNY | 8 | Arch Joint ' | 8/22/1986 | 2/11/2014 |
| Go to map | Whitehorse | YA96004 | Quartz | BARNY | 9 | Arch Joint ' | 8/22/1986 | 2/11/2014 |
| Go to map | Whitehorse | YA96005 | Quartz | BARNY | 10 | Arch Joint ' | 8/22/1986 | 2/11/2014 |
| Go to map | Whitehorse | YA96006 | Quartz | BARNY | 11 | Arch Joint ' | 8/22/1986 | 2/11/2014 |
| Go to map | Whitehorse | YA96007 | Quartz | BARNY | 12 | Arch Joint ' | 8/22/1986 | 2/11/2014 |
| Go to map | Whitehorse | YA96008 | Quartz | BARNY | 13 | Arch Joint ' | 8/22/1986 | 2/11/2014 |
| Go to map | Whitehorse | YA96009 | Quartz | BARNY | 14 | Arch Joint ' | 8/22/1986 | 2/11/2014 |
| Go to map | Whitehorse | YA96015 | Quartz | MUS | 12 | Arch Joint ' | 8/22/1986 | 2/11/2014 |
| Go to map | Whitehorse | YA96017 | Quartz | MUS | 14 | Arch Joint ' | 8/22/1986 | 2/11/2014 |
| Go to map | Whitehorse | YA96019 | Quartz | MUS | 16 | Arch Joint ' | 8/22/1986 | 2/11/2014 |
| Go to map | Whitehorse | YA96867 | Quartz | BARNY | 19 | Arch Joint ' | 2/11/1987 | 2/11/2014 |
| Go to map | Whitehorse | YA96868 | Quartz | BARNY | 20 | Arch Joint ' | 2/11/1987 | 2/11/2014 |
| Go to map | Whitehorse | YA96869 | Quartz | BARNY | 21 | Arch Joint ' | 2/11/1987 | 2/11/2014 |
| Go to map | Whitehorse | YA96870 | Quartz | BARNY | 22 | Arch Joint ' | 2/11/1987 | 2/11/2014 |
| Go to map | Whitehorse | YA96871 | Quartz | BARNY | 23 | Arch Joint ' | 2/11/1987 | 2/11/2014 |
| Go to map | Whitehorse | YA96872 | Quartz | BARNY | 24 | Arch Joint ' | 2/11/1987 | 2/11/2014 |
| Go to map | Whitehorse | YA96873 | Quartz | BARNY | 25 | Arch Joint ' | 2/11/1987 | 2/11/2014 |
| Go to map | Whitehorse | YA96874 | Quartz | BARNY | 26 | Arch Joint ' | 2/11/1987 | 2/11/2014 |
| Go to map | Whitehorse | YA96875 | Quartz | BARNY | 27 | Arch Joint ' | 2/11/1987 | 2/11/2014 |
| Go to map | Whitehorse | YA96876 | Quartz | BARNY | 28 | Arch Joint ' | 2/11/1987 | 2/11/2014 |
| Go to map | Whitehorse | YA96877 | Quartz | BARNY | 29 | Arch Joint ' | 2/11/1987 | 2/11/2014 |
| Go to map | Whitehorse | YA96878 | Quartz | BARNY | 30 | Arch Joint ' | 2/11/1987 | 2/11/2014 |
| Go to map | Whitehorse | YA96879 | Quartz | BARNY | 31 | Arch Joint ' | 2/11/1987 | 2/11/2014 |
| Go to map | Whitehorse | YA96880 | Quartz | BARNY | 32 | Arch Joint ' | 2/11/1987 | 2/11/2014 |
| Go to map | Whitehorse | YA97896 | Quartz | BARNY | 33 | Arch Joint ' | 6/23/1987 | 2/11/2014 |
| Go to map | Whitehorse | YA97897 | Quartz | BARNY | 34 | Arch Joint ' | 6/23/1987 | 2/11/2014 |
| Go to map | Whitehorse | YA97898 | Quartz | BARNY | 35 | Arch Joint ' | 6/23/1987 | 2/11/2014 |
| Go to map | Whitehorse | YA97899 | Quartz | BARNY | 36 | Arch Joint ' | 6/23/1987 | 2/11/2014 |
| Go to map | Whitehorse | YA97900 | Quartz | BARNY | 37 | Arch Joint ' | 6/23/1987 | 2/11/2014 |
| Go to map | Whitehorse | YA97901 | Quartz | BARNY | 38 | Arch Joint ' | 6/23/1987 | 2/11/2014 |
| Go to map | Whitehorse | YA97902 | Quartz | BARNY | 39 | Arch Joint ' | 6/23/1987 | 2/11/2014 |
| Go to map | Whitehorse | YA97904 | Quartz | BARNY | 41 | Arch Joint ' | 6/23/1987 | 2/11/2014 |
| Go to map | Whitehorse | YA97905 | Quartz | BARNY | 42 | Arch Joint ' | 6/23/1987 | 2/11/2014 |
| Go to map | Whitehorse | YA97906 | Quartz | BARNY | 43 | Arch Joint ' | 6/23/1987 | 2/11/2014 |
| Go to map | Whitehorse | YA97908 | Quartz | BARNY | 45 | Arch Joint ' | 6/23/1987 | 2/11/2014 |
| Go to map | Whitehorse | YA97910 | Quartz | BARNY | 47 | Arch Joint ' | 6/23/1987 | 2/11/2014 |
| Go to map | Whitehorse | YA97911 | Quartz | BARNY | 48 | Arch Joint ' | 6/23/1987 | 2/11/2014 |
| Go to map | Whitehorse | YA97912 | Quartz | BARNY | 49 | Arch Joint ' | 6/23/1987 | 2/11/2014 |
| Go to map | Whitehorse | YB08307 | Quartz | BARNY | 50 | Arch Joint ' | 10/2/1987 | 2/11/2014 |

report total:

| Map | District | GrantNumb | RegType | ClaimNam | ClaimNbr | Claim Own | OperationF | ClaimExpir |
|---|---|---|---|---|---|---|---|---|
| Go to map | Whitehorse | 71435 | Quartz | ROSS | 4 | Northern P | ######## | 12/5/2020 |
| Go to map | Whitehorse | 71434 | Quartz | ROSS | 3 | Northern P | ######## | 12/5/2020 |
| Go to map | Whitehorse | 71433 | Quartz | ROSS | 2 | Northern P | ######## | 12/5/2020 |
| Go to map | Whitehorse | 71432 | Quartz | ROSS | 1 | Northern P | ######## | 12/5/2020 |
| Go to map | Whitehorse | 70829 | Quartz | QUILL | | Northern P | 8/9/1955 | 12/5/2020 |
| Go to map | Whitehorse | 66572 | Quartz | JEEP | 268 | Northern P | 8/22/1953 | 12/5/2020 |
| Go to map | Whitehorse | 66571 | Quartz | JEEP | 267 | Northern P | 8/22/1953 | 12/5/2020 |
| Go to map | Whitehorse | 66569 | Quartz | JEEP | 265 | Northern P | 8/22/1953 | 12/5/2020 |
| Go to map | Whitehorse | 64836 | Quartz | JEEP | 244 | Northern P | 9/14/1952 | 12/5/2020 |
| Go to map | Whitehorse | 64834 | Quartz | JEEP | 242 | Northern P | 9/14/1952 | 12/5/2020 |
| Go to map | Whitehorse | 64832 | Quartz | JEEP | 240 | Northern P | 9/14/1952 | 12/5/2020 |
| Go to map | Whitehorse | 64830 | Quartz | JEEP | 236 | Northern P | 9/14/1952 | 12/5/2020 |
| Go to map | Whitehorse | 64828 | Quartz | JEEP | 234 | Northern P | 9/14/1952 | 12/5/2020 |
| Go to map | Whitehorse | 64742 | Quartz | JEEP | 96 | Northern P | 8/6/1952 | 12/5/2020 |
| Go to map | Whitehorse | 64587 | Quartz | ROSS | 96 | Northern P | 7/16/1952 | 12/5/2020 |
| Go to map | Whitehorse | 64122 | Quartz | JEEP | 238 | Northern P | 9/14/1952 | 12/5/2020 |
| Go to map | Whitehorse | 64087 | Quartz | ROSS | 86 | Northern P | 7/16/1952 | 12/5/2020 |
| Go to map | Whitehorse | 64086 | Quartz | ROSS | 85 | Northern P | 7/16/1952 | 12/5/2020 |
| Go to map | Whitehorse | 64085 | Quartz | ROSS | 95 | Northern P | 7/16/1952 | 12/5/2020 |
| Go to map | Whitehorse | 64084 | Quartz | ROSS | 94 | Northern P | 7/16/1952 | 12/5/2020 |
| Go to map | Whitehorse | 64077 | Quartz | ROSS | 16 | Northern P | 7/9/1952 | 12/5/2020 |
| Go to map | Whitehorse | 64076 | Quartz | ROSS | 15 | Northern P | 7/9/1952 | 12/5/2020 |
| Go to map | Whitehorse | 64066 | Quartz | ROSS | 25 | Northern P | 7/7/1952 | 12/5/2020 |
| Go to map | Whitehorse | 63044 | Quartz | RED | 8 | Northern P | 7/8/1952 | 12/5/2020 |
| Go to map | Whitehorse | 63043 | Quartz | RED | 7 | Northern P | 7/8/1952 | 12/5/2020 |
| Go to map | Whitehorse | 63042 | Quartz | RED | 6 | Northern P | 7/8/1952 | 12/5/2020 |
| Go to map | Whitehorse | 63041 | Quartz | RED | 5 | Northern P | 7/8/1952 | 12/5/2020 |
| Go to map | Whitehorse | 63040 | Quartz | RED | 4 | Northern P | 7/8/1952 | 12/5/2020 |
| Go to map | Whitehorse | 63039 | Quartz | RED | 3 | Northern P | 7/8/1952 | 12/5/2020 |
| Go to map | Whitehorse | 63038 | Quartz | RED | 2 | Northern P | 7/8/1952 | 12/5/2020 |
| Go to map | Whitehorse | 63037 | Quartz | RED | 1 | Northern P | 7/8/1952 | 12/5/2020 |
| Go to map | Whitehorse | 63036 | Quartz | BETTY | 8 | Northern P | 7/3/1952 | 12/5/2020 |
| Go to map | Whitehorse | 63035 | Quartz | BETTY | 7 | Northern P | 7/3/1952 | 12/5/2020 |
| Go to map | Whitehorse | 63034 | Quartz | BETTY | 6 | Northern P | 7/3/1952 | 12/5/2020 |
| Go to map | Whitehorse | 63033 | Quartz | BETTY | 5 | Northern P | 7/3/1952 | 12/5/2020 |
| Go to map | Whitehorse | 63032 | Quartz | BETTY | 4 | Northern P | 7/3/1952 | 12/5/2020 |
| Go to map | Whitehorse | 63031 | Quartz | BETTY | 3 | Northern P | 7/23/1952 | 12/5/2020 |
| Go to map | Whitehorse | 63030 | Quartz | BETTY | 2 | Northern P | 7/23/1952 | 12/5/2020 |
| Go to map | Whitehorse | 63029 | Quartz | BETTY | 1 | Northern P | 7/23/1952 | 12/5/2020 |
| Go to map | Whitehorse | 63028 | Quartz | MAC | 8 | Northern P | 7/3/1952 | 12/5/2020 |
| Go to map | Whitehorse | 63027 | Quartz | MAC | 7 | Northern P | 7/3/1952 | 12/5/2020 |
| Go to map | Whitehorse | 63026 | Quartz | MAC | 6 | Northern P | 7/3/1952 | 12/5/2020 |
| Go to map | Whitehorse | 63025 | Quartz | MAC | 5 | Northern P | 7/3/1952 | 12/5/2020 |
| Go to map | Whitehorse | 63024 | Quartz | MAC | 4 | Northern P | 7/3/1952 | 12/5/2020 |
| Go to map | Whitehorse | 63023 | Quartz | MAC | 3 | Northern P | 7/3/1952 | 12/5/2020 |
| Go to map | Whitehorse | 63022 | Quartz | MAC | 2 | Northern P | 7/3/1952 | 12/5/2020 |
| Go to map | Whitehorse | 63021 | Quartz | MAC | 1 | Northern P | 7/3/1952 | 12/5/2020 |
| Go to map | Whitehorse | 63020 | Quartz | SAM | 8 | Northern P | 7/3/1952 | 12/5/2020 |
| Go to map | Whitehorse | 63019 | Quartz | SAM | 7 | Northern P | 7/30/1952 | 12/5/2020 |
| Go to map | Whitehorse | 63018 | Quartz | SAM | 6 | Northern P | 7/3/1952 | 12/5/2020 |
| Go to map | Whitehorse | 63017 | Quartz | SAM | 5 | Northern P | 7/3/1952 | 12/5/2020 |

| | | | | | | | |
|---|---|---|---|---|---|---|---|
| Go to map | Whitehorse | 63016 | Quartz | SAM | 4 | Northern P | 7/3/1952 12/5/2020 |
| Go to map | Whitehorse | 63015 | Quartz | SAM | 3 | Northern P | 7/3/1952 12/5/2020 |
| Go to map | Whitehorse | 63014 | Quartz | SAM | 2 | Northern P | 7/3/1952 12/5/2020 |
| Go to map | Whitehorse | 63013 | Quartz | SAM | 1 | Northern P | 7/3/1952 12/5/2020 |
| Go to map | Whitehorse | 63006 | Quartz | IRISH | 6 | Northern P | 7/3/1952 12/5/2020 |
| Go to map | Whitehorse | 63003 | Quartz | IRISH | 3 | Northern P | 7/3/1952 12/5/2020 |
| Go to map | Whitehorse | 63002 | Quartz | IRISH | 2 | Northern P | 7/3/1952 12/5/2020 |
| Go to map | Whitehorse | 63001 | Quartz | IRISH | 1 | Northern P | 7/3/1952 12/5/2020 |
| Go to map | Whitehorse | 60798 | Quartz | RAM | 8 | Northern P | 7/2/1952 12/5/2020 |
| Go to map | Whitehorse | 60797 | Quartz | RAM | 7 | Northern P | 7/2/1952 12/5/2020 |
| Go to map | Whitehorse | 60796 | Quartz | RAM | 6 | Northern P | 7/2/1952 12/5/2020 |
| Go to map | Whitehorse | 60795 | Quartz | RAM | 5 | Northern P | 7/2/1952 12/5/2020 |
| Go to map | Whitehorse | 60794 | Quartz | RAM | 4 | Northern P | 7/2/1952 12/5/2020 |
| Go to map | Whitehorse | 60793 | Quartz | RAM | 3 | Northern P | 7/2/1952 12/5/2020 |
| Go to map | Whitehorse | 60792 | Quartz | RAM | 2 | Northern P | 7/2/1952 12/5/2020 |
| Go to map | Whitehorse | 60791 | Quartz | RAM | 1 | Northern P | 7/2/1952 12/5/2020 |
| Go to map | Whitehorse | 60790 | Quartz | WAGONEI | 8 | Northern P | 6/27/1952 12/5/2020 |
| Go to map | Whitehorse | 60789 | Quartz | WAGONEI | 7 | Northern P | 6/27/1952 12/5/2020 |
| Go to map | Whitehorse | 60788 | Quartz | WAGONEI | 6 | Northern P | 6/27/1952 12/5/2020 |
| Go to map | Whitehorse | 60787 | Quartz | WAGONEI | 5 | Northern P | 6/27/1952 12/5/2020 |
| Go to map | Whitehorse | 60786 | Quartz | WAGONEI | 4 | Northern P | 6/27/1952 12/5/2020 |
| Go to map | Whitehorse | 60785 | Quartz | WAGONEI | 3 | Northern P | 6/27/1952 12/5/2020 |
| Go to map | Whitehorse | 60784 | Quartz | WAGONEI | 2 | Northern P | 6/27/1952 12/5/2020 |
| Go to map | Whitehorse | 60783 | Quartz | WAGONEI | 1 | Northern P | 6/27/1952 12/5/2020 |
| Go to map | Whitehorse | 60782 | Quartz | DISCOVEI | 8 | Northern P | 7/3/1952 12/5/2020 |
| Go to map | Whitehorse | 60781 | Quartz | DISCOVEI | 7 | Northern P | 7/3/1952 12/5/2020 |
| Go to map | Whitehorse | 60780 | Quartz | DISCOVEI | 6 | Northern P | 7/3/1952 12/5/2020 |
| Go to map | Whitehorse | 60779 | Quartz | DISCOVEI | 5 | Northern P | 7/3/1952 12/5/2020 |
| Go to map | Whitehorse | 60778 | Quartz | DISCOVEI | 4 | Northern P | 7/3/1952 12/5/2020 |
| Go to map | Whitehorse | 60777 | Quartz | DISCOVEI | 3 | Northern P | 7/3/1952 12/5/2020 |
| Go to map | Whitehorse | 60776 | Quartz | DISCOVEI | 2 | Northern P | 7/3/1952 12/5/2020 |
| Go to map | Whitehorse | 60775 | Quartz | DISCOVEI | 1 | Northern P | 7/3/1952 12/5/2020 |
| Go to map | Whitehorse | 60774 | Quartz | QUILL | 8 | Northern P | 7/2/1952 12/5/2020 |
| Go to map | Whitehorse | 60773 | Quartz | QUILL | 7 | Northern P | 7/2/1952 12/5/2020 |
| Go to map | Whitehorse | 60772 | Quartz | QUILL | 6 | Northern P | 7/2/1952 12/5/2020 |
| Go to map | Whitehorse | 60771 | Quartz | QUILL | 5 | Northern P | 7/2/1952 12/5/2020 |
| Go to map | Whitehorse | 60770 | Quartz | QUILL | 4 | Northern P | 7/2/1953 12/5/2020 |
| Go to map | Whitehorse | 60769 | Quartz | QUILL | 3 | Northern P | 7/2/1952 12/5/2020 |
| Go to map | Whitehorse | 60768 | Quartz | QUILL | 2 | Northern P | 7/2/1952 12/5/2020 |
| Go to map | Whitehorse | 60767 | Quartz | QUILL | 1 | Northern P | 7/2/1952 12/5/2020 |

report total:

| Status | QuartzLea | TotalExces | NTS MapN | NonStdSiz | Ops Number |
|---|---|---|---|---|---|
| Active | OW00121 | | 115G06 | | 5E+08 |
| Active | OW00120 | | 115G06 | | 5E+08 |
| Active | OW00119 | | 115G05 | | 5E+08 |
| Active | OW00118 | | 115G05 | | 5E+08 |
| Active | OW00117 | | 115G05 | Full Quartz | 5E+08 |
| Active | OW00171 | | 115G06 | | 5E+08 |
| Active | OW00170 | | 115G06 | | 5E+08 |
| Active | OW00169 | | 115G06 | | 5E+08 |
| Active | OW00168 | | 115G05 | | 5E+08 |
| Active | OW00167 | | 115G05 | | 5E+08 |
| Active | OW00166 | | 115G05 | | 5E+08 |
| Active | OW00165 | | 115G05 | | 5E+08 |
| Active | OW00164 | | 115G05 | | 5E+08 |
| Active | OW00163 | | 115G05 | | 5E+08 |
| Active | OW00161 | | 115G06 | Full Quartz | 5E+08 |
| Active | OW00162 | | 115G05 | | 5E+08 |
| Active | OW00158 | | 115G06 | | 5E+08 |
| Active | OW00157 | | 115G06 | | 5E+08 |
| Active | OW00160 | | 115G05 | | 5E+08 |
| Active | OW00159 | | 115G05 | Full Quartz | 5E+08 |
| Active | OW00155 | | 115G06 | | 5E+08 |
| Active | OW00154 | | 115G06 | | 5E+08 |
| Active | OW00156 | | 115G06 | | 5E+08 |
| Active | OW00153 | | 115G05 | | 5E+08 |
| Active | OW00152 | | 115G05 | | 5E+08 |
| Active | OW00151 | | 115G05 | | 5E+08 |
| Active | OW00150 | | 115G05 | | 5E+08 |
| Active | OW00149 | | 115G05 | | 5E+08 |
| Active | OW00148 | | 115G05 | | 5E+08 |
| Active | OW00147 | | 115G05 | | 5E+08 |
| Active | OW00146 | | 115G06 | | 5E+08 |
| Active | OW00145 | | 115G05 | | 5E+08 |
| Active | OW00144 | | 115G05 | | 5E+08 |
| Active | OW00143 | | 115G05 | | 5E+08 |
| Active | OW00142 | | 115G05 | | 5E+08 |
| Active | OW00141 | | 115G05 | | 5E+08 |
| Active | OW00140 | | 115G05 | | 5E+08 |
| Active | OW00139 | | 115G05 | | 5E+08 |
| Active | OW00138 | | 115G05 | | 5E+08 |
| Active | OW00137 | | 115G05 | | 5E+08 |
| Active | OW00136 | | 115G05 | | 5E+08 |
| Active | OW00135 | | 115G05 | | 5E+08 |
| Active | OW00134 | | 115G05 | | 5E+08 |
| Active | OW00133 | | 115G05 | | 5E+08 |
| Active | OW00132 | | 115G05 | | 5E+08 |
| Active | OW00131 | | 115G05 | | 5E+08 |
| Active | OW00130 | | 115G05 | | 5E+08 |
| Active | OW00129 | | 115G05 | | 5E+08 |
| Active | OW00128 | | 115G05 | | 5E+08 |
| Active | OW00127 | | 115G05 | | 5E+08 |
| Active | OW00126 | | 115G05 | | 5E+08 |

| | | | |
|---|---|---|---|
| Active | OW00125 | 115G05 | 5E+08 |
| Active | OW00124 | 115G05 | 5E+08 |
| Active | OW00123 | 115G05 | 5E+08 |
| Active | OW00122 | 115G05 | 5E+08 |
| Active | OW00116 | 115G05 | 5E+08 |
| Active | OW00115 | 115G05 | 5E+08 |
| Active | OW00114 | 115G05 | 5E+08 |
| Active | OW00113 | 115G05 | 5E+08 |
| Active | OW00112 | 115G05 | 5E+08 |
| Active | OW00111 | 115G05 | 5E+08 |
| Active | OW00110 | 115G05 | 5E+08 |
| Active | OW00109 | 115G05 | 5E+08 |
| Active | OW00108 | 115G05 | 5E+08 |
| Active | OW00107 | 115G05 | 5E+08 |
| Active | OW00106 | 115G05 | 5E+08 |
| Active | OW00105 | 115G05 | 5E+08 |
| Active | OW00104 | 115G05 | 5E+08 |
| Active | OW00103 | 115G05 | 5E+08 |
| Active | OW00102 | 115G05 | 5E+08 |
| Active | OW00101 | 115G05 | 5E+08 |
| Active | OW00100 | 115G05 | 5E+08 |
| Active | OW00099 | 115G05 | 5E+08 |
| Active | OW00098 | 115G05 | 5E+08 |
| Active | OW00097 | 115G05 | 5E+08 |
| Active | OW00096 | 115G05 | 5E+08 |
| Active | OW00095 | 115G05 | 5E+08 |
| Active | OW00094 | 115G05 | 5E+08 |
| Active | OW00093 | 115G05 | 5E+08 |
| Active | OW00092 | 115G05 | 5E+08 |
| Active | OW00091 | 115G05 | 5E+08 |
| Active | OW00090 | 115G05 | 5E+08 |
| Active | OW00089 | 115G05 | 5E+08 |
| Active | OW00088 | 115G05 | 5E+08 |
| Active | OW00087 | 115G05 | 5E+08 |
| Active | OW00086 | 115G05 | 5E+08 |
| Active | OW00085 | 115G05 | 5E+08 |
| Active | OW00084 | 115G05 | 5E+08 |
| Active | OW00083 | 115G05 | 5E+08 |
| Active | OW00082 | 115G05 | 5E+08 |
| Active | OW00081 | 115G05 | 5E+08 |

## TECHNICAL SUMMARY

| | |
|---|---|
| Navigation | Differentially–corrected GPS |
| Data reduction grid interval | 20 metres |
| Terrain clearance | Helicopter 57 m<br>Electromagnetic sensor 30 m<br>Magnetometer 30 m |
| Data sampling interval | 0.1 second |
| Magnetometer / sensitivity | Cesium / 0.01 nT |
| Electromagnetic system | DIGHEM$^V$ |

| Frequency | Sensitivity | Coil Orientation |
|---|---|---|
| 1000 Hz | .06 ppm | Vertical coaxial |
| 5500 Hz | .12 ppm | Vertical coaxial |
| 900 Hz | .12 ppm | Horizontal coplanar |
| 7200 Hz | .24 ppm | Horizontal coplanar |
| 56000 Hz | .60 ppm | Horizontal coplanar |

## ELECTROMAGNETIC ANOMALIES

| Grade | Anomaly | Conductance |
|---|---|---|
| 7 | ● | >100 siemens |
| 6 | ◕ | 50–100 siemens |
| 5 | ◑ | 20–50 siemens |
| 4 | ◔ | 10–20 siemens |
| 3 | ⊕ | 5–10 siemens |
| 2 | ○ | 1–5 siemens |
| 1 | ◌ | < 1 siemens |
| – | ✳ | Questionable anomaly |

Anomaly identifier

Interpretive symbol

Depth is greater than
- . 15 m
- : 30 m
- ⋮ 45 m
- ⋮ 60 m

Inphase and Quadrature of coaxial coil is greater than
- . 5 ppm
- .. 10 ppm
- ... 15 ppm
- .... 20 ppm

| Interpretive symbol | Conductor ("model") |
|---|---|
| B | Bedrock conductor |
| D | Narrow bedrock conductor ("thin dike") |
| S | Conductive cover ("horizontal thin sheet") |
| H | Broad conductive rock unit, deep conductive weathering, thick conductive cover ("half space") |
| E | Edge of broad conductor ("edge of half space") |
| L | Culture, e.g. power line, metal building or fence |

## FLIGHT LINES WITH EM ANOMALIES

Flight number
Flight direction
Flight line number
Reflight Number
Line Number
Area Number
Fiducials identified on profiles
Dip direction
EM anomaly (see EM legend)
Conductor axis (on EM maps only)
Arcs indicate the conductor has a thickness > 10m
Magnetic correlation in nT (gammas)

## INTERPRETATION LEGEND

Structural Breaks

Conductive Zone

## LOCATION MAP




NTS: 115G/5,6 | UTM ZONE: 7 NAD83 | SCALE: 1:250,000

# CORONATION MINERALS INC.
## WELLGREEN PROPERTY, YUKON

## ELECTROMAGNETIC ANOMALIES

| | | |
|---|---|---|
| FUGRO DIGHEM$^V$ SURVEY | NTS: 115G/5,6 | GEOPHYSICIST: |
| DATE: JUNE, 2008 | JOB: 08032 | SHEET: 1 |

Fugro Airborne Surveys

0 1 2 Km
0 1 Mi
Scale 1:20 000

**FUGRO AIRBORNE SURVEYS**

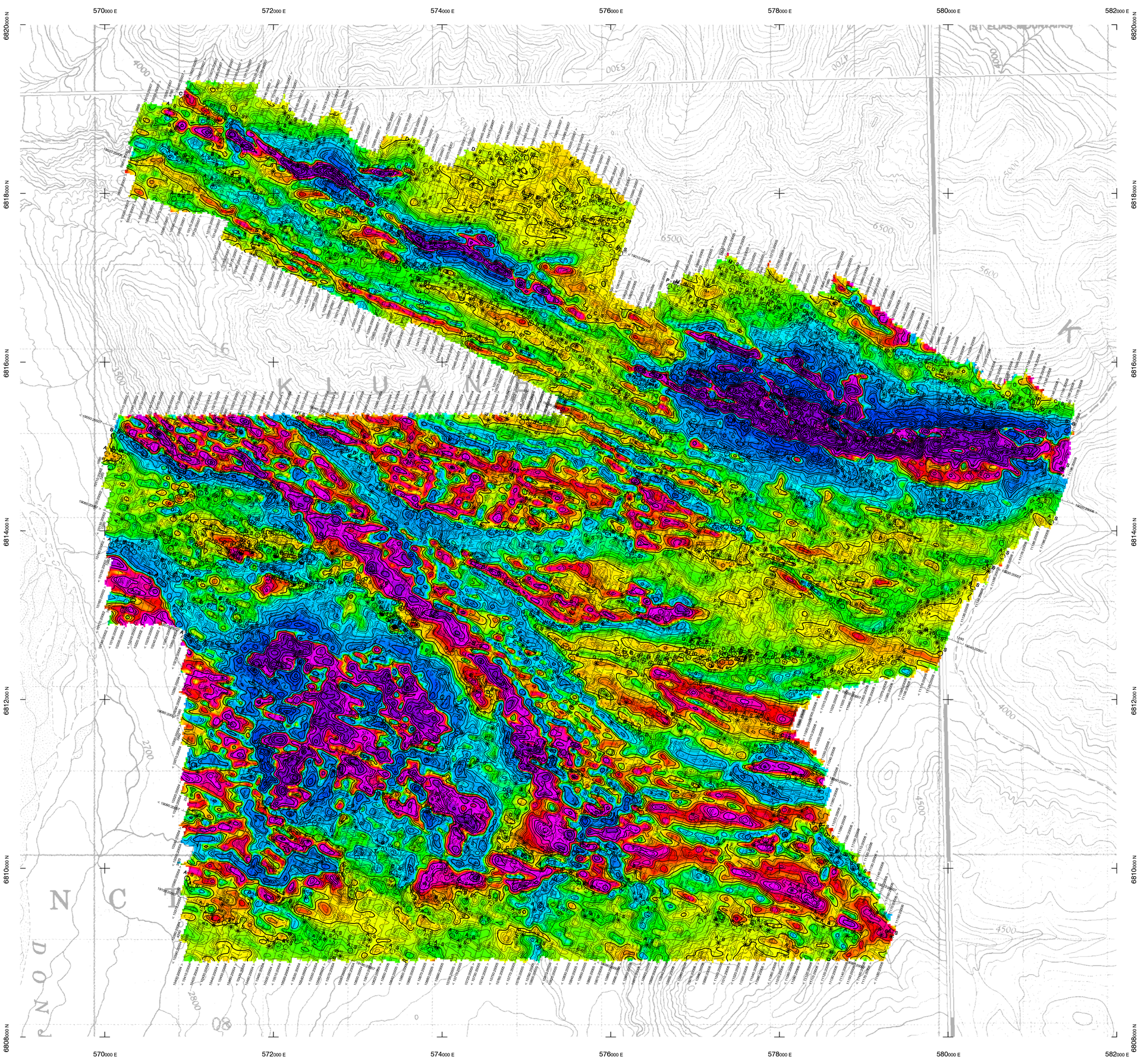


## TECHNICAL SUMMARY

| | |
|---|---|
| Navigation | Differentially–corrected GPS |
| Data reduction grid interval | 20 metres |
| Terrain clearance | Helicopter 57 m<br>Electromagnetic sensor 30 m<br>Magnetometer 30 m |
| Data sampling interval | 0.1 second |
| Magnetometer / sensitivity | Cesium / 0.01 nT |
| Electromagnetic system | DIGHEM$^V$ |

| Frequency | Sensitivity | Coil Orientation |
|---|---|---|
| 1000 Hz | .06 ppm | Vertical coaxial |
| 5500 Hz | .12 ppm | Vertical coaxial |
| 900 Hz | .12 ppm | Horizontal coplanar |
| 7200 Hz | .24 ppm | Horizontal coplanar |
| 56000 Hz | .60 ppm | Horizontal coplanar |

nT/m

7.00 6.00 5.00 4.00 3.00 2.50 2.00 1.50 1.00 1.50 1.00 0.95 0.90 0.85 0.80 0.75 0.70 0.65 0.60 0.55 0.50 0.45 0.40 0.35 0.30 0.25 0.20 0.15 0.10 0.05 0.00 -0.05 -0.10 -0.15 -0.20 -0.25 -0.30 -0.35 -0.40 -0.45 -0.50 -0.55 -0.60 -0.65 -0.70 -0.75 -0.80 -0.85 -0.90 -0.95 -1.00 -1.10 -1.20 -1.30 -1.50 -2.00 -2.50 -3.00 -4.00 -5.00 -6.00 -7.00

## ELECTROMAGNETIC ANOMALIES

| Grade | Anomaly | Conductance |
|---|---|---|
| 7 | ● | >100 siemens |
| 6 | ◕ | 50–100 siemens |
| 5 | ◒ | 20–50 siemens |
| 4 | ◔ | 10–20 siemens |
| 3 | ⊕ | 5–10 siemens |
| 2 | ○ | 1–5 siemens |
| 1 | ◌ | < 1 siemens |
| – | ✳ | Questionable anomaly |

Anomaly identifier; Interpretive symbol; Depth is greater than . 15 m .. 30 m ... 45 m .... 60 m; Inphase and Quadrature of coaxial coil is greater than . 5 ppm .. 10 ppm ... 15 ppm .... 20 ppm

| Interpretive symbol | Conductor ("model") |
|---|---|
| B | Bedrock conductor |
| D | Narrow bedrock conductor ("thin dike") |
| S | Conductive cover ("horizontal thin sheet") |
| H | Broad conductive rock unit, deep conductive weathering, thick conductive cover ("half space") |
| E | Edge of broad conductor ("edge of half space") |
| L | Culture, e.g. power line, metal building or fence |

## FLIGHT LINES WITH EM ANOMALIES

Flight number; Flight direction; Flight line number; 11020 Reflight Number, Line Number, Area Number; Fiducials identified on profiles; Dip direction; EM anomaly (see EM legend); Conductor axis (on EM maps only); Arcs indicate the conductor has a thickness > 10m; Magnetic correlation in nT (gammas)

## CALCULATED VERTICAL GRADIENT CONTOURS

2.5 nT/metre
0.5 nT/metre
0.1 nT/metre
0.05 nT/metre

## LOCATION MAP




# CORONATION MINERALS INC.

WELLGREEN PROPERTY, YUKON

## CALCULATED VERTICAL MAGNETIC GRADIENT

| | | |
|---|---|---|
| FUGRO DIGHEM$^V$ SURVEY | NTS: 115G/5,6 | GEOPHYSICIST: |
| DATE: JUNE, 2008 | JOB: 08032 | SHEET: 1 |
| Fugro Airborne Surveys | | |

0 1 2 Km
0 1 Mi
Scale 1:20 000

FUGRO AIRBORNE SURVEYS

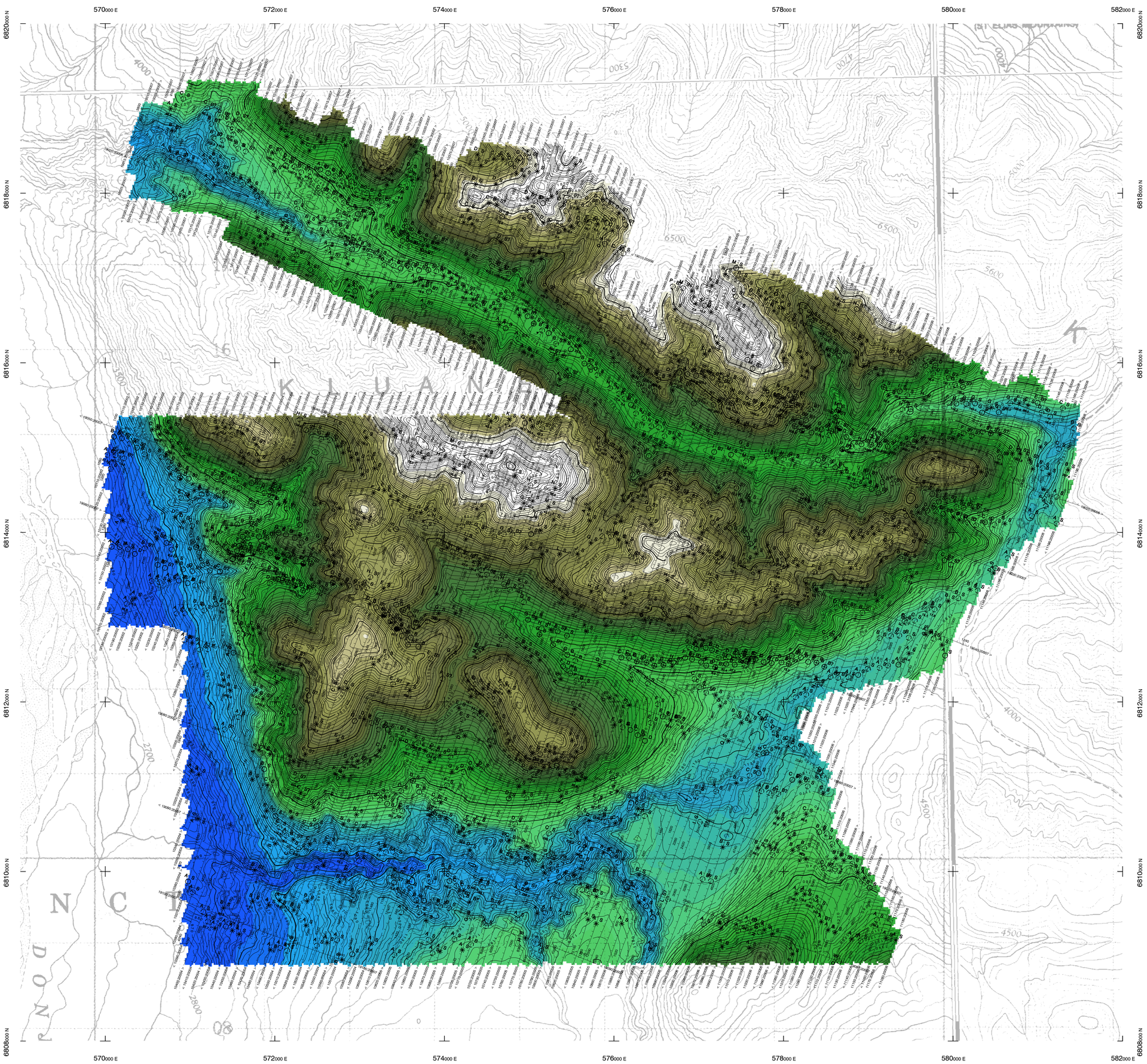


## TECHNICAL SUMMARY

| | |
|---|---|
| Navigation | Differentially–corrected GPS |
| Data reduction grid interval | 20 metres |
| Terrain clearance | Helicopter 57 m<br>Electromagnetic sensor 30 m<br>Magnetometer 30 m |
| Data sampling interval | 0.1 second |
| Magnetometer / sensitivity | Cesium / 0.01 nT |
| Electromagnetic system | DIGHEM$^V$ |

| Frequency | Sensitivity | Coil Orientation |
|---|---|---|
| 1000 Hz | .06 ppm | Vertical coaxial |
| 5500 Hz | .12 ppm | Vertical coaxial |
| 900 Hz | .12 ppm | Horizontal coplanar |
| 7200 Hz | .24 ppm | Horizontal coplanar |
| 56000 Hz | .60 ppm | Horizontal coplanar |

m: 1791, 1729, 1688, 1653, 1624, 1602, 1579, 1558, 1536, 1514, 1494, 1475, 1456, 1437, 1419, 1400, 1382, 1364, 1346, 1328, 1312, 1295, 1279, 1263, 1243, 1225, 1207, 1192, 1180, 1170, 1163, 1156, 1146, 1130, 1106, 1074, 1036, 990, 942

## ELECTROMAGNETIC ANOMALIES

| Grade | Anomaly | Conductance |
|---|---|---|
| 7 | ● | >100 siemens |
| 6 | ◕ | 50–100 siemens |
| 5 | ◑ | 20–50 siemens |
| 4 | ◔ | 10–20 siemens |
| 3 | ⊕ | 5–10 siemens |
| 2 | ○ | 1–5 siemens |
| 1 | ◌ | < 1 siemens |
| – | ✳ | Questionable anomaly |

Anomaly identifier; Interpretive symbol; Depth is greater than . 15 m, : 30 m, ⋮ 45 m, ⋮ 60 m; Inphase and Quadrature of coaxial coil is greater than . 5 ppm, .. 10 ppm, ... 15 ppm, .... 20 ppm

| Interpretive symbol | Conductor ("model") |
|---|---|
| B | Bedrock conductor |
| D | Narrow bedrock conductor ("thin dike") |
| S | Conductive cover ("horizontal thin sheet") |
| H | Broad conductive rock unit, deep conductive weathering, thick conductive cover ("half space") |
| E | Edge of broad conductor ("edge of half space") |
| L | Culture, e.g. power line, metal building or fence |

## FLIGHT LINES WITH EM ANOMALIES

Flight number; Flight direction; Flight line number; Reflight Number; Line Number; Area Number; Fiducials identified on profiles; Dip direction; EM anomaly (see EM legend); Conductor axis (on EM maps only); Arcs indicate the conductor has a thickness > 10m; Magnetic correlation in nT (gammas)

## DIGITAL ELEVATION CONTOURS

. . . . . 50 m.

. . . . . 10 m.

. . . . . 5 m.

This Digital Elevation Model (DEM) has been computed from GPS "Z" values minus the aircraft altimeter data recorded during the course of a helicopter–borne geophysical survey flown at a nominal line spacing of 100 metres, azimuth 20 degrees. Elevation values have been interpolated/gridded between survey lines. Every effort has been made to make the model a useful general reference. No guarantee can be made that this model is a true representation of the height above sea level and it may contain radar altimeter responses from buildings and in some instances dense timber. Users of the product should be aware of the topographic limitations mapped herewithin.
DO NOT USE THIS MAP FOR NAVIGATION PURPOSES.

## LOCATION MAP




NTS: 115G/5,6 UTM ZONE: 7 NAD83 SCALE: 1:250,000

# CORONATION MINERALS INC.
## WELLGREEN PROPERTY, YUKON

## DIGITAL ELEVATION MODEL

| | | |
|---|---|---|
| FUGRO DIGHEM$^V$ SURVEY | NTS: 115G/5,6 | GEOPHYSICIST: |
| DATE: JUNE, 2008 | JOB: 08032 | SHEET: 1 |
| Fugro Airborne Surveys | | |

0 1 2 Km
0 1 Mi
Scale 1:20 000

**FUGRO AIRBORNE SURVEYS**

570000 E 572000 E 574000 E 576000 E 578000 E 580000 E 582000 E

6820000 N 6818000 N 6816000 N 6814000 N 6812000 N 6810000 N 6808000 N

K L U A N E

N C I D O N I

## TECHNICAL SUMMARY

| | |
|---|---|
| Navigation | Differentially–corrected GPS |
| Data reduction grid interval | 20 metres |
| Terrain clearance | Helicopter 57 m<br>Electromagnetic sensor 30 m<br>Magnetometer 30 m |
| Data sampling interval | 0.1 second |
| Magnetometer / sensitivity | Cesium / 0.01 nT |
| Electromagnetic system | DIGHEM$^V$ |

| | Frequency | Sensitivity | Coil Orientation |
|---|---|---|---|
| | 1000 Hz | .06 ppm | Vertical coaxial |
| | 5500 Hz | .12 ppm | Vertical coaxial |
| | 900 Hz | .12 ppm | Horizontal coplanar |
| | 7200 Hz | .24 ppm | Horizontal coplanar |
| | 56000 Hz | .60 ppm | Horizontal coplanar |

nT
1451.6
1112.9
899.7
731.6
605.3
510.2
442.2
384.0
323.1
270.4
224.0
183.1
145.6
114.4
84.6
58.6
34.0
10.1
-10.4
-29.0
-45.7
-62.1
-79.6
-95.2
-110.1
-124.5
-138.0
-153.0
-167.1
-181.5
-195.0
-208.9
-222.6
-237.8
-252.4
-267.5
-281.7
-296.6
-313.4
-330.4
-346.0
-358.6
-371.0
-381.8
-391.1
-400.0
-410.7
-420.4
-430.9
-440.8
-452.4
-464.3
-475.9
-487.8
-499.5
-511.1
-524.0
-538.9
-554.8
-573.6
-614.1
-671.7
-775.9

## ELECTROMAGNETIC ANOMALIES

| Grade | Anomaly | Conductance |
|---|---|---|
| 7 | ● | >100 siemens |
| 6 | ◕ | 50–100 siemens |
| 5 | ◒ | 20–50 siemens |
| 4 | ◔ | 10–20 siemens |
| 3 | ⊕ | 5–10 siemens |
| 2 | ○ | 1–5 siemens |
| 1 | ◌ | < 1 siemens |
| – | ✳ | Questionable anomaly |

Anomaly identifier; Interpretive symbol; Depth is greater than: . 15 m, : 30 m, ⋮ 45 m, ⋮ 60 m; Inphase and Quadrature of coaxial coil is greater than: . 5 ppm, .. 10 ppm, ... 15 ppm, .... 20 ppm

| Interpretive symbol | Conductor ("model") |
|---|---|
| B | Bedrock conductor |
| D | Narrow bedrock conductor ("thin dike") |
| S | Conductive cover ("horizontal thin sheet") |
| H | Broad conductive rock unit, deep conductive weathering, thick conductive cover ("half space") |
| E | Edge of broad conductor ("edge of half space") |
| L | Culture, e.g. power line, metal building or fence |

## FLIGHT LINES WITH EM ANOMALIES

Flight number; Flight direction; Flight line number; Reflight Number; Line Number; Area Number; Fiducials identified on profiles; Dip direction; EM anomaly (see EM legend); Conductor axis (on EM maps only); Arcs indicate the conductor has a thickness > 10m; Magnetic correlation in nT (gammas)

## RESIDUAL MAGNETIC INTENSITY CONTOURS

250 nT
50 nT
10 nT
5 nT
magnetic low

Magnetic inclination within the survey area: 76 degrees N
Magnetic declination within the survey area: 23 degrees E

## LOCATION MAP




NTS: 115G/5,6 UTM ZONE: 7 NAD83 SCALE: 1:250,000

# CORONATION MINERALS INC.

WELLGREEN PROPERTY, YUKON

## RESIDUAL MAGNETIC INTENSITY

| | | |
|---|---|---|
| FUGRO DIGHEM$^V$ SURVEY | NTS: 115G/5,6 | GEOPHYSICIST: |
| DATE: JUNE, 2008 | JOB: 08032 | SHEET: 1 |

Fugro Airborne Surveys

0 1 2 Km
0 1 Mi
Scale 1:20 000

FUGRO AIRBORNE SURVEYS

## TECHNICAL SUMMARY

| | |
|---|---|
| Navigation | Differentially–corrected GPS |
| Data reduction grid interval | 20 metres |
| Terrain clearance | Helicopter 57 m<br>Electromagnetic sensor 30 m<br>Magnetometer 30 m |
| Data sampling interval | 0.1 second |
| Magnetometer / sensitivity | Cesium / 0.01 nT |
| Electromagnetic system | DIGHEM$^V$ |

| Frequency | Sensitivity | Coil Orientation |
|---|---|---|
| 1000 Hz | .06 ppm | Vertical coaxial |
| 5500 Hz | .12 ppm | Vertical coaxial |
| 900 Hz | .12 ppm | Horizontal coplanar |
| 7200 Hz | .24 ppm | Horizontal coplanar |
| 56000 Hz | .60 ppm | Horizontal coplanar |

ohm•m
18250
16043
14453
12896
11248
9718
8301
7166
6251
5499
4849
4302
3863
3486
3197
2952
2736
2557
2404
2269
2145
2025
1911
1811
1711
1617
1530
1450
1373
1301
1238
1178
1121
1071
1024
977
933
890
852
816
779
746
714
683
653
625
600
574
547
522
498
474
451
428
405
379
352
326
300
274
245
212
181

## ELECTROMAGNETIC ANOMALIES

| Grade | Anomaly | Conductance |
|---|---|---|
| 7 | ● | >100 siemens |
| 6 | ◕ | 50–100 siemens |
| 5 | ◒ | 20–50 siemens |
| 4 | ◔ | 10–20 siemens |
| 3 | ⊕ | 5–10 siemens |
| 2 | ○ | 1–5 siemens |
| 1 | ◌ | < 1 siemens |
| – | ✳ | Questionable anomaly |

Anomaly identifier

Depth is greater than
. 15 m
: 30 m
⋮ 45 m
⋮ 60 m

Interpretive symbol

Inphase and Quadrature of coaxial coil is greater than
. 5 ppm
.. 10 ppm
... 15 ppm
.... 20 ppm

| Interpretive symbol | Conductor ("model") |
|---|---|
| B | Bedrock conductor |
| D | Narrow bedrock conductor ("thin dike") |
| S | Conductive cover ("horizontal thin sheet") |
| H | Broad conductive rock unit, deep conductive weathering, thick conductive cover ("half space") |
| E | Edge of broad conductor ("edge of half space") |
| L | Culture, e.g. power line, metal building or fence |

## FLIGHT LINES WITH EM ANOMALIES

Flight number
Flight direction
Flight line number
11020
Reflight Number
Line Number
Area Number
Fiducials identified on profiles
Dip direction
EM anomaly (see EM legend)
Conductor axis (on EM maps only)
Arcs indicate the conductor has a thickness > 10m
Magnetic correlation in nT (gammas)

## RESISTIVITY CONTOURS

1000
800
600
500
400
300
250
200
150
125
100

Contours in ohm–m at 10 intervals per decade. Apparent resistivity calculated using a pseudo–layer half–space model (Fraser 1978).

## LOCATION MAP




NTS: 115G/5,6 | UTM ZONE: 7 NAD83 | SCALE: 1:250,000

# CORONATION MINERALS INC.
## WELLGREEN PROPERTY, YUKON

## APPARENT RESISTIVITY
## 56,000 Hz COPLANAR

| | | |
|---|---|---|
| FUGRO DIGHEM$^V$ SURVEY | NTS: 115G/5,6 | GEOPHYSICIST: |
| DATE: JUNE, 2008 | JOB: 08032 | SHEET: 1 |
| Fugro Airborne Surveys | | |

0 1 2 Km
0 1 Mi
Scale 1:20 000

**FUGRO AIRBORNE SURVEYS**

570000 E | 572000 E | 574000 E | 576000 E | 578000 E | 580000 E | 582000 E

6820000 N | 6818000 N | 6816000 N | 6814000 N | 6812000 N | 6810000 N | 6808000 N

K L U A N E

N C

D O N

## TECHNICAL SUMMARY

| | |
|---|---|
| Navigation | Differentially–corrected GPS |
| Data reduction grid interval | 20 metres |
| Terrain clearance | Helicopter 57 m<br>Electromagnetic sensor 30 m<br>Magnetometer 30 m |
| Data sampling interval | 0.1 second |
| Magnetometer / sensitivity | Cesium / 0.01 nT |
| Electromagnetic system | DIGHEM$^V$ |

| Frequency | Sensitivity | Coil Orientation |
|---|---|---|
| 1000 Hz | .06 ppm | Vertical coaxial |
| 5500 Hz | .12 ppm | Vertical coaxial |
| 900 Hz | .12 ppm | Horizontal coplanar |
| 7200 Hz | .24 ppm | Horizontal coplanar |
| 56000 Hz | .60 ppm | Horizontal coplanar |

ohm•m: 8758, 8108, 7630, 7273, 6986, 6760, 6550, 6362, 6180, 6024, 5883, 5742, 5613, 5454, 5214, 4889, 4504, 4099, 3690, 3315, 2964, 2665, 2410, 2202, 2029, 1874, 1740, 1626, 1523, 1427, 1343, 1267, 1196, 1131, 1072, 1011, 953, 902, 858, 817, 778, 740, 704, 673, 642, 613, 584, 556, 527, 500, 471, 443, 414, 385, 356, 328, 302, 277, 250, 218, 185, 153, 121

## ELECTROMAGNETIC ANOMALIES

| Grade | Anomaly | Conductance |
|---|---|---|
| 7 | ● | >100 siemens |
| 6 | ◕ | 50–100 siemens |
| 5 | ◒ | 20–50 siemens |
| 4 | ◔ | 10–20 siemens |
| 3 | ⊕ | 5–10 siemens |
| 2 | ○ | 1–5 siemens |
| 1 | ◌ | < 1 siemens |
| – | ✳ | Questionable anomaly |

Anomaly identifier; Interpretive symbol; Depth is greater than . 15 m, : 30 m, ⁝ 45 m, ⋮ 60 m; Inphase and Quadrature of coaxial coil is greater than . 5 ppm, .. 10 ppm, ... 15 ppm, .... 20 ppm

| Interpretive symbol | Conductor ("model") |
|---|---|
| B | Bedrock conductor |
| D | Narrow bedrock conductor ("thin dike") |
| S | Conductive cover ("horizontal thin sheet") |
| H | Broad conductive rock unit, deep conductive weathering, thick conductive cover ("half space") |
| E | Edge of broad conductor ("edge of half space") |
| L | Culture, e.g. power line, metal building or fence |

## FLIGHT LINES WITH EM ANOMALIES

Flight number; Flight direction; Flight line number; Reflight Number; Line Number; Area Number; Fiducials identified on profiles; Dip direction; EM anomaly (see EM legend); Conductor axis (on EM maps only); Arcs indicate the conductor has a thickness > 10m; Magnetic correlation in nT (gammas)

## RESISTIVITY CONTOURS

1000, 800, 600, 500, 400, 300, 250, 200, 150, 125, 100

Contours in ohm–m at 10 intervals per decade. Apparent resistivity calculated using a pseudo–layer half–space model (Fraser 1978).

## LOCATION MAP

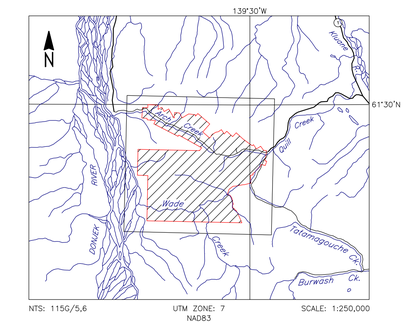


NTS: 115G/5,6 | UTM ZONE: 7 NAD83 | SCALE: 1:250,000

CORONATION MINERALS INC.
WELLGREEN PROPERTY, YUKON

APPARENT RESISTIVITY
7200 Hz COPLANAR

| | | |
|---|---|---|
| FUGRO DIGHEM$^V$ SURVEY | NTS: 115G/5,6 | GEOPHYSICIST: |
| DATE: JUNE, 2008 | JOB: 08032 | SHEET: 1 |

Fugro Airborne Surveys

0 1 2 Km
0 1 Mi
Scale 1:20 000

FUGRO AIRBORNE SURVEYS